Hygrothermal Properties of Cross Laminated Timber and Moisture Response of Wood at High Relative Humidity

by

George AlSayegh

A Thesis submitted to the Faculty of Graduate and Postdoctoral Affairs in partial fulfillment of the requirements for the degree of

Master of Applied Science

in

Civil and Environmental Engineering

Carleton University
Ottawa, Ontario

Your file Votre référence
ISBN: 978-0-494-94251-2

Our file Notre référence
ISBN: 978-0-494-94251-2

Abstract

Cross Laminated Timber (CLT) is a new wood-based material composed of cross laminated wood boards that form a structural panel. This study focuses on identifying the appropriate methods to determine the hygrothermal properties of CLTs fabricated with Canadian and European Lumber. The laboratory tests carried out in this study will help establish heat, air and moisture response properties to be used for hygrothermal simulation to assess the durability of CLTs in building envelope construction.

Measurement of water vapour permeability, liquid water absorption, sorption isotherms, thermal conductivity, and air permeability were performed on three Canadian CLT specimens composed of Hem-Fir, Eastern Spruce-Pine-Fir, and Western Spruce-Pine-Fir and one European specimen composed of Spruce.

The hygrothermal properties of CLT, considered in this study, appear to be similar to commonly used wood specimens reported in the literature. However, liquid water absorption coefficients of CLT were found to be generally lower than common wood species, possibly due to the presence of glue between the wood layers which limits the moisture movement across the specimen. On the other hand, the air permeability across the CLT specimens varied due to the glue discontinuity within the specimen which led some CLTs to be permeable, however all the European specimens were found to be impermeable.

This study also critically analyzed the significance of equilibrium moisture content (EMC) of wood at high relative humidity, measured by means of a pressure plate apparatus and humidity chambers, on the moisture management performance of a wood-frame stucco wall, using the

hygrothermal simulation tool hygIRC-2D. The simulation results indicate that the prediction of the moisture response of a wood-frame stucco wall assembly depends significantly on the method adopted to derive the EMC of wood at high RH.

Acknowledgements

This thesis would not have been possible without the support of my supervisors, friends and family who have been there with me until the end.

I would like to thank my research and academic supervisors, Dr. Phalguni Mukhopadhyaya and Dr. Ehab Zalok, for their tremendous support.

Dr. Phalguni Mukhopadhyaya, my supervisor at NRC, was there every step of the way. Without his guidance, time and wise thoughts throughout this study it would have been impossible to complete this task on time. It has been a great journey, Thank You!!!

Dr. Ehab Zalok, my supervisor at Carleton University, offered me this great opportunity. He always provided me with lots of great advice and support to complete this thesis through reviewing and offering suggestions, Thank You!!!

I owe my deepest gratitude for the kind assistances and continuous supports to both of you.

I would like to thank Dr. Jieying Wang from FPInnovations for being involved in reviewing the results in this study, and providing outstanding recommendations.

I would like to thank NRC's Building Envelope and Structures team for their guidance and assistance in performing the experiments, especially Gordon Sherrer. It was a pleasure working with you.

I would like to thank my friends at Carleton University for their support and motivation especially Amin Fereidooni, Adam Walker, Ali Kassim, Anton Matachniouk, Graziela Girardi, Hassan AlMadhoon, James Diak, Omar Abdelalim, Osama Salem and ...

I would like to thank my siblings for cheering me up, especially my sister, Joyce, who has supported me in this mission.

For my parents, Zuhair and Victoria Alsayegh, who have been long waiting for this moment, I would like to thank you for your support, motivation and belief in me. I present this thesis to you.

Thank you all,

George Alsayegh

Table of Contents

List of Figures

List of Tables

Nomenclature

Symbols

A	Area (m^2)
A_w	Absorption Coefficient ($kg/(m^2 \cdot s^{1/2})$)
C	Thermal conductance ($W/(m^2 \cdot K)$)
dx	Thickness (m)
E	Heat flux sensor output (V)
J_a	Air flow rate (m^3/s)
K	Permeance ($kg/m^2 \cdot Pa \cdot s$)
k	Permeability ($kg/m \cdot Pa \cdot s$)
m	Mass of specimen (kg)
Δm	Difference in mass (kg)
MC	Moisture Content represented by mass of moisture per mass of dry material (kg/kg)
p	Pressure (pa)
Δp	Pressure difference (pa)
q	Heat flux(W/m^2)
R	Thermal resistance ($(m^2 \cdot K)/W$)
RH	Relative humidity (%)
T	Temperature (°C)

t Time (s)

WVT Water vapour transport (kg / (m^2·s))

λ Thermal conductivity (W/(m·K))

Subscripts

a Air

d Dry

v Vapour

w Wet

Chapter 1 **Introduction**

1.1 **Introduction**

As time advances, the search for more sustainable solutions is still underway in the construction industry. Innovative building construction materials and assemblies are being developed to help reduce the carbon footprint that the construction industry is presently creating. Cross Laminated Timber (CLT) is considered one of these innovative ideas that will have a future by replacing current conventional methods of constructing buildings made of concrete and steel. CLT is a material composed of large layers of lumber that are stacked perpendicular to each other and glued together to form a large solid panel (FPInnovations 2010). These panels have a higher structural capacity than timber framing and can form walls, floor slabs and roofs. Its high structural capacity is due to the dense use of wood in the panel together with the glue application. Moreover, with appropriate design and construction techniques, CLT can help builders construct large-scale buildings using renewable wood-based materials while still satisfying the objectives of the building code.

In 2010, Canadian researchers from FPInnovations, an organization responsible for wood research, and four Canadian universities initiated an investigation on the potential of using CLT in the construction industry (FPInnovations 2010). Based on the lessons learned from the European construction industry, the large-scale adoption of CLT in the construction industry will potentially increase local and global market demand for Canadian wood, as Canada has the third largest wood resource in the world (FAO 2003). The construction industry will benefit from the tolerance of the building, precision of the material, speed in constructing, flexibility in designing and safety in operation.

A known example of CLT use in construction is the nine-storey Stadthaus building in Hackney, London, UK, which is the tallest mixed-use wood structure to date and is the first building that is built from pre-fabricated CLT panels (TRADA 2009a). The CLT structure, consisting of eight floors, is built on top of a concrete ground floor. Four Austrian crew members worked on the CLT structure, and completed it in 27 working days. The entire building was completed to the client's satisfaction in 49 weeks, compared to an estimated 72 weeks using reinforced concrete. The building met the fire requirements achieving 60 minutes fire resistance using CLT alone, and 90 minutes with the addition of plasterboards. The thermal resistance requirement of (U = 0.13 $W/m^2/K$) was met by the addition of 100 mm of wood fibre insulation to the 128 mm thick CLT walls. In addition, the tolerance of the building was within 5mm, compared to 10 mm with concrete (TRADA 2009b).

1.2 **Rational for the Study**

Hygrothermal properties, such as the transmission and storage of heat, air and moisture, have significant influence on the long-term performance and durability of construction materials and constructed facilities. This is one of the major concerns for designers and builders interested in using CLT based on Canadian wood species. Published literatures, such as Time (1998), Kumaran et al. (2002), Wu (2007) and Glass and Zelinka (2010), provide information on the hygrothermal properties of wood. However, very limited information exists on the hygrothermal properties of CLT or the test methods to be followed to determine its properties in North America.

Equilibrium moisture content (EMC) is one of the critical hygrothermal properties of a construction material. EMC is defined as that "*moisture content at which wood is neither gaining*

nor losing moisture" (Glass and Zelinka 2010). In wood, the moisture content varies with the RH. A controlled environmental chamber is used to determine the EMC of wood at RH levels up to ≈ 95% (ASTM C1699 2009). For RH higher than 95%, it is difficult, if not impossible, to maintain the RH in an environmental chamber at a constant (±1%) RH (Kumaran 2009). Hence, it has been always a challenge to define the EMC of a material at a RH between ≈ 95% and 100% RH. The use of a pressure plate apparatus to determine the EMC at RH greater than 95% is gaining acceptance among researchers and professionals (Kumaran 2009). However, the impact of the EMC obtained from a pressure plate test apparatus on the overall moisture management performance of a whole wall assembly is still unknown, which will be investigated in the succeeding chapters in more details.

1.3 **Research Objectives**

The main objectives of this study were to investigate the hygrothermal properties of CLT composed of Canadian wood species used in building construction compared to CLT composed of European species, and to investigate the significance of an appropriate methodology to determine EMC of wood at high RH on the overall moisture management performance of a wall assembly. More specifically, the objectives were:

Objective 1: To identify suitable methods for the determination of the hygrothermal properties of CLT.

Objective 2: To conduct tests on CLT specimens to determine hygrothermal properties and to perform a critical analysis of tests results.

Objective 3: To identify various possibilities to define EMC curves, especially at high RH (> 95%) for wood-based materials.

Objective 4: To determine the impact of EMC variation in wood-based materials on the moisture management performance of exterior wood-frame stucco wall assembly.

To accomplish the overall objectives of this study both experimental and modeling approaches were used. The research included testing four different CLT specimens for various hygrothermal properties including EMC, water vapour permeability, liquid water absorption, thermal conductivity and air permeability. The test results were validated against the experimental work conducted by other studies such as Time (1998), Wu (2007) and Raji et al. (2009). On the other hand, a parametric study, with different EMC curves (i.e. EMC as a function of RH) of wood material, on a wood-frame stucco wall assembly is conducted to evaluate the impact of EMC variation at high RH on the moisture management performance of the wall assembly. These EMC curves were generated from sorption isotherm and pressure plate experiments.

1.4 **Thesis Structure and Organization**

This thesis is organized into seven chapters. Chapter 1 is an introduction to the context of the research problem and research objectives. Chapter 2 provides a review of CLT: its properties and applications in the construction industry. Chapter 3 reviews details on the hygrothermal properties and the methods to analyse the moisture response of building materials is also provided. Chapter 4 details the overall research methods, including specifications of the CLT specimens investigated and the methods for data analysis. Chapter 5 presents the results and discussion for the experimental work. Chapter 6 discusses the impact of EMC on wood

durability that was determined through modeling. Chapter 7 presents the overall conclusions of this study and recommendations for future work.

Chapter 2 **Background**

This chapter will discuss how CLT became part of the building system and how important it will become in the next few years. A good understanding of the CLT manufacturing process and CLT applications will help to assess the best methods to determine its hygrothermal responses.

2.1 **Cross Laminated Timber (CLT)**

Cross Laminated Timber (CLT) is a solid wood panel composed of wood layers that are laid perpendicular to one another, and glued together. Each layer contains boards that are set adjacent to each other, Figure 2.1. CLT panels can be produced using a variety of wood types and sizes and different gluing agents (TRADA 2009b, FPInnovations 2010, GLTRA 2011). In the early 1990s, a number of companies in Switzerland (Lausanne and Zurich) began manufacturing CLT products using proprietary approaches. This led various academic and industrial research organisations to study the behaviour of CLT products (FPInnovations 2010). In the early 2000s, the construction of CLT panels in Europe, specifically Austria, increased dramatically following an increased focus on sustainable solutions (e.g. green building movement), enhanced efficiencies, building code changes (e.g. Netherlands), and improved marketing and distribution channels (FPInnovations 2010).

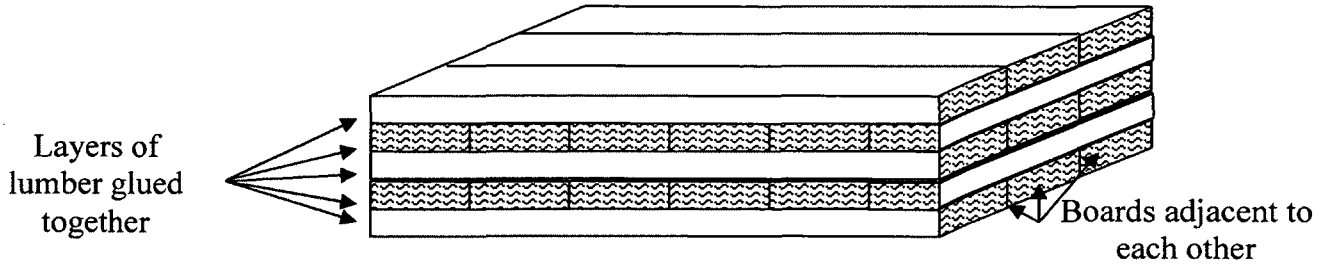

Figure 2.1 Cross laminated timber (CLT) arrangement

In North America, wood studies concerned with dimensional stability suggested cross laminating wood two decades ago, prior to the production of CLT in Europe (Rowell et al. 1981). However, the subject did not receive enough interest from the wood industry to further investigate, as it was believed that preservation of forests was the main concern. New interest in CLT development in North America only started in the last few years. Since 2009, research in this field has included a variety of topics such as evaluation of structural durability, fire and environmental performance of CLT.

The high load-bearing capacity of CLT panels allows engineers to use wood in constructing higher buildings, such as multi-story timber buildings, as opposed to the conventional wood frame method which is limited to four storey buildings in Canada, (FPInnovations 2010). Furthermore, CLT panels have an attractive natural appearance, which enhances its use as a cladding material or internal decoration. The various applications of CLT will increase its market share due to its ease of installation. Figure 2.2 shows CLT panels used in a modern timber housing system. Common CLT applications, some are shown in Figure 2.2, include the following (TRADA 2009b):

a. load and non-load bearing walls,
b. solid partitions,
c. floor and ceiling elements,
d. roof elements,
e. stairs,

- cantilever floors, and
- load bearing lift shafts.

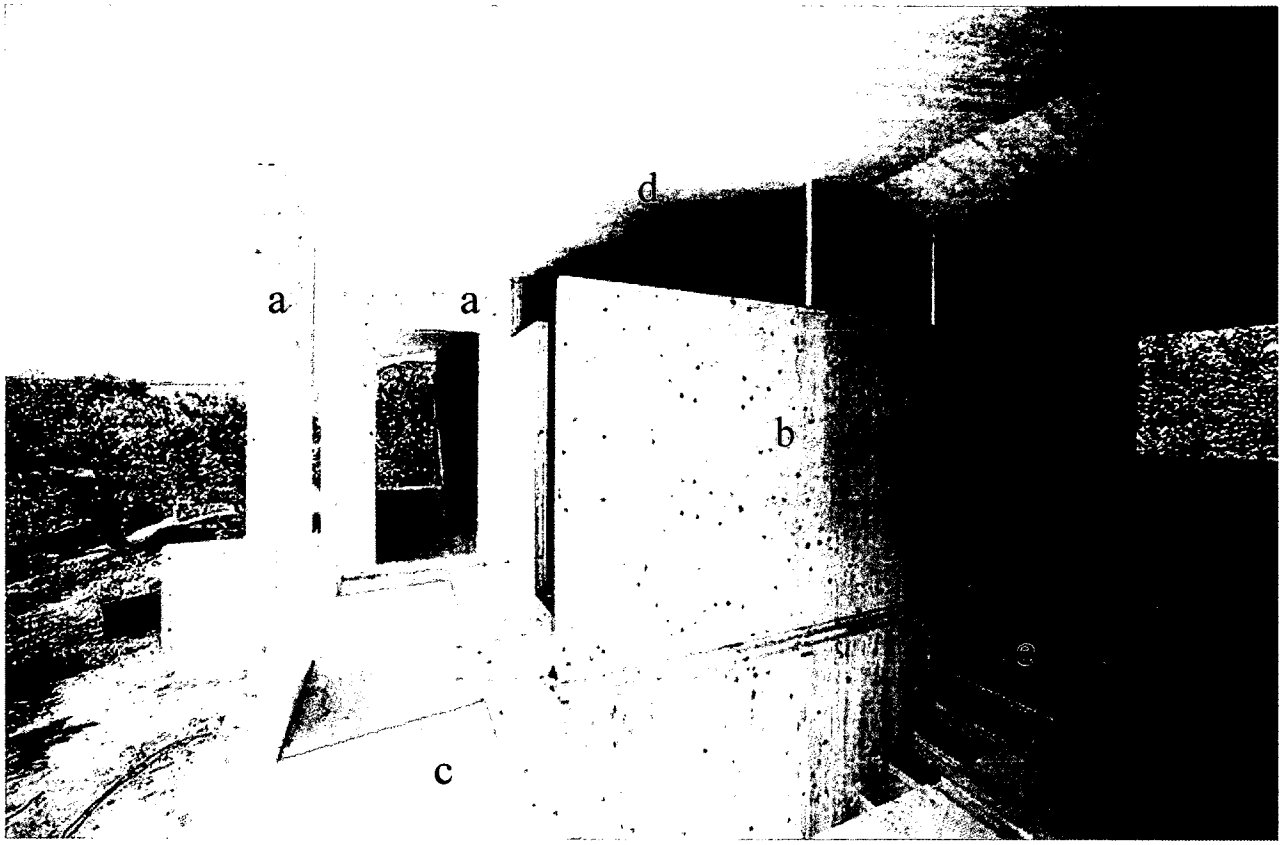

Figure 2.2 CLT panels applications in a modern housing system (KLH 2012)

2.2 Composition of CLT

To manufacture CLT that would conform well with building requirements, both wood and glue should have certain characteristics. According to the Canadian Wood Council's (CWC) wood design manual (CWC 2010), the timber used for construction in Canada is categorized into four different combinations of softwood species:

1- Douglas Fir-Larch, which includes species such as Douglas Fir and Western Larch,

2- Hem-Fir, which includes species such as Pacific Coast Hemlock and Amabilis Fir,

3- Spruce-Pine-Fir (SPF), which includes species such as most Spruce, Jack Pine, Lodge Pole Pine, Balsam Fir and Alpine Fir, and

4- Northern Species, which are Canadian species, graded in accordance with National Lumber Grades Authority rules.

The performance of a CLT panel is based on the performance of the wood layers within the panel. The four different combinations of softwood species mentioned above could be used in manufacturing CLT panels. However, there is no code that specifies which type of timber species should be used in the CLT products. Therefore, it is essential to identify the best combination of softwood species to use in CLT. In Europe, the most common species used for manufacturing CLT panels are Spruce and Douglas Fir; however, Pine and Larch may also be used (GLTRA 2011).

The last major component is the gluing agent. In Europe, the layers making up CLT are glued together using one of two common types of adhesives: Polyurethane Reactive (PUR) and Melamine Urea Formaldehyde (MUF). The adhesive is applied in layers of 0.1 mm to 0.3 mm thick (GLTRA 2011), which accounts for less than 1% of the total mass of the CLT structure. PUR and MUF are advantageous gluing agents due to their rapid curing time, transparency at the joints and resistance to fire. In Canada, a variety of gluing agents are available, however the appropriate glue is the one which can adapt to the Canadian climate and resist the applicable loads. The wood handbook (Frihart and Hunt 2010) refers to various glues for wood based products that can be used in North America; however, there is no reference to the type of glue that has to be utilized for CLT; hence, it is expected that the glue used in similar product, such as "Glue Laminated Timber", would be a good option for CLT.

2.3 CLT Design

The design of a CLT panel has two different dimensional considerations: micro-dimensions and macro-dimensions. For the micro-dimensions, the thicknesses and layer arrangement of the panels are considered along with the overall length of the panel. The loading resistance is considered in choosing the length and the structural thickness of the CLT panel, whereas the architectural features and different protection features are considered in the design of the non-structural outer layers. Further details on the design of CLT panels are discussed in Section 2.5.1. For the macro-dimensions, the overall dimensions of the CLT units are considered for the final assembly design. The dimensions of the panels are limited by the manufacturer's capacity, and certain design factors. Factories can manufacture panels with an optimal thickness of up to 300 mm. The length and the width of the panels are different in every project; however, they are limited by the factory capacity as well as the logistical factors such as transportation, handling and storage limitations. Most truck trailers can only accommodate 2.95 m widths and 20 m lengths. Although manufacturers can produce panels up to 4.8 m wide and 60 m long (GLTRA 2011), transportation arrangements need to be in place to handle the oversized load.

2.4 Constructing CLT Structures

After designing CLT panel, prefabrication takes place at a factory prior to being transported and erected at the building site. This strategy has been used by many builders to simplify construction and reduce manpower. Prefabrication is used for other construction elements such as precast concrete elements (slabs, walls and columns), service elements (mechanical, electrical and plumbing connections), and bathroom pods (residential fully fitted bathrooms). The prefabrication strategy was recommended by top construction experts in the UK, including Sir

John Egan (TRADA 2009b). Manufacturing CLT can also be an application for low-grade wood, which are small in dimension and low in quality (FPInnovations 2010). The low-grade wood could be used in the less functional layers of the CLT panel, usually the middle layer in which this area resists the least load during bending. Besides the outer layer of the CLT, there could be an additional layer made up of other materials derived from other timber products to enhance the panel's architectural look (GLTRA 2011).

Manufacturing prefabricated units reduces manpower since the processes can be automated. The repetitive and non-critical actions, normally performed by a person, are generally performed by automated machines. As a result, the overall cost of a project is more dependent on the material and manufacturing costs rather than labour costs.

Since CLT panels are prefabricated, the system is precise with a faster and safer construction process than a conventional one. Prefabrication can also influence planning ideas, such as the design of the building and its assembly procedures, and reduce several of the unknowns and deficiencies within the design. The safety of a project can also be better managed through the use of prefabrication, since most of the work for a building is performed at the factory, in a controlled environment. Once on-site, the CLT panels are erected and tightened into place using light-weight equipment. This requires considerably less time than conventional construction methods, therefore the potential for lost hours, due to circumstances such as harsh weather or severe site conditions, is minimised.

Although these advantages make prefabrication attractive, it has certain limitations such as increased technical work, transportation care and storage care. Prefabrication requires more professional and technical work than practical work. Careful planning is also required to avoid

transportation and storage issues. Once production has begun, changes to the design can mean higher costs since most prefabricated units complement one another, therefore changes to the design can impact the final product. Transportation of large prefabricated CLT panels (20 m by 2.95 m) may also require special arrangements since not all roads can accommodate heavy or oversized trucks. In addition, once on-site the units must be handled with care and properly stored to avoid damage due to accidents or adverse weather conditions. Minimising the potential for problems which could arise during CLT construction requires a high degree of engineering, both upfront and throughout the entire construction process.

Manufacturing CLT panels involves a number of different processes, from conditioning the timber boards to the delivery of the panels to the CLT assembler (GLTRA 2011). The following steps, as illustrated in Figure 2.3, are used in the manufacturing of CLT panels at the factory, prior to being transported to a construction site:

1. The softwood boards are dried to moisture content (MC) of 10 ±2% to reach their serviceable MC (GLTRA 2011).
2. The boards undergo visual or mechanical grading to determine their strength. Normal strength timber is used for the outer layers, and defective and knotted parts of the boards are removed if necessary.
3. In the event that the boards do not satisfy the required length or width of the panel, they are finger-jointed with other boards to increase their length or width.
4. Once a wood layer has been prepared for assembly, adhesive is applied in a layer (0.1 to 0.3 mm thick, not exceeding 1% of the total mass) and then another wood layer is placed perpendicular to the previous layer. The layer arrangement, thicknesses, and type of material are based on the particular design requirements.

5. After all of the layers are in place, pressure is applied using a hydraulic press. However, depending on the panel thickness and the kind of adhesive used during the gluing process, vacuum and clamping presses can also be used.
6. After the glue has cured, the panels are planed or sanded for a smooth surface and then transported to the CLT assembler, where the panels are adjusted to the customers' requirements for fitting with other components. Computer numeric control (CNC) plasma cutting or blade cutting is used to adjust the panel for the fittings.

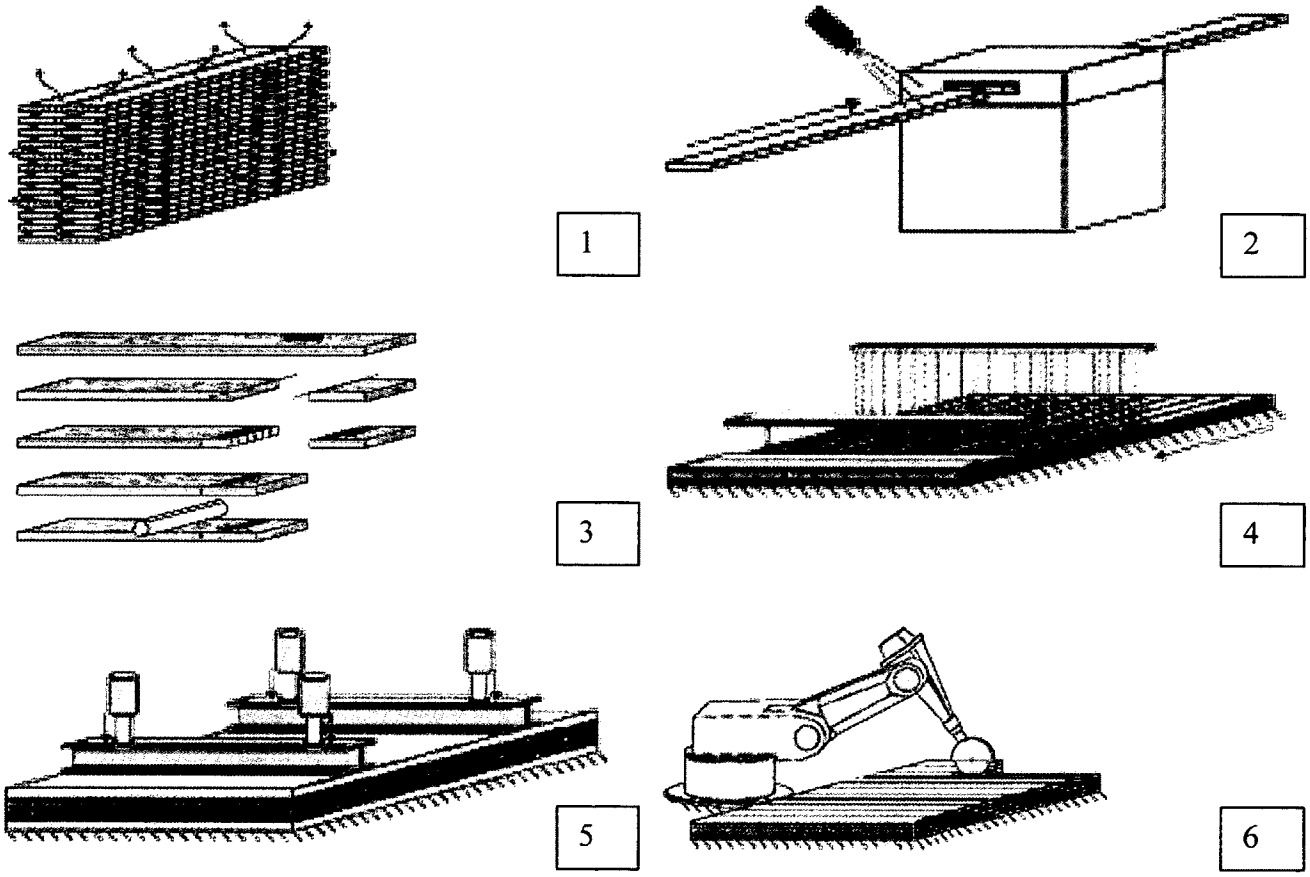

Figure 2.3 Manufacturing process for CLT (GLTRA 2011). Note: numbering refers to steps mentioned above.

2.5 CLT Performance

2.5.1 Structural Performance

The structural analysis of the CLT and its design specifications are not yet incorporated in the Canadian Building Code and the wood design standard (CSA-O86-09 2009); however, the available wood design code (CSA-O86-09 2009) for plain wood can be followed as a guide in designing CLT based structures:

Due to the fact that the resistance provided by the boards which are laid perpendicular to the direction of the normal stress is negligible, it is assumed that the stress distribution over the cross section only exists in the layers parallel to the normal stress. Hence the applied loads are resisted by the board layers parallel to the span in case of horizontal assembly and parallel to the height in case of vertical assembly. Based on the cross section of the resisting layers and their grade, the overall resistance of the CLT member under bending and normal forces can be estimated (CWC 2010). Figure 2.4 illustrates how the stress would appear in case of normal (n) and bending forces (m) assuming the wood boards in the CLT have similar grade. In case of a normal force, the stresses (σ) in the wood layers resisting the force are uniform across the board layers parallel to the normal force. In case of bending moment, the stress at the neutral axis is zero and will vary linearly to the maximum stress value at the farthest distance from the neutral axis (d/2). Similarly, the wood grading and loading factors can be determined based on the wood details stipulated in the Canadian wood design code (CSA-O86-09 2009).

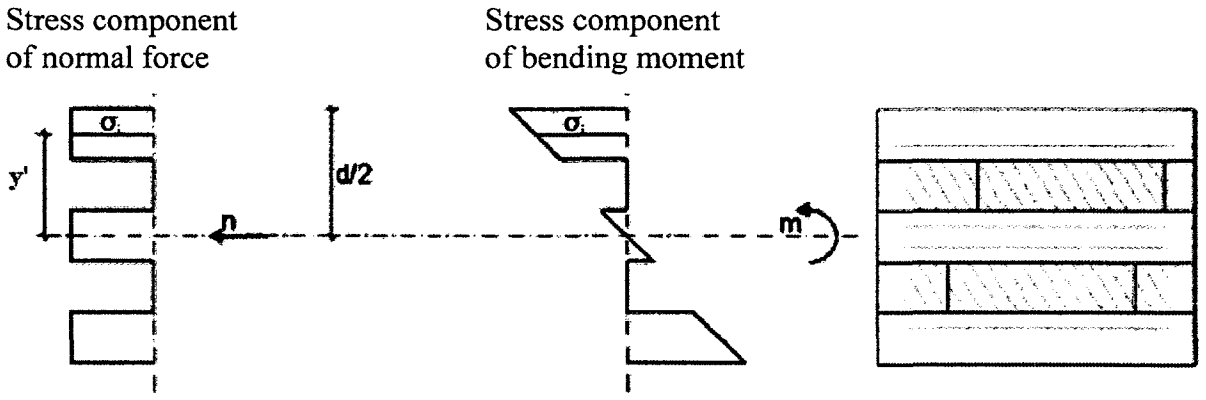

Figure 2.4 Load profile on CLT (modified) (GLTRA 2011)

2.5.2 **Durability Performance**

CLT durability depends on the moisture management performance of the wood. In Europe, wood is not recommended to be exposed to moisture so its moisture content does not exceed 20% (TRADA 2009b), and the same applies in Canada (Baker 1969). The exposure of wood to moisture can promote its decay. It allows fungus and biological elements to grow on the wood. These biological elements use wood as a substrate and cause decay, which results in a loss of wood structural strength and hygiene (Baker 1969).

The moisture movement happens within the cells of the wood. These cells, which are mainly longitudinal, are called tracheids. These tracheids are reproduced in layers radial to the tree circumference and are connected to each other by pits along the tangential direction. It is worth mentioning that pits are a pair of complementary gaps in the secondary walls of adjacent cells and are capable to transferring moisture between the cells in the tangential direction. Other than trachieds, there are other longitudinal cells that help moisture to travel through wood in the longitudinal direction such as resin canal and parenchyma cells that are found in certain softwoods.

On the other hand moisture can also travel in the radial direction, e.g. Rays which are cells in the radial direction, transfer the water and nutrients horizontally to the cambium layer (Bowyer et al. 2007). The moisture movement in pits, rays and other cells in the radial and tangential directions are limited compared to moisture movement in the longitudinal direction (Siau 1995). These directions and further illustration of the wood anatomy is illustrated in Figure 2.5.

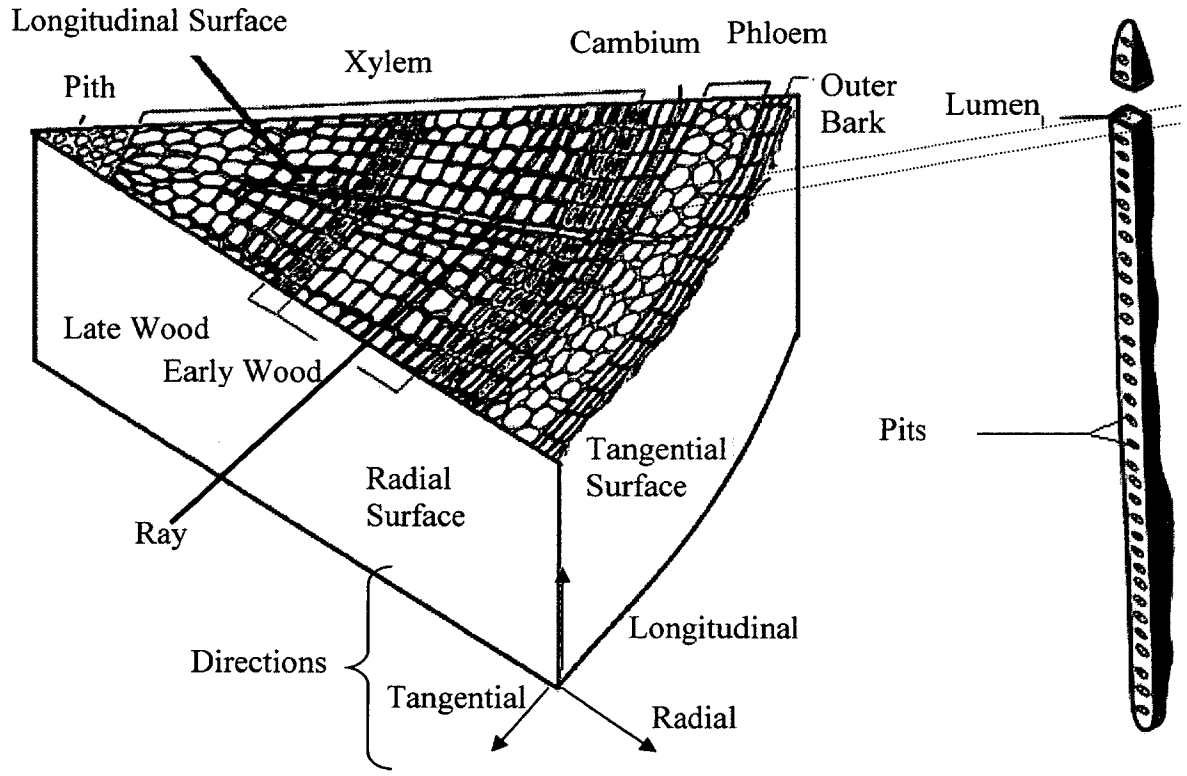

Figure 2.5 Schematic of cells in wood (adopted from Siau 1995)

Wood is greatly influenced by its moisture content (MC). Wood expands and shrinks as the MC increases and decreases respectively. Due to the fact that wood is an anisotropic material, increase or decrease in the MC of wood results in different amount of deformation in different directions: radial, tangential and longitudinal. This phenomenon is illustrated in Figure 2.6 in

more details. Glass and Zelinka (2010) reported that the deformation in the radial direction is approximately twice as much as in tangential direction; however, as shown in Figure 2.6, the deformation in the longitudinal direction is slight compared to other directions. This behavior of wood is a crucial fact to be considered during preparation of timber for construction. After a tree is cut, the EMC of the wood decreases during the drying process. This change in MC results in the different amount of shrinkage of wood in different directions, as shown Figure 2.7. To minimise this deformation, especially during serviceability, wood is dried to a MC based on the service location and the intended use (Bergman 2010). Common methods of drying wood include air drying and kiln drying. For building construction purposes in Canada, wood is dried to an average MC of 12% (CWC 2010).

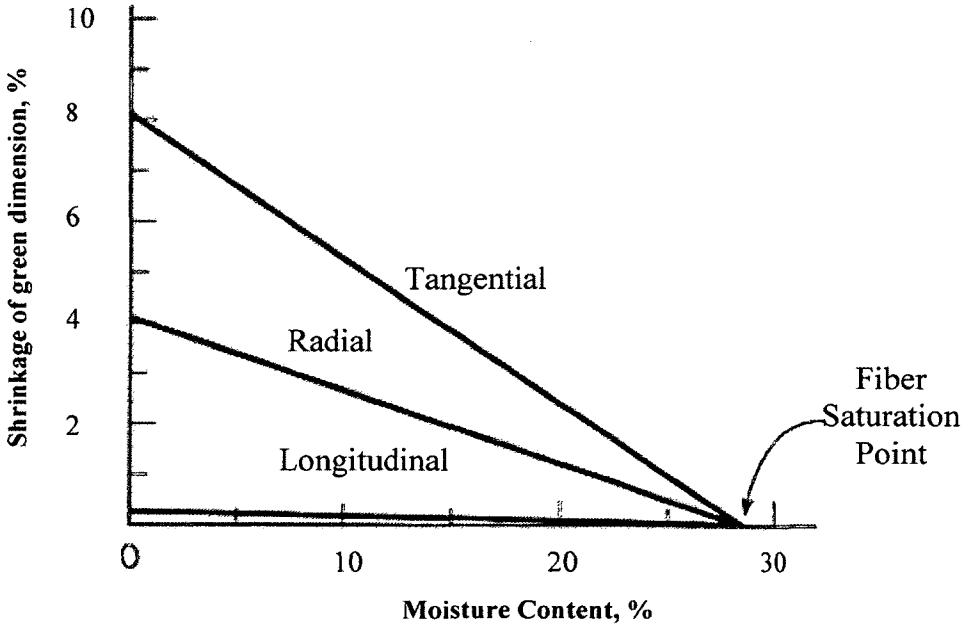

Figure 2.6 Shrinkage of wood in each direction (Mamlouk and Zaniewski 1999)

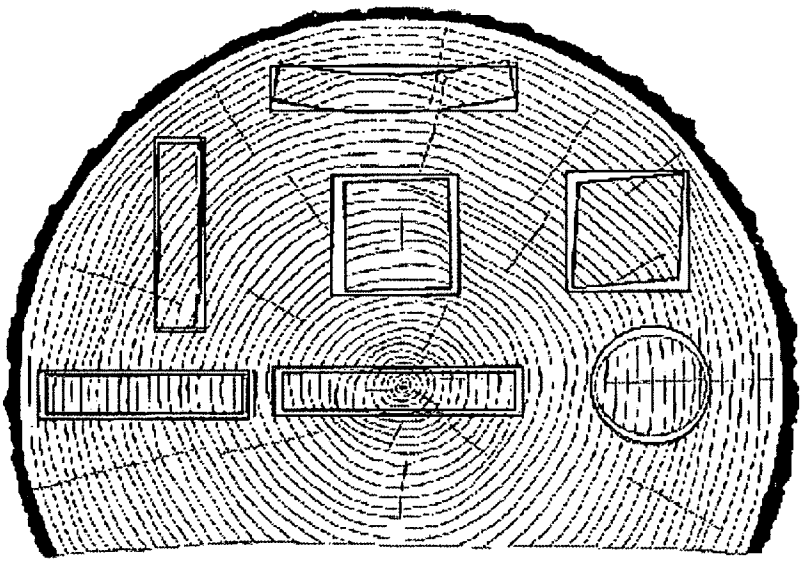

Figure 2.7 Wood shrinkage (Glass and Zelinka 2010)

2.5.3 **Fire Performance**

Fire protection is essential to reduce the potential of harm of life as a result of fire in buildings (CWC 2000). This can be done by minimizing the risk of harm to people from fire. As CLT is a solid structure made of wood, it is prone to burn as it is a combustible material; when wood burns, a char layer forms and slows the burning of the wood inside. The process of char forming after wood burn is called "charring" and the rate of this process happening is defined differently in every region. For example, wood in Europe has a charring rate of 0.65 mm/min as specified by European Timber Design Code (EN-1995-1-2), however in Canada the rate is 0.6 mm/min as proposed by Lie (1977), therefore this rate also applies to CLT. According to Schaffer (1967), the charring rate of wood is influenced by density, thermal conductivity, moisture content and permeability. Wood resistance to fire is a function of the thickness of the member, and the severity of fire exposure. Increasing the thickness of the CLT layers or adding additional layers can help enhance the fire performance of the CLT structure. This is because thicker cross-

sections will require longer time to char. Furthermore, adding gypsum board on the exposed surface of the wood will increase the fire resistance of the CLT member by 30 minutes using regular gypsum board, based on analysing the fire and sound resistance of walls in Canadian National Building Code A-9.10.3.1.

Chapter 3 **Literature Review**

As discussed earlier, a proper understanding of the manufacturing process and application of cross laminated timber (CLT) will help to assess the best methods to determine its hygrothermal response. Thereafter, attention must turn to the deterioration mechanisms in wood due to heat, air, and moisture (HAM) transport phenomena, which affect wood and other wood-based materials that are similar to CLT. Finally, the methods to analyze the hygrothermal response of building envelopes will also be discussed.

3.1 **Heat Air and Moisture Transport**

The main principle of building durability is that "*buildings should be suited to their environment (and) laws of physics must be followed*" (Lstiburek 1999). The durability of a building is affected by environmental factors such as rain, temperature, humidity and interior climate, which can lead to rot, decay and corrosion. The hygrothermal properties of a material are used to describe the material responses to such changing environmental conditions. Building physicists refer to hygrothermal properties as "*heat, air, and moisture transport*" (Kumaran 2001). A building is considered durable when its materials are prepared to respond efficiently to these environmental loads by not deteriorating.

Heat-air-moisture (HAM) transport mechanisms within a material affect the moisture management and long-term performance of the material. Understanding HAM transfer in a building can help estimate the favourable conditions for the development and movement of biological elements, as well as the decay of the material. This can also help to determine preventative measures to control the response of a material to HAM transport and their effect on durability.

3.2 Wood Deterioration

Wood deterioration is the result of wood degrading organisms, such as termites and fungi. The development of these wood degrading organisms depends on three environmental factors: moisture content (MC), oxygen supply, and temperature (Lebow and White 2007). Baker (1969), Scheffer (1973), Carll and Highley. (1999) and Morrell (2002) all agree that "*...most fungi require wood at moisture levels above the fibre saturation point, but once they colonize the substrate, they can continue to grow at MCs as low as 20%*". According to Glass and Zelinka (2010), Fibre saturation point is point within the moisture content range at which only the cell walls are completely saturated as bound water while no water exists in cell lumina. The presence of fungi can threaten the long-term structural strength of a building, and can pose a health risk to the occupants.

Infections can enter lumber at different stages, such as in the forest, in the storage area, during drying, at the building site or during operation (Hukka and Viitanen 1999). CLT is most vulnerable to biological elements during transportation and storage, prior to being erected on site. Manufacturers should protect the material from any infection, such as that caused by moisture exposure that can affect the quality of the product. However, the protection should also continue during the life of the structure, which is why building scientists and designers are concerned with the HAM transfer within buildings.

3.3 Hygrothermal Analysis

The presence of water on wooden structures at certain temperatures increases the likelihood of fungus growth. A hygrothermal analysis helps predict HAM movement and storage within the wall assemblies. Different analytical tools are available to perform this task manually, including

the Dew Point method, the Glaser Diagram and the Kieper Diagram (Mukhopadhyaya et al. 2006). These tools and other computer-based models use the hygrothermal properties of a material to predict its hygrothermal responses to HAM, which are all aspects of hygrothermal phenomena. Every material, whether used alone or combined with other materials, has its own hygrothermal performance. The performance of these materials can be calculated from the properties of each material, which are derived using standard test methods. These standard test methods, that reflect the acceptance of various scientists and researchers and help academic and commercial organisations eliminate erroneous results, have been created by various organisations, though predominantly by the American Society for Testing and Materials (ASTM) and International Organisation for Standardization (ISO). The hygrothermal properties of a material used in modeling tools, as well as various other testing methods, are discussed next.

3.4 Moisture Storage

Moisture storage in material is measured by determining the equilibrium moisture content (EMC). Determining the moisture storage of wood for varying relative humidity (RH) is critical since certain moisture levels will activate the fungus and other biological elements causing decay. The moisture content (MC), which represents the moisture storage, is expressed as the weight of water in the material per dry weight of the dry material, as shown in Equation 3.1.

$$MC = \frac{m - m_d}{m_d} \times 100\% \qquad \text{Equation 3.1}$$

Where, MC is moisture content (kg/kg), m is the mass of the moist material (kg), and m_d is the mass of the dry material (kg). On the other hand, EMC is calculated by measuring the moisture content at steady state for various RH.

The MC of a material is affected by changes in RH and temperature (Siau 1995, Kumaran 2009, Glass and Zelinka 2010). The EMC of material is determined through a process known as sorption, which is classified as either adsorption or desorption (Siau 1995, ASTM C1498 2004). Adsorption occurs when moisture is added or absorbed in the material until the steady state is reached, while desorption is when the material releases the moisture to the atmosphere and reaches steady state. The EMC of wood is usually higher in desorption than in adsorption. This phenomenon is known as hysteresis, and it initiates when the wood desorption causes the cellulose chain in wood to bond when loosing water (Siau 1995). During adsorption, these bonds between the chains, that will not break until fiber saturation and the compressive stress on wood will lower the EMC. The ratio of desorption to adsorption is estimated to be 1:0.85 at an RH of from 80% to 90% (Skaar 1972).

Moisture storage in wood can be classified in two groups: bound or hygroscopic water and free or capillary water (Siau 1995). The EMC of building material can be measured using sorption isotherm (ASTM C1498 2004), except it is limited up to 95% RH (ASTM C1699 (2009). According to Kumaran (2009), moisture storage occurs in two different ranges. As shown in Figure 3.1, The first is a hygroscopic range, which starts from 0% RH to a RH at which the moisture in the material will start condensing. In this range, the material absorbs and releases moisture from the environment as vapour and so the moisture exists in wood as hygroscopic water within the pores of the material. The second range is from the condensation point to 100% RH in which the material moisture content increases dramatically. It would be worth noting that the hygroscopic range varies between materials as it could range up to 98% RH (Kumaran 1996). As condensation occurs, the moisture increases dramatically to saturate the material with water to reach maximum moisture content (Kumaran 2009) and eventually water will exist in wood as

capillary water and hygroscopic water (Siau 1995). As shown in Figure 3.1, this level of saturation is also referred to as full saturation and it is not similar to fiber saturation. According to the Tiemann (1906), the fibre saturation point is defined as "*the moisture content corresponding to the saturation of the cell wall with no capillary water in the voids*" (Siau 1995). Saturation of the cell walls is calculated based on an extrapolation of the first hygroscopic range to get the EMC at 95% to 100% (Siau 1995). The moisture storage properties of a material are determined using two different methods: sorption method (ASTM C1498 2004) and pressure plate apparatus method (ASTM C1699 2009). Both methods will be discussed next.

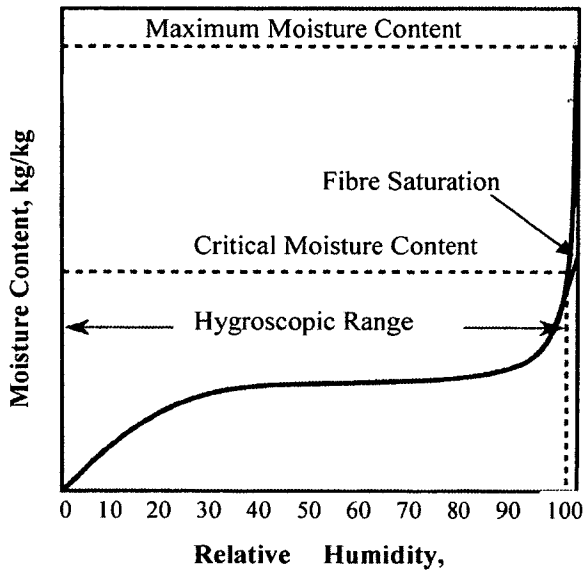

Figure 3.1 Sorption Isotherm of material (extracted from Kumaran 1996)

3.4.1 **Hygroscopic Sorption Isotherm**

Sorption isotherm is the relationship between EMC of the material and RH of the environment at a specific temperature (ASTM C1498 2004). As Straube and Burnett (2005) found it difficult to control and measure wood at high RH once it is above 95%, the hygroscopic range can be

considered to be around 0% RH to 95% RH, which till moisture condenses. At hygroscopic range, moisture in ambient air is considered water vapour. EMC within this range can be determined by sorption isotherm, which in turn is the average of adsorption measurements and desorption measurement. Sorption, adsorption and desorption can be mathematically modeled using equation 3.2, which is derived by Hailwood and Horrobin (1946).

$$MC = \frac{RH}{A+B\cdot RH-C\cdot RH^2} \qquad \text{Equation 3.2}$$

Where, MC is the moisture content (%), RH is the relative humidity (%/100) and A, B, and C are constants depending on the model used.

Hailwood and Horrobin's (1946) equation, shown as Equation 3.2, was one of the first equations capable of modeling sorption curves. Most of the mathematical models, such as Dent (Dent 1977) and the GAB (Saidani-Scott 1993), are derived from Hailwood and Horrobin's equation (Time 1998).

Test methods such as the chamber method and DVS1000 are used to determine the EMC of a material. The chamber method, as discussed in ASTM 1498 (2010), uses temperature and humidity controlled chambers. The chamber's humidity can be controlled either through a humidifier or saturated salts that adjusts the RH. The humidity chambers control the humidity using a mechanical method while saturated salts control humidity chemically depending on the used type of saturated salts. After measuring the dry weight of the samples, the set is placed in multiple chambers; each chamber contains a specific RH value. To account for adsorption, the specimens are placed in the chambers starting with the lowest RH and then measured for equilibrium weight before moving the sample to a chamber with a higher RH. Conversely,

saturated samples are tested for desorption by decreasing the RH in the chambers followed by measurement of their equilibrium weights. After measuring the equilibrium weight of the specimens, the results are substituted into equation 3.1 to determine the EMC during desorption and adsorption.

There are various other methods for determining the EMC of material in the hygroscopic range such as the DVS1000 that was used by Burke et al. (2008). The DVS1000 is a complete instrument that tests material for sorption at isothermal and non-isothermal conditions. A first run starts by measuring the sorption at isothermal condition by weighing at real time. In each run, the specimens are exposed to different RH, as each run ends when the material reaches steady state. The change in the RH is applied by changing saturated salts that can expose material to different RH. The non-isothermal measurement is calculated using the isothermal measurements at various temperatures. During the isothermal sorption test at 40°C by Burke et al. (2008), the condensation on the material hindered the results at high RH of 92% causing the experiment to halt. Burk et al. (2008) reported to have accurate results but faced some problems during the tests.

Various researchers have determined the sorption properties of wood (Tveit 1966, Ahlgren 1972, Absentz 1993, Time 1998 and Raji et al. 2009). These properties will be used to relate the sorption of CLT to that of wood. The data from their research are presented using the Hailwood and Horrobin model in Table 3.1 and plotted in Figure 3.2. The uncertainties of these models have been represented by the sum of square of residual, S_r, which is calculated using the following equation.

$$S_r = \sum_{i=1}^{n}(MC_i - MC_{HH})^2 \qquad \text{Equation 3.3}$$

Where MC_i is the measured value of the moisture content at a certain RH, MC_{HH} is the corresponding value using the Hailwood and Horrobin model, and n is the number of measure values.

Table 3.1: Parameters based on Hailwood and Horrobin model to determine the curves

	Method	Temp (°C)	*A*	*B*	*C*	S_r/n
Tviet (1966)	Sorption	25	1.047315	0.130558	0.001079	0.285
Ahlgren (1972)	Adsorption	20	1.388877	0.138648	0.001194	1.080
Absetz (1993)	Adsorption	20	3.380826	0.116223	0.001060	0.046
Time (1998)	Adsorption	26	0.584371	0.156113	0.001151	0.780
Raji et al. (2009)	Adsorption	20	0.014695	0.116358	0.095120	*
Wood Handbook (Glass and Zelinka 2010)	Sorption	22	-	-	-	

Note: Raji et al. (2009) results were converted from GAB model to Hailwood and Horrobin model (Appendix A). Sr/n is the sum of squares of residuals divided by the number of measuring points. * Raji et al.(2009) reported a standard deviation between data points and GAB model to be less than 2.2%.

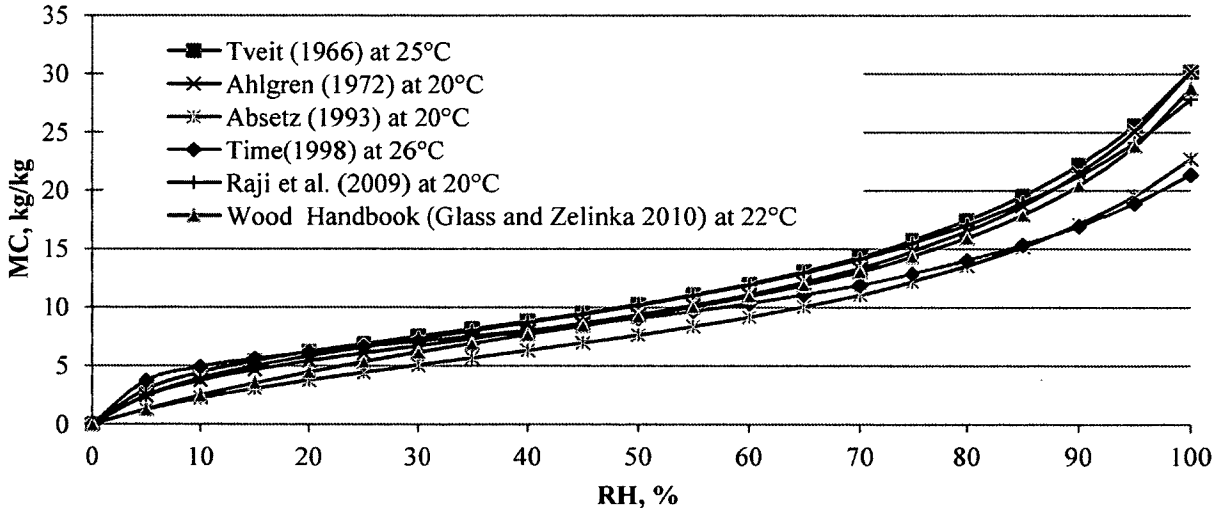

Figure 3.2 Adsorption values for wood

Tveit (1966) researched the sorption properties of spruce using 14 different combinations of temperature and RH, ranging from 5 to 45 °C and 10 to 97% RH (Time 1998). The specimens were cylindrical, 80 mm in diameter and 13 mm in thickness. Specimens were equilibrated to 75 % RH, and then measurements were taken at 55 %, 35 %, 12 % (for desorption) and 95 % RH (for adsorption).

Ahlgren (1972) tested the adsorption of various building materials, including spruce. Two to three specimens were used, but the dimensions of the specimens were not discussed. The measurements were performed using a 'two pressure apparatus'.

Absetz (1993) performed sorption studies comparing the sapwood and heart wood of spruce and pine (Time 1998). Although there were no differences in the EMC of the sapwood and heart wood for spruce, there were significant differences for pine. The results for spruce during adsorption are presented in Table 3.1.

Time (1998) also researched sorption for spruce and pine, and reported the differences in the results obtained from previous research by Absetz (1993), Ahlgren (1972), and Tveit (1966). He experimented the adsorption of spruce at 26 °C. The results are plotted in Figure 3.2.

The Wood Handbook, published by the U.S. Department of Agriculture (Glass and Zelinka 2010), reported general EMC models for wood. Simpson (1973) showed that the models were a good fit to EMC, RH and temperature data. The model presented in Figure 3.2 was generated based on the sorption model at 22°C, which is an average of adsorption and desorption. The Forest Products Laboratory in the U.S. Department of Agriculture specifies the generic model, presented as Equation 3.4, to determine the sorption of wood at various temperatures (Glass and Zelinka 2010):

$$MC = \frac{1800}{W}\left[\frac{K(RH)}{1-K(RH)} + \frac{K_1K(RH)+2K_1K_2K^2(RH)^2}{1+K_1K(RH)+K_1K_2K^2(RH)^2}\right] \quad \text{Equation 3.4}$$

$$W = 349 + 1.29T + 0.0135T^2$$
$$K = 0.805 + 0.000736T - 0.00000273T^2$$
$$K_1 = 6.27 - 0.00938T - 0.000303T^2$$
$$K_2 = 1.91 + 0.0407T - 0.000293T^2$$

Where, RH is relative humidity (%/100), MC is moisture content (%) and T is the temperature in (°C).

Finally, Raji et al. (2009) published work on advanced systems in wood construction, known as 'Stacked Laminated Solid Wood Planks'. These systems are composed of one layer of adhesive, applied along the height of the wall, as shown in Figure 3.3. The experiment tested solid pine glued together with an adhesive seal. The sorption of the wall was measured, and the results were published using the GAB model. More information on the conversion of the variables in the models is provided in Appendix A.

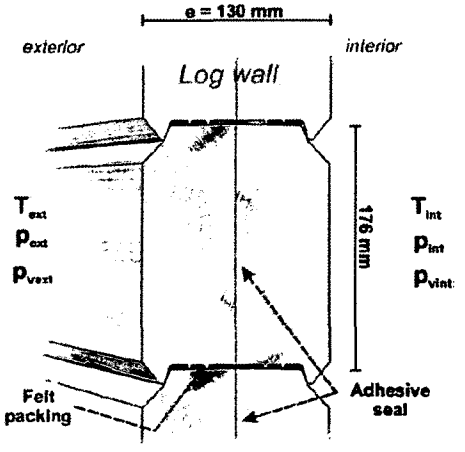

Figure 3.3 Stacked laminated solid-wood planks (Raji et al. 2009)

3.4.2 EMC at High RH

At a high RH of greater than 95%, the moisture in wood is composed of capillary water and hygroscopic water, which cannot be extrapolated from sorption measurements as it measures the hygroscopic water and does not measure the capillary water. It is experimentally impossible to differentiate capillary water and hygroscopic water, especially since they both overlap during measuring (Saiu 1995). Moreover, full saturation and fibre saturation are two different concepts for moisture presence in wood. Full saturation, or maximum MC, is the EMC of wood fully submerged in liquid water and does not reflect the extrapolated EMC at the fibre saturation point. Figure 3.1 shows the difference between these two ranges which show how MC at hygroscopic range increases with RH in steady way. When the moisture starts condensing on the material, the MC in the material will increase dramatically. It is experimentally impossible to measure EMC of wood at high RH using sorption due to condensation which occurs in the chamber at high humidity. To determine the EMC of wood at high RH, an alternative testing method is required, such as the pressure plate apparatus test (Kumaran 2009). This test, identified as ASTM C1699 (2009), is used to determine the EMC of a material for levels between 95% and 100% RH. For this method, the pressure is adjusted to match the RH in the pressure plate to the atmospheric RH level. Pressure plate apparatus experiments with RH lower than 96% require very high pressure, and therefore require extra effort to extract results.

Wang et al. (2011) have expressed concern over the relationship between MC and RH, specifically near saturation. Various studies have produced different results for the EMC of wood at 100% RH. Traditional sorption experiments require saturated salts or water to reflect 100% RH. The EMC of wood at 100% RH is about 0.3 kg/kg (Almeida and Hernandez 2006, Thygesen and Elder 2009, Glass and Zelika 2010). However, this MC is based on an extrapolation since it

is "*difficult to precisely control and measure a high RH once it is above 95%*" (Wang et al. 2011, Straube and Burnett 2005).

The pressure plate apparatus has been used by various researchers for sorption measurements and they all reported different results (Cloutier and Fortin 1991, 1993, Almeida and Hernandez 2006, Thygesen et al. 2010 and Mukhopadhyaya et al. 2011). Cloutier and Fortin (1991) determined the sorption for yellow birch (hardwood) using pressure plate apparatus for near-saturation RH and traditional sorption at low RH. The results from the tests show a reasonable overlap for EMC from 0 kg / kg to 1.18 kg / kg, as shown in Figure 3.4 published by Almeida and Hernandez (2006). Thygesen et al. (2010) used a pressure plate apparatus to measure sorption at low RH. The results did not show any significant discontinuities in the EMC measurements; however, there was no dramatic increase in EMC at high RH up to 99.5% (Wang et al. 2011). The maximum MC Thygesen et al. (2010) reached was 0.4 kg / kg. The results "*indicated that lower degrees of pit aspiration (pit closure) lead to high amounts of capillary moisture in wood*" (Wang et al. 2011, Thygesen et al 2010, Engelund et al. 2010). Experiments by Mukhopadhyaya et al. (2011) tested red pine for sorption using ASTM C1498 (2004) and for pressure plate using ASTM C1699 (2009). Both Mukhopadhyaya's experiments were conducted at NRC-IRC's laboratories. The MC data obtained by Mukhopadhyaya et al (2011) and Almeida and Hernandez (2006) for sorption test and pressure plate test is presented in Figure 3.4. As noticed in the figure, the EMC of yellow birch differs at high RH.

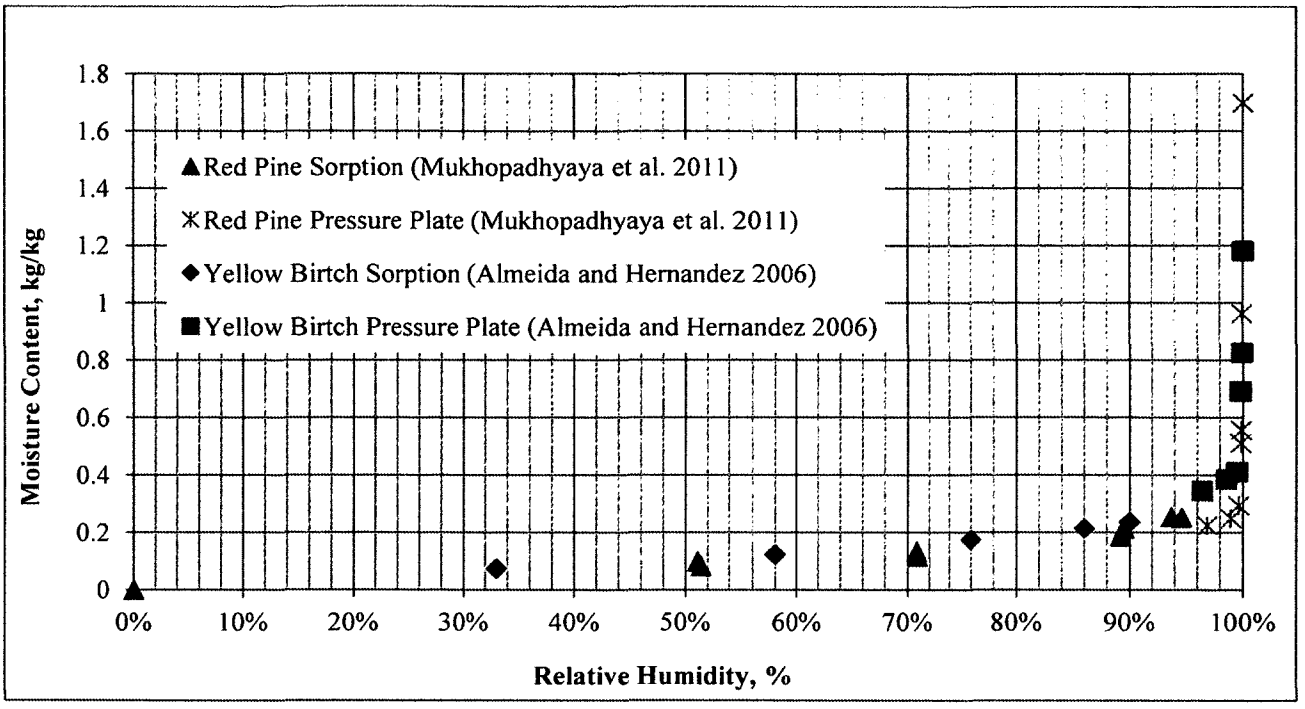

Figure 3.4 Sorption and pressure plate for red pine by Mukhopadhyaya et al. (2011) and for Yellow Birch by Almeida and Hernandez (2006)

3.5 **Moisture Transmission**

Moisture movement through a material is classified into three different stages (ISO 15148 2002). The first stage considers moisture transmission in pure water vapour form, when exposed to low RH ranges. At this stage, the Dry cup method is commonly used to measure the water vapour movement, as will be discussed later in this section. At higher RH of up to 95%, the second stage considers moisture transmission, in form of water vapour, through the moist material in which the material contains capillary water. During the previous two stages, the permeability of the specimen increases with an increase in moisture flow (ISO 15148 2002). At a RH above 95%, movement of moisture through the specimen is affected by condensation; therefore the third stage of moisture movement is governed by the liquid water transport through the specimen. The

first two stages cover the movement of moisture for a RH of up to 95 %, and can be classified as water vapour transmission. At a RH above 95%, the moisture movement is classified as liquid water transport (ISO 15148 2002).

Wood is an anisotropic and heterogeneous substance; as a result moisture movement in wood depends on the area of exposure. In particular, moisture travels faster in the wood's longitudinal direction than the tangential and radial direction; therefore moisture transmission in a building material is reflected by the orientation at which the material is installed. Wood framing and CLT are exposed to the atmosphere and other materials in their radial and tangential directions, therefore moisture transport experiments on wood specimens are performed in those directions (Siau 1995). In case the longitudinal direction is exposed to moisture, it is always protected due to its fast moisture absorption.

3.5.1 **Water Vapour Transmission**

Water Vapour Transmission (WVT) is calculated by determining the rate of moisture movement, in vapour form, through the material. The rate is dependent on the average RH surrounding the material and the area of exposure. Gravimetric methods, such as cup methods, are commonly used to determine the WVT through a material. ISO 12572 (2001) uses the cup methods to determine the moisture movement across the specimen. These methods require the material to seal a cup which contains saturated salts representing different RH, desiccant as shown in Figure 3.5 or water. The cups are then placed in a temperature and humidity-controlled chamber to allow time for the moisture to move from high RH environment to the lower RH environment. The moisture movement is calculated by measuring the weight of moisture absorbed, or desorbed, by the saturated salts in the cups, and is calculated based on the weight change in the

cup per area of exposure. ASTM E96 (2010) offers a similar version of the ISO12572 (2001) cup method, in which the complication of using multiple saturated salts in the cup are replaced with only two RH controlling substances. The use of each substance represents a method, and so the methods are classified as either desiccant method or water method. The desiccant method uses desiccant filled cup to represent 0% RH on one surface of the specimen; conversely, the water method uses a water-filled cup to represent 100% RH. These cups, which hold the sample, are exposed to various RH on the other surface using humidity chambers. The WVT rate is measured by determining the steady water vapour flow in unit time. The following equation is used to determine the water vapour transport:

$$WVT = (\Delta m/t)/A \qquad \text{Equation 3.5}$$

Where WVT is the water vapour transport (kg/ (m^2 ·s)), Δm is the cup mass change (kg), t is the time during the weight change (s) and A is the test surface area (m^2).

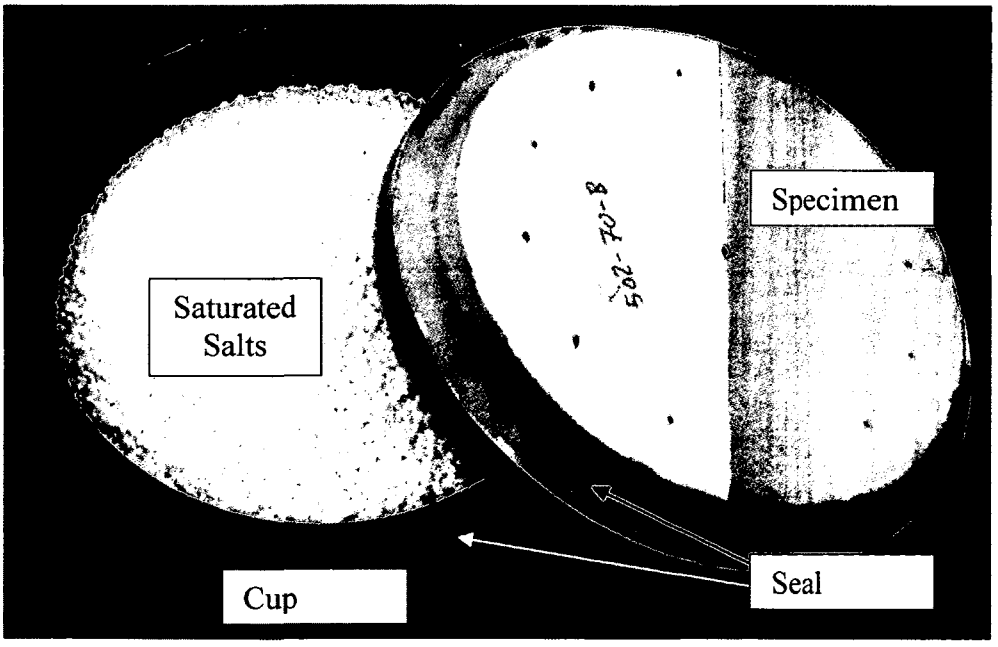

Figure 3.5 Sample on a cup according to ASTM E96 (2010)

There are various other standard methods to quantify the WVT, such as ASTM F372-99 that was withdrawn in 2009 because it was not commonly used, ASTM F1249-06 and ASTM E398-03 (Cammalleri and Lagus 2009). These standards specify precisely how to place the specimen and how to expose it to different RH, under isothermal conditions. Some of these standards use advanced or alternative methods, such as infrared sensors to detect the moisture content of the specimen. Since an infrared sensor was not available at NRC at the time of this project, the water vapour permeability was determined using standard ASTM E96 (2010) in this study.

Previous experiments

Various experiments have been conducted on plain wood, including spruce and pine. Tveit (1966) measured the WVT in spruce in the longitudinal and transverse (tangential and radial) directions, and demonstrated that water vapour permeability is greater in the longitudinal direction. The data presented in Figure 3.6 are for water vapour permeability of spruce in the transverse direction. On the other hand, Wu (2007) tested WVT for various materials including spruce wood. The WVT results for spruce in the transverse direction were similar to Tviet (1966).

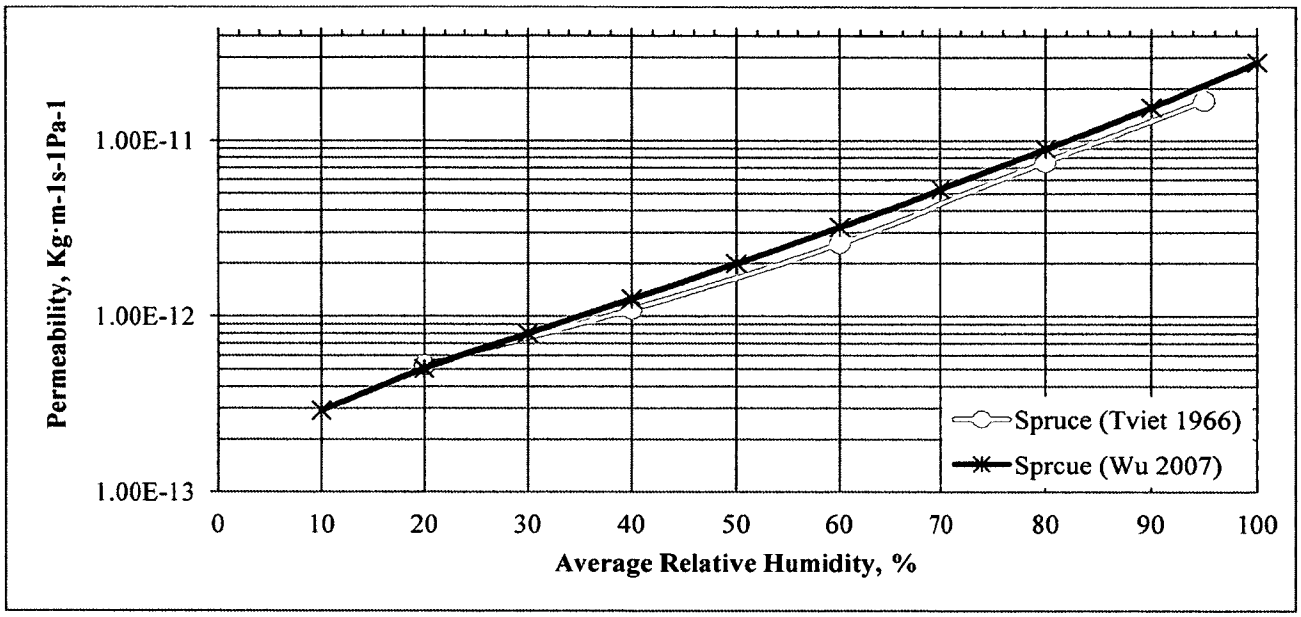

Figure 3.6 Water vapour permeability of spruce wood

Raji et al. (2009) studied the effect of lamination on WVT using samples of stacked laminated solid wood panels, made of scotch pine, imported from Finland. After the specimens WVT became constant, specimens were sliced to thin slices, using microtome, and weighed their moisture content. Wood samples without the laminated layer had a linear MC profile, whereas the laminated samples showed a lower MC at the lower RH side of the lamination. The experiment demonstrated that a laminated layer on the timber acts as a seal, thus reducing the diffusion of moisture, and the overall WVT through the specimen.

Sonderegger et al. (2010) used neutron imaging, which uses infrared sensors, to quantify the moisture movement across laminated spruce specimens. The study tested the effects of increasing the number of lamina (1, 3 and 5), and the behaviour of different adhesives, including epoxy, PVAC, Urea and PUR. Low MC levels were detected surrounding the bond lines in the

specimens. The experiments also demonstrated that WVT through specimens with more adhesive layer are slower in water vapour transport.

3.5.2 **Liquid Water Transport**

At a RH greater than 95%, moisture transport is faster due to the hydraulic pressure by the water and the negative suction pressure (ISO15148 2002). To account for cases where wood is in contact with water, the absorption of liquid water is considered. The mechanism of water absorption is called wicking, or capillary action (Siau 1995). When the material is exposed to liquid and air, an interaction occurs which draws moisture into the material at a rate which is dependent on the rate at which air can be released from the material. For wood, absorption of moisture is higher in the longitudinal direction, therefore when CLT members are installed in a building, the longitudinal direction of the wood should not be exposed.

ISO 15148 (2002) provides a standard method to determine the water absorption coefficient by exposing the material to liquid water and measuring its weight at different intervals. The water absorption coefficient, A_w ($kg \cdot m^{-2} \cdot s^{-1/2}$), is the measurement of mass moisture absorption through a specific area of the material, and can be calculated using Equation 3.6:

$$A_w = \left(\frac{m_2 - m_1}{A\sqrt{\Delta t}}\right) \qquad \text{Equation 3.6}$$

Where, m_1(kg) and m_2(kg) are the mass of the specimen before and after the absorption period, Δt(s) is the time duration between readings, and A (m^2) is the area in contact with the liquid water.

Wu (2007) measured the water absorption coefficient for various materials including spruce. The water absorption coefficient of the spruce specimens was 0.012 $\pm 8.22 \times 10^{-5}$ $kg/m^2 \cdot s^{1/2}$. This

coefficient could help compare the results of the study to wood especially since Wu used the same instruments used in this study.

3.6 Thermal Conductivity

Fourier's law is used to determine the thermal conductivity (W/m·K) based on knowing thermal conductance ($W/m^2 \cdot K$) of a material. The thermal conductance quantifies the thermal conductivity of the material per unit thickness. Moreover, the thermal resistance ($(m^2 \cdot K)/W$), another term for describing thermal conductivity in a material, is the reciprocal of the thermal conductance. The same relation applies between thermal resistance and thermal resistivity ((m·K)/W). Various factors affect the thermal conductivity of wood such as density, moisture content, grain direction, extractive content, structural defects, fibril angle and temperature (Glass and Zelinka 2010). The thermal conductivity of wood increases when the wood's moisture content, density, temperature and extractive content increases. Thermal conductance and thermal resistance are calculated as follows:

$$C = S \cdot E/\Delta T \qquad \text{Equation 3.7}$$

$$R = 1/C \qquad \text{Equation 3.8}$$

Where C is the thermal conductance, $W/(m^2 \cdot K)$, S is the calibration factor of the heat flux sensor, E the is heat flux sensor output in volts (V), ΔT is the temperature difference across the specimen (°C) and R is the thermal resistance of the material ($(m^2 \cdot K)/W$).

Using the available thermal conductivity data of a material, the temperature gradient within a building envelope assembly can be estimated at steady state. The temperature gradient within a building envelope will then help locate areas within the material where the dew point

temperature, which is the temperature at which the moisture in air condenses, has been reached (Latta and Garden 1964). The thermal conductivity of the building wall is calculated based on the sum of thermal resistance of each material within the wall. Example as shown in Figure 3.7, the temperature indoor is 24°C while the outdoor is -6°C and assuming the thermal conductivity of material A is 0.1, material B is 0.25 and material C is 0.5. The thickness of A, B and C is 40mm, 60mm and 20mm respectively. As the thermal resistance of the wall equals the sum of the resistance of each material used, the thermal conductance is the reciprocal of thermal resistance and the thermal conductivity is the property of thermal conductance, the equivalent thermal conductivity of the wall is the reciprocal of the sum of the thermal resistance of each matrial, which is the reciprocal of the thermal conductivity. By knowing the thermal resistance of each material, the temperature gradient within a wall assembly could be estimated. These relations and final results are calculated in Table 3.2.

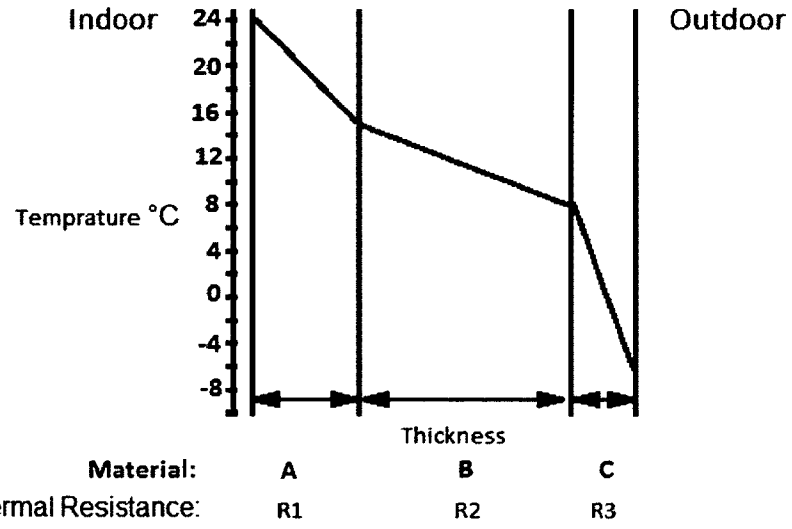

Figure 3.7 Temperature gradient within the building wall materials

Table 3.2: Thermal conductivity calculation example

	A	B	C
Conductivity(λ) (W/m·K)	0.10	0.20	0.50
Thickness (dx) (m)	0.04	0.06	0.02
Conductance($C = \lambda/(dx)$) (W/m²·K)	2.5	3.33	25.0
Resistance ($R = 1/C$) (m·K/W)	0.40	0.30	0.04
Overall Resistance(ΣR) (m·K/W)	0.74		
Overall Conductance($C = 1/\Sigma R$) (W/m²·K)	1.35		
Temperature measured	25°C	$\Delta T_{total} = 31$°C	-6°C
Temperature gradient ($\Delta T_x = \Delta T_{total}(R_x/R_{Total})$)	16.8	12.6	1.6
Temperature gradiant calculated within the wall	25°C	8.2°C	-4.4°C	-6°C

A few devices are available on the market to determine the thermal conductivity of a material. Most labs in the U.S. and Canada use ASTM Standards such as ASTM C177 (2010), which measures thermal conductivity, using the guarded-hot-plate apparatus. Another standard that can be used is ASTM C518 (2010), which uses a heat flow meter apparatus to measure the thermal conductivity of the material. Due to the extensive testing using thermal conductivity test, the imprecision of the test is 2.12% at two standard deviation level based on testing non-identical similar specimens at two different labs (ASTM C518 2010).

Previous research

Various researchers have measured the thermal conductivity of wood. The wood manual, by Glass and Zelinka (2010), specifies the thermal conductivity of softwood to be approximately 0.08 to 0.17 W/(m·K), depending on its moisture content. The wood handbook (Glass and Zelinka 2010) specifies the conductivity of various wood species as shown in Table 3.3. Also, Table 3.3 shows that the conductivity of the material is dependent on the density of the material.

Table 3.3: Thermal conductivity of selected softwoods (specific gravity from the source (Glass and Zelinka 2010) has been converted to density by multiplying by 1000kg/m^3)

Species	Density (kg/m^3)	Thermal Conductivity (W/(m·K)	
		Oven-dry	12% MC
Fir (Balsam)	370	0.09	0.11
Pine (Eastern white, Sugar)	370	0.09	0.11
Spruce (Engelmann, White)	370	0.09	0.11
Fir (White)	410	0.10	0.12
Hemlock (Eastern)	420	0.10	0.12
Pine (lodgepole, ponderosa, western white)	400-430	0.10	0.12
Spruce (Red, Stika)	420	0.10	0.12
Pine (Jack, Red)	450-460	0.11	0.13
Hemlock (Western)	480	0.11	0.14
Douglas-fir	500-520	0.12	0.14
Pine (Loblolly, Pitch, Shortleaf)	530-540	0.12	0.15
Pine (Longleaf, Slash)	610-620	0.14	0.17

Raji et al. (2009) tested a laminated pine specimen for thermal conductivity. Results ranged between 0.08 and 0.14 W/m·K for a MC less than 0.1 kg/kg, and between 0.22 and 0.3 W/m·K at higher MC. It was determined that an increase in thermal conductivity was due to the nature of pine, since no difference was found between the specimens with and without adhesive.

3.7 **Air Permeability**

Air tightness affects both the hygrothermal performance, the acoustical performance and *"performance at the building level such as thermal comfort, primary energy consumption and fire safety*" (Hens 2011). Bomberg and Brown (1993) identified air transport as a critical factor in environmental control. This is because air movement within a specimen brings with it the movement of moisture and heat. Breathable materials dry more effectively, whereas air entrapment can affect the thermal performance of a material (TRADA 2009b).

Prior to 1986, there were no standard tests for breathability. Bomberg and Kumaran (1986) helped create a standard test to determine air flow resistance. Air permeability can be measured

by determining the air flow through the specimen at different pressure differentials across the specimen. Air permeability is represented by the following equation:

$$k_a = l\frac{J_a}{(A \cdot \Delta p)} \qquad \text{Equation 3.9}$$

Where, k_a is the air permeability (kg/m·Pa·s), J_a is the air flow rate across the specimen (m^3/s), A is the exposed surface area across the specimen (m^2), and Δp is the air pressure difference across the specimen (Pa). Note that the weight in J_a is based on the conversion of air density from kg to m^3 which is 1kg to $83.3m^3$ at 20°C. The performance of the material can be described in air permeance ($kg/m^2 \cdot Pa \cdot s$)

Wu (2007) reported air permeance of spruce to be (7.2 ±1) x 10^{-9} kg/m·Pa·s using pressure differences ranging from 50 to 350 Pa. Moreover, Raji et al. (2009) tested specimens with and without laminate, and found that specimens with laminate had low air permeability. It was concluded that the difference in air permeability will have minimal influence due to the very low permeability of wood at large thicknesses.

3.8 **Hygrothermal Modeling**

The hygrothermal activity within a wall is critical for determining when the moisture level in the material will affect its durability. Moreover, because different geographic regions have different environmental factors, they must be analysed individually since the effects on the building material will differ. To facilitate the analysis for designers, modeling and simulation tools have been developed to help adjust the assemblies to meet a region's requirement of not being "*too wet for too long*" (Mukhopadhyaya et al. 2006). ISO13788 (2002) describes how to determine the condensation within envelopes based on the Glaser method, through simple calculation.

However, the WUFI ORNL/IBP software developed by Oak Ridge National Laboratories (ORNL) and Fraunhofer Institute for Building Physics (IBP) allows realistic calculation of the transient coupled one-dimensional heat and moisture transport in multi-layer building components exposed to natural weather, unlike the outdated Glaser method which considers steady state for hygrothermal analysis (ORNL 2012). At a faster processing time, software applications are capable of generating different scenarios of how moisture is transported and stored in the material. Depending on the modeling tools used, a range of parameters is required to run the models. In general, parameters include the geometry of the enclosures, the material's properties, and the boundary conditions (Barreira et al. 2010).

Modeling the hygrothermal effects on a building helps the designer to estimate the durability of the building in terms of moisture and heat distribution, although the understanding of the HAM transfer helps in making improvements to the design. Modeling can use input from historic data or manually adjusted data to estimate the effects of moisture and heat on the building. Every software tool has its own models to estimate moisture.

3.8.1 **Modeling Setup**

Most modeling software comes pre-loaded with generic examples to highlight the effectiveness of the application. Due to the limited database of the software, wall assembly details require special value inputs that vary with software.

Such special values are the geometric properties of the material including the orientation, location and dimensions of the material within the assembly. These properties represent the assembly's dimensions, and the thickness of each material used. A one dimensional case differs from two dimensional cases in the amount of data processed and the complication of the model.

A one dimensional geometric property only considers one line through the wall assembly, and does not include the vertical interaction between the materials. On the other hand, two dimensional geometric properties considers the interaction of neighbouring material through a sectional cut, and so a matrix of the 2D section is composed to calculate the HAM transport across the matrix. As complications can arise, 3D geometric properties forming a 3D matrix can calculate the HAM transport throughout the matrix, however the amount of data processed is extensive compared to 1D and 2D.

After deciding on the locations and dimensions of the material, the software requires the user to input the properties of the particular material specified for the assembly. These properties include density, porosity, heat capacity, thermal conductivity, EMC, water vapour permeability and water absorption. Each application requires a special representation of the data, based on the particular modeling method used by the software. These conditions are usually determined by testing the material, as described in the previous section. In two dimensional modeling software, the two dimensional properties of the material are considered.

Boundary conditions are the environmental conditions surrounding the assembly. In building envelopes, the standard boundary conditions are indoor and outdoor (Barreira et al. 2010). While indoor conditions are usually controlled by limited parameters, such as (A) temperature, (B) RH, (C) air pressure and (D) interior stack effect, the outer boundary conditions are dependent on the climate surrounding the building, which depends on the region. Outer boundary conditions include (1) temperature, (2) RH/ dew point/ vapour pressure, (3) air pressure, (4) solar radiation, (5) wind speed, (6) wind direction, (7) horizontal rain, (8) long wave radiation, (9) cloud index (i.e. fraction of sky covered with clouds) and (10) water leakage. Table 3.4 presents various boundary conditions that are considered by different hygrothermal modeling packages.

Table 3.4: Boundary condition requirements for various HAM software applications (Barreira et al. 2010). Letters and numbers represent the boundary conditions mentioned above.

Name	Type	Originating Location	Boundary Condition (External)										B.C. (Internal)			
			1	2	3	4	5	6	7	8	9	10	A	B	C	D
MOIST-EXP	1/2D-HAM	USA	X	X	X	X	X	X	X	X	X	X	X	X	X	X
HAM-Tools	1D-HAM	Swed./Den.	X	X	X	X	X	X	X	X	X		X	X	X	
DELPHIN 5	1/2D-HAMPS	Germany	X	X	X	X	X	X	X	X			X	X	X	
Bsim2000	1D-HM	Denmark	X	X	X	X	X	X		X	X		X	X	X	
IDA-ICE	1D-HAM	Sweden	X	X	X	X	X	X		X			X	X		
WUFI	1/2D-HM	Germ./USA	X	X		X	X	X	X	X	X		X	X		
MATCH	1D-HAM	Denmark	X	X		X	X		X	X	X		X	X		
hygIRC-1D	1D-HAM	Canada	X	X		X	X	X	X		X	X	X	X		X
HAMLab	1D-HAM	Netherlands	X	X			X	X		X	X		X	X		
MOIST	1D-HM	USA	X	X		X	X	X			X		X	X		
UMIDUS	1D-HM	Brazil	X	X		X	X	X					X	X		
1D-HAM	1D-HAM	Sweden	X	X	X	X				X			X	X		
GLASTA	1D-HM	Belgium	X	X		X				X			X			
EMPTIED	1D-HAM	Canada	X	X	X								X	X	X	

3.8.2 **Available Hygrothermal Modeling Software**

Various software packages are commercially available and many are verified by experimental hygrothermal testing models. Different versions of these application softwares are available; however, details provided by researchers may vary with respect to their features. Although some of the information related to these software versions may be outdated, the main functional comparison still applies for the software applications discussed in this text.

The software applications which have been on the market for the past few decades include WUFI Kuenzel and Kiessl 1997), hygIRC (Maref et al. 2002, Karagiozis 1993 and Djebbar et al. 2002a,b), and Moist (Burch and Chi 1997). These softwares will be discussed along with software applications such as HamLab (van Schijndel 2005), Glasta (Physibel 2007), Emptied (Rousseau 1999), Delfin (Nicolai et al. 2007), 1DHam (Hagentoft and Blomberg 2000), Bsim2000 (Rode and Grau 2004), IDA-ICE (Kurnitski and Vuolle 2000), HAM tools

(Kalagasidis 2004), Match (Rode 1990), Umidus (Mendes et al. 1999) and Moist-Expert (Karagiozis 2001). The list could be longer, since other newer models with a concentration on energy efficiency, which is the new trend, are under development.

HAM are the main functional considerations of most durability modeling software. Some software applications simplify the modeling process by eliminating the air factor in the model, which makes it easier to determine the results. Other software use more complex models to do this, including measurements of the pollutant and salt transport to determine additional outcomes. Delphin is one of the most comprehensive software applications used to estimate the pollution and energy efficiency in a building (Barreira et al. 2010).

For additional simplicity, some models function in one dimension, considering only the envelope thickness. Two-dimensional analysis can consider a sectional cut through an envelope, which could be either a wall or a roof. One dimensional modeling does not take into consideration adjacent materials; as a result, the durability of a material can be determined much faster than with a two-dimensional model. Examples of software which use two-dimensional modeling are Delphin, Moist-Expert, and Wufi (Barreira et al. 2010). The National Research Council of Canada also developed its software (hygIRC) to work in two dimensions. Three-dimensional models are also available but these require a tremendous amount of processing time.

Straube and Burnett (2005) point out that the variation between the software is in the mathematical sophistication of the models, which depends on the degree of information considered within the following parameters: moisture transfer dimension; type of flow (steady-state, quasi-static or dynamic); quality and availability of information and stochastic nature of various data (material properties, weather, construction quality, etc.).

Modeling software require the material properties to be input in a specific way, since many material properties can be presented differently, using different standards. For example, data input in 1D-Ham is different from hygIRC. 1D-Ham requires that the properties be presented according to the constants of the equations described in their manual. On the other hand, hygIRC requires the data points from the measurements to be entered from the material properties field, and these data points can be interpolated in different ways.

Many modeling tools are available on the market, and the difference between an average tool and a more successful tool is its validation. The validation is done by comparing modeling data to experimental test data (Barreira et al. 2010). Examples of well validated tools are hygIRC, Wufi, Moist, Match, and HAMLab, as they have been benchmarked with experimental studies.

3.8.3 **hygIRC-2D**

This section presents an overview of the state-of-the-art simulation program that was developed by Institute of Research in Construction (IRC) of the National Research Council (NRC) of Canada. A great advantage in using hygIRC-2D is simulating a structure based on a two-dimensional cross-section. Sections of the structure are rendered into a group of squared elements within a matrix. The geometric details of the wall assembly can be specified by the user, specifically the wall elements dimensions and matrix elements sizes. The analyses of every element in every material, in the structure, are determined as a function of time, and are calculated hourly.

After specifying the boundary conditions, the software requires the hygrothermal properties of material used in the structure. Boundary conditions include any proposed outdoor weather data set in any proposed period of time (Maref et al. 2002), the indoor proposed environment, and

geometric details. These hygrothermal properties, such as the ones explained previously, are calculated based on small scale tests. Major organisations such as ASHRAE and ASTM verified hygrothermal properties (Kumaran (2001) as a reference point and the building science community uses it in simulations. The hygrothermal properties of the materials used in this study are based on Kumaran (2001) material properties. All these details are processed in the unique part of the software, which is the model that will calculate the HAM transport within the elements.

Advanced hygrothermal models have been developed for more than 15 year by a joint research between IRC and the Technical Research Centre of Finland (VTT Finland) (Maref et al. 2002). Based on the outcomes of this joint research, hygIRC is the current hygrothermal model used by IRC to simulate the HAM transport. The model is based on well-know HAM transport equations such as Fourier's law of heat conduction, Fick's law of diffusion of mater, Darcy's law of fluid flow, Navier-Stokes equations, and equations that define conservation of energy, mass and momentum (Maref et al. 2002). In hygIRC-2D, a matrix is created of rectangular elements to represent the building structure. The model simulates the response of each element to changing environmental condition on an hourly basis and produces information on temperature and RH distribution surrounding the element within time (Maref et al. 2002). Equations used in hygIRC-2D are better described in Karagiozis (1993) (1997), Karagiozis et al. (1996) and Djebbar et al. (2002a) (2002b), however the governing equations used in this model are given below.

Moisture Balance:

$$\rho_d \frac{\partial(u)}{\partial t} = -\nabla\{g_l + g_v\} \qquad \text{Equation 3.10}$$

$$g_v = -\underbrace{\delta_P(u,T)\nabla P_v}_{\textit{Vapour diffusion}} + \underbrace{\rho_v V_a}_{\textit{Vapour airflow}}$$ Equation 3.11

$$g_l = -\underbrace{\rho_d D_w(u,T)\nabla u}_{\textit{Liquid diffusion}} + \underbrace{k_w(u)\rho_w g}_{\textit{Liquid gravity}}$$ Equation 3.12

$$k_w = \rho_d \frac{D_w(u,T)}{\frac{\partial P_c}{\partial u}}$$ Equation 3.13

Energy balance:

$$\frac{\partial(\rho_T(u,T)C_p(u,T)T)}{\partial t} = \underbrace{-\nabla\left(\rho_a(\mathrm{T})C_{P_a}(\mathrm{T})\vec{V}_a\mathrm{T}\right)}_{\textit{Airflow convective heat}} + \underbrace{\nabla(\mathrm{k(u,T)}\nabla\mathrm{T})}_{\textit{Heat conduction}} + \underbrace{L_v(\nabla(\rho_d\delta_p(u,T)\nabla P_v))}_{\textit{Evaporation/condensation}} - \underbrace{L_{ice}(\rho_d u\frac{\partial f_i}{\partial t})}_{\textit{Freeze/thaw heat}}$$

Equation 3.14

Where:

u Moisture content (kg/kg)

g_l Liquid moisture mass flow rate (kg/s/m^2)

g_v Vapour moisture mass flow rate (kg/s/m^2)

k_w Liquid moisture permeability (kg/m·s·Pa)

P_c Capillary suction pressure (Pa)

P_v Vapour moisture pressure (Pa)

T Temperature (K)

t Time (s)

$\vec{V_a}$ Air velocity vector (m/s)

ρ_d Density of the dry porous material (kg/m^3)

ρ_v Vapour moisture partial density (kg/m^3)

ρ_w Liquid moisture partial density (kg/m^3)

D_w Liquid moisture diffusivity (m^2/s)

δ_p Vapour water permeability (kg/m·s·Pa)

$\vec{g}$ Gravitational vector (m/s^2)

C_p Effective specific heat capacity (J/kg·K)

C_{Pa} Dry-air specific heat capacity (J/kg·K)

f_l Liquid fraction having a value 0 to 1

k Effective thermal conductive (W/m·K)

L_v Enthalpy of evaporation/condensation (J/kg)

L_{ice} Enthalpy of freeze/thaw(J/kg)

ρ_T Actual total density of the material including moisture contribution (kg/m^3)

The output of this software includes analysis of the RH and temperature changes within the elements throughout the simulated duration. So after processing the simulation, the data can be reviewed using post processing graphic software, which allows the reviewer to identify the locations with high moisture condition and the duration of exposure (Maref et al. 2002). The data extracted from the software present the moisture content, the temperature of each element and the RH surrounding it. The response of the material is evaluated in different methods including analysing the moisture content which is tracked in every element of the matrix.

Chapter 4 **Research Methods: Experimental and Modeling**

The objective of this research is to determine the hygrothermal properties of CLT using an experimental approach. This chapter includes a detailed description of the material used in the experimental work, as well as tests conducted to determine the hygrothermal properties of CLT. The hygrothermal properties measured include thermal conductivity, liquid water absorption, water vapour permeability, equilibrium moisture content (EMC), and air flow permeability.

4.1 **Specimens Details**

Four different sets of CLT specimens were used for testing. Three of these sets of CLT specimens contained wood harvested in Canada, such as Eastern Spruce-Pine-Fir, Hem-Fir and Western Spruce-Pine-Fir referred to in this study as ESPF, Hem-Fir, and WSPF, respectively. These sets were then manufactured in a laboratory, in Vancouver, B.C. The fourth set was a manufactured CLT from Europe, made from European spruce. This set will be referred to as Euro in this study. The dimensions and the compositions of the specimens are provided in this section.

Initial dimensions of the CLT specimens were recorded before cutting the specimens for testing. Each Canadian set included five layers of wood, whereas the European set included only three layers of wood. The Canadian specimens were composed of two sets of lumber with different dimensions: the thicker set's measurements were 689 mm (27" 1/8) long by 137 mm (5" 3/8) wide and 33.3 mm (1" 5/16) thick; while the thinner set's measurements were 689 mm (27" 1/8) long by 137 mm (5" 3/8) wide and 14.3mm (9/16) thick. The thicker lumber was used for the 1st, 3rd and 5th layers, while the thinner lumber was used for the 2nd and 4th layers. Details and illustrations are provided in Table 4.1 and Figure 4.1.

Table 4.1: Dimensions of lumber in test specimens

	Region	Number of layer	Dimensions (layer 1,3, and 5) (L x W x H) (mm)	Dimensions (layer 2 and 4) (L x W x H) (mm)
Hem-Fir	Canada	5	689 x 137 x 33.3	689 x 137 x 14.3
ESPF	Canada	5	689 x 137 x 33.3	689 x 137 x 14.3
WSPF	Canada	5	689 x 137 x 33.3	689 x 137 x 14.3
Euro	Europe	3	* x 114 x 33.3	* x 114 x 22.2

*Data not available due to finger jointing.

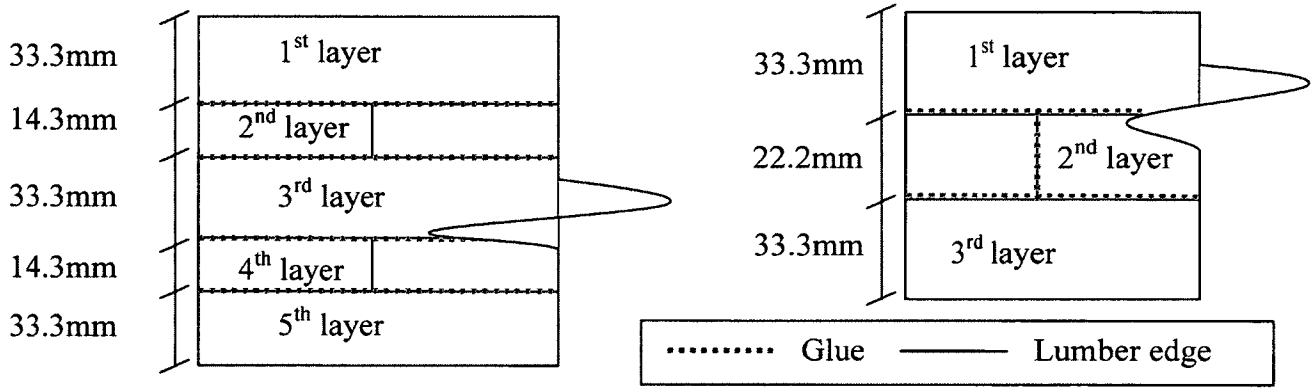

Figure 4.1 Canadian (left) and European (right) specimen thickness and glue application (not to scale)

Unlike the Canadian specimens, the European specimens were cut from larger CLT specimens. Finger joints were used to extend the length of the lumber before it was glued together. As a result, the length of the lumber cannot be determined by visual inspection, only the width and the thickness of the lumbers were recorded. The specimens were composed of two sets of finger jointed lumber with different dimensions: the thicker set's measurements were 114 mm (4" 1/2) wide by 33.3 mm (1" 5/16) thick while the thinner set's measurements were 114 mm (4" 1/2) wide by 22.2 mm (7/8) thick. The thicker lumber was used for the outer layers, while the thinner lumber was used for the inner layer (Table 4.1 and Figure 4.1).

The Canadian and European specimens had different types of glue and different application methods as provided by the source, FPInnovations. Emulsion polymer isocyanate was the glue used for the Canadian specimens. It was applied between the layers of the CLT. Conversely, polyurethane was used on the European specimens, and the glue was applied in two different areas. The first area was between the CLT's layers, and the second area was at the sides of the adjacent boards in each layer, combining every three boards together (Figure 4.1).

Prior to any experimental work, checks in the wood were observed. Figure 4.2 shows the specimen with the largest number of checks, which was due to a low RH, of around (20 $\pm$10)%, in the laboratories during winter. These checks could cause the material to be more permeable to heat, air and moisture (HAM) transfer, specifically at the location of the checks. To get a representative and comparable data on the material tested, all experiments were conducted with specimens without checks, except for the thermal conductivity test which measured large size material.

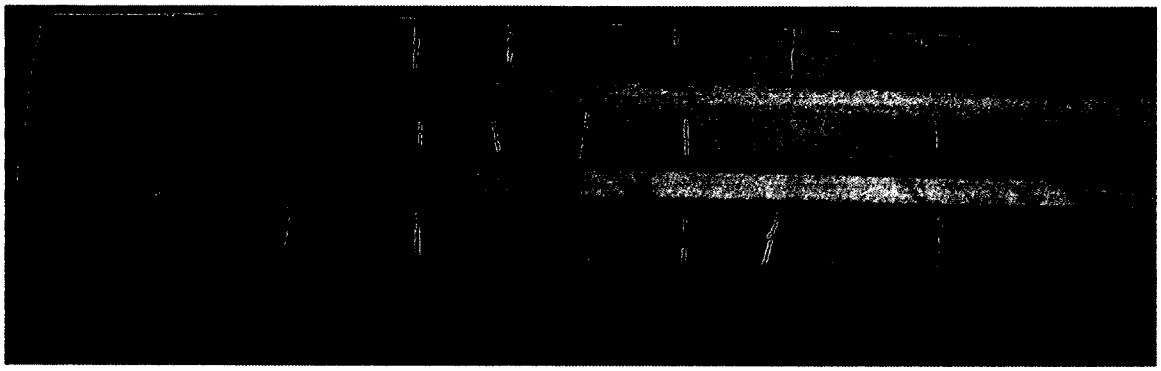

Figure 4.2 Checks developed in the lab during winter

4.2 Thermal Conductivity

The thermal conductivity of the CLT specimens was determined using a heat flow meter apparatus, shown in Figure 4.3. The meter was set in accordance to standard ASTM C518 (2010). The heat flow meter apparatus measured the thermal resistance of material by comparing the thermal resistance of the material to the thermal resistance of a common specimen, which is used to calibrate the apparatus (ASTM C518 2010). As the thickness of the material was recorded at the beginning of the test and the temperature differential and heat flux sensor output was recorded by a computer instantaneously, the computer measured the thermal conductance of the material based on Equation 3.7 and used the thickness to calculate the thermal conductivity of the material.

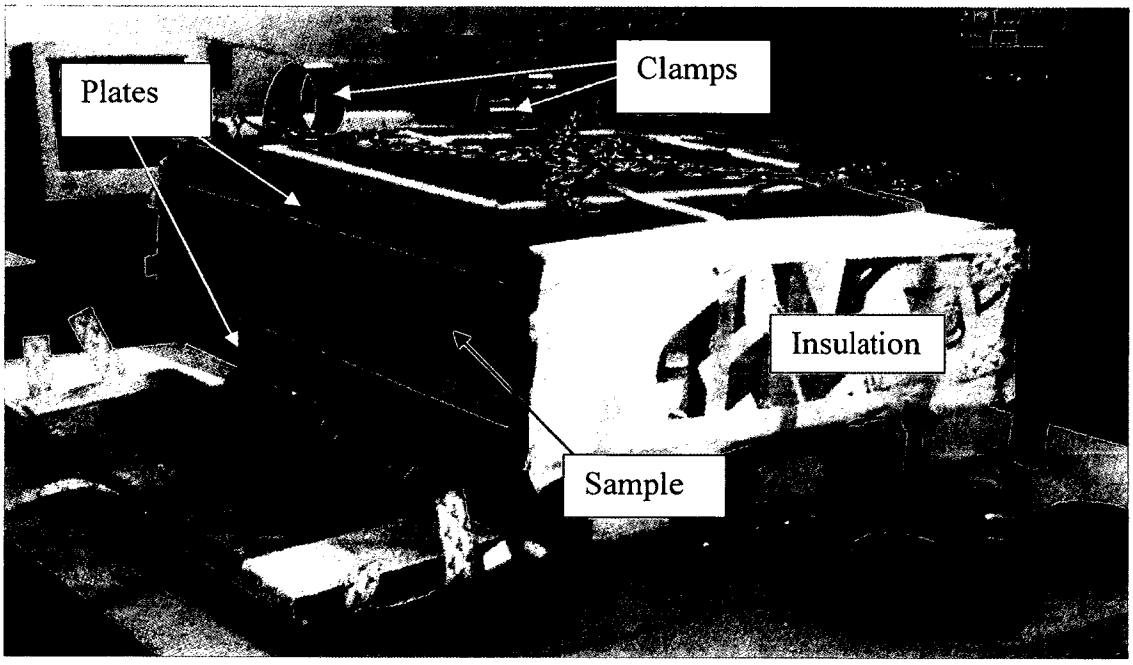

Figure 4.3 Heat flow meter apparatus

The heat flow meter apparatus available at IRC had two heat flux sensors as illustrated in Figure 4.4 and was used to measure the thermal conductivity of the CLT. The apparatus can test materials with dimensions of up to 610 mm x 610 mm (2ft x 2 ft) and computes the thermal resistance of a material from the temperature differential of the plates, using heat flux sensors located at the centre of each plate surrounding the specimen. The calculated value is dependent on a calibration factor, which is set using a specific calibration material. As it is essential to calibrate the apparatus prior to testing in order to get accurate measurements, this was performed by the lab technicians, as required by the standard. Since the calibration is performed, the imprecision of this experiment was comparable to the imprecision reported by ASTM C518 (2010), which was 2.12%, based on testing a similar but not identical specimens in an inter-laboratory imprecision at two standard deviations.

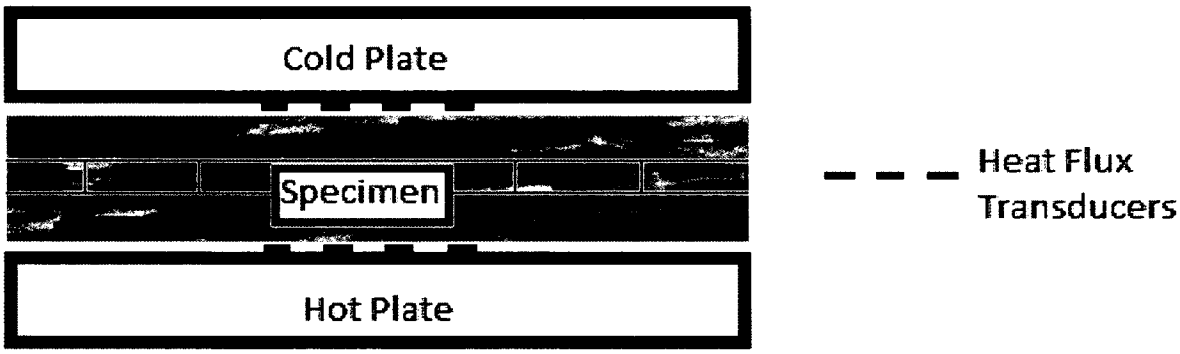

Figure 4.4 Heat flow meter apparatus with two areas for heat flux sensors

Since solid wood samples of various wood species have been previously tested by various researchers, the purpose of the experiments in this study was to determine the effect of lamination on the CLT specimens. The CLT specimens were tested with the manufactured thickness (reported in section 4.1). However, the edges of the specimens were cut to 610 mm x

610 mm (2ft x 2ft) in order to fit into the apparatus. One specimen from each set of CLTs was used for this test. Since the samples were not perfectly flat and hard to deform, rubber pads were used as a '*blanket and batt-type*' material in accordance to ASTM C518 (2010). The final results were calculated by subtracting the pads' thermal resistance from the calculated thermal resistance of the pads and the CLT together. The MC of the material was not recorded; however, the material was considerably dry as it was stored in the lab for 6 months at (20 ±10) % RH. At the beginning of the test, the thickness of the material was recorded to identify the thermal conductance of the material. The recording process required twelve hours of stable thermal conductance measurements.

4.3 Water Absorption

The water absorption properties of CLTs were determined following ISO 15148 (2002). CLT specimens were tested for liquid water absorption by submerging a surface of the specimen in liquid water, while the opposite surface was exposed to air and the sides were sealed.

The apparatus used to measure water absorption included a water tank, top loading stand and a specimen container with adjustable height. The water tank contains circulating water that maintains the water level within the tank while keeping the temperature constant. The container holds the specimens from the sides so they can be easily placed on the stand, and the height can be easily adjusted to ensure that the specimens are immersed in water to a specific height (Figure 4.5).

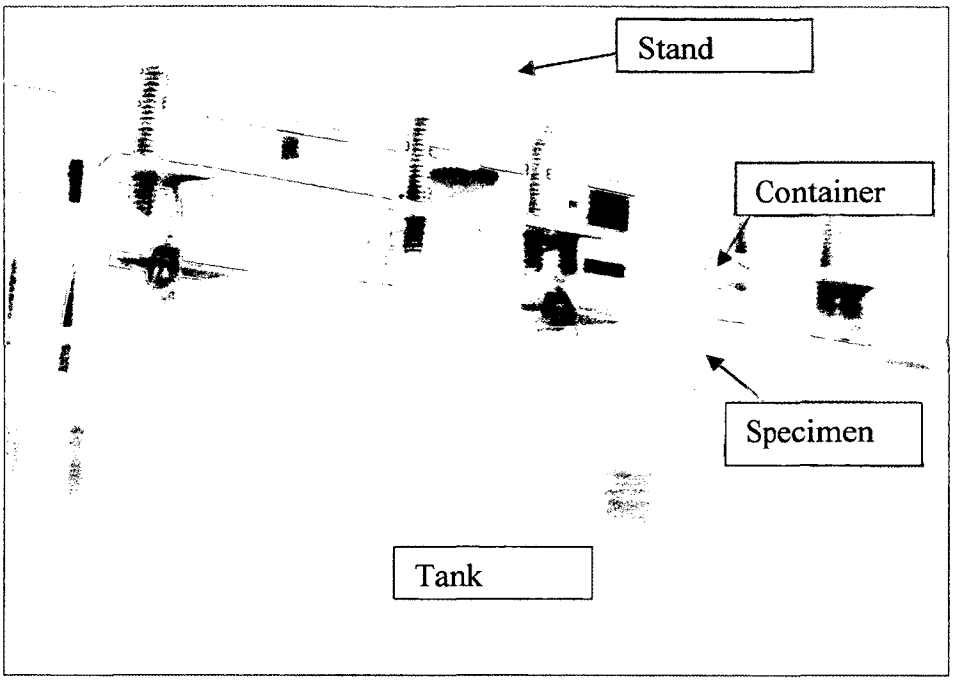

Figure 4.5 Partial immersion test for CLT specimen, IRC

Because CLT is very thick and the apparatus cannot handle large sizes, the specimens were cut to representative sizes to include one lamina. Moreover, because each individual test specimens surface is less than $1x10^4$ mm^2, six specimens were used to satisfy a total surface area of $3x10^4$ mm^2 required by ISO 15148 (2002). After the CLT specimens were tested for thermal transmission, which is a non-destructive test, they were cut into 100 mm x 50 mm smaller specimens with a thickness of 25 mm. The specimens included a layer of lamination to account for the lamination effect without considering abutting boards (Figure 4.6). The top of the specimen was exposed to the lab atmosphere, while the bottom was exposed to temperature controlled water at 21 ±1 °C.

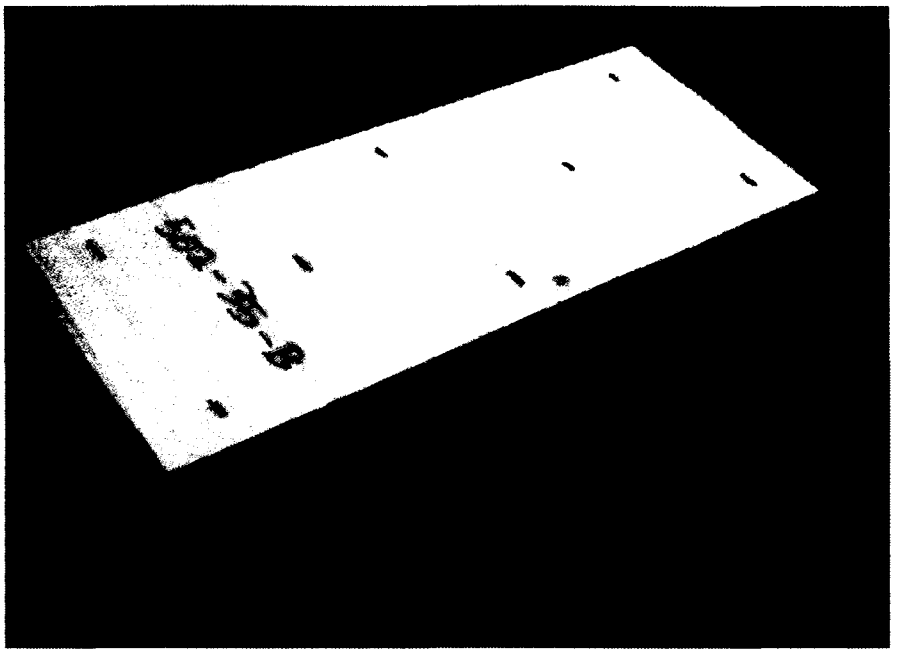

Figure 4.6 Specimen for partial immersion without edge wax

As specified by ISO 15148, the edges of the specimen were required to be sealed with vapour tight sealant. The sealant used was a wax that is composed of beeswax and rosin of equal weights applied at 135°C. The first batch of six specimens was Hem-Fir and had a brush application of wax on its outer edges in addition to an additional protective wax layer. The additional layer of wax was applied to cover the first layer and protect it.

During the test of the first batch, it was noticed that the seal broke on the edges, shown on a similar dummy specimen in Figure 4.7, which caused to rethink of another method for sealing the material for this experiment.

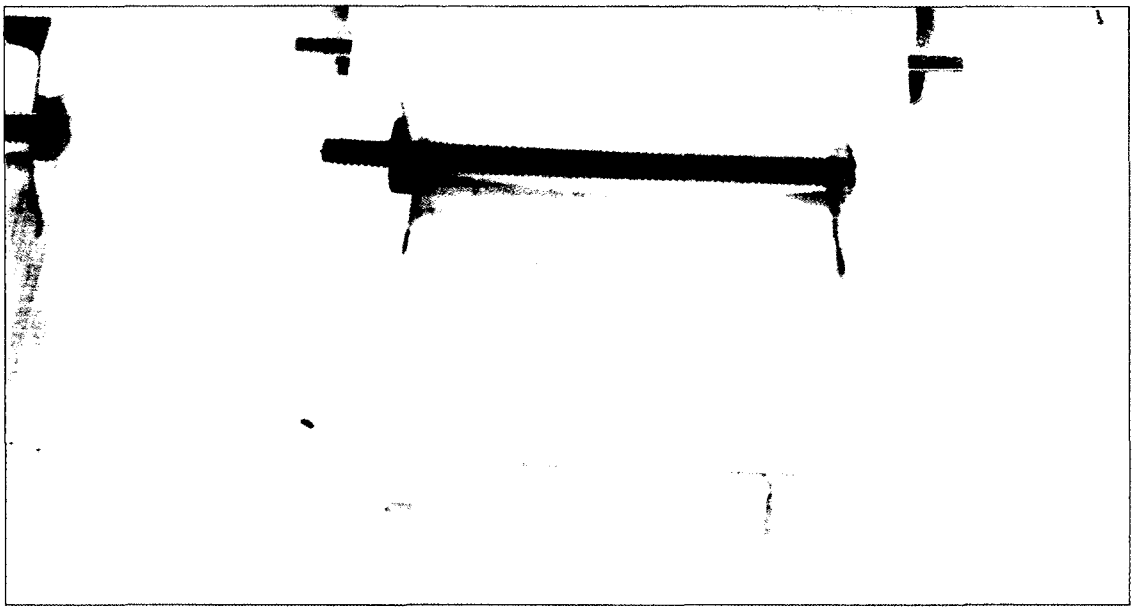

Figure 4.7 Break in the wax with the use of tape due to dummy specimen swelling

To avoid sealant failure, five different methods of sealing were tested. A basic inaccurate test composed of one specimen for each case was performed. The purpose was to identify a method that would not allow the edge of the specimens to be exposed to moisture, thereby reducing the rate of moisture transport.

Wood specimens, from ESPF CLT specimens, were used in this basic test. All the specimens were of same shape and no checks were observed among them. The size of the specimens was 120mm x 50mm x 15mm. No lamination was included.

Two sealing materials were considered as options for testing in different application methods. First was the wax, composed of 50% bees wax and 50% rosin, as specified in ASTM E96 (2005). The second was aluminum tape. To apply the seal, a brush and a heated wax container were required.

Five different sealing applications were performed on the materials including:

1- Normal brushing application of the wax on the edge of the specimen. 1) The wax was applied on the edge of the specimen using a brush. 2) The specimen was dried and cooled. 3) Another application was done to protect the first application.

2- Special enforced application of the wax was applied on the edge of the specimen. 1) The sides of the specimen were heated by abutting the edge of the specimen to the heated container. 2) A brush application of wax was applied to the edges. 3) The sides of the specimen were heated by abutting the edges to the heated container. 4) Step 2 and 3 were repeated. 5) The wax was applied to the areas with no wax visible. 6) The specimen was dried and cooled.7) A simple application of normal brushing was done to protect the bottom layer.

3- The wax was applied on top of an aluminum tape covering the center portion of the specimen. 1) The tape was applied at the center of the specimen to cover the center portion of the edges. 2) The steps in method 1 was applied on top of the tape

4- The wax was applied on top of an aluminum tape covering the center portion of the specimen. 1) The tape was applied at the center of the specimen to cover the center portion of the edges. 2) The steps in method 2 was applied on top of the tape

5- The wax was applied on top of an aluminum tape covering the full edges of the specimen. 1) The tape was applied at the edges of the specimen to cover the full portion of the edges. 2) The steps in method 1 was applied on top of the tape

The specimens were tested as proposed by ISO 15148 (2002) (shown in Figure 4.8). The best method was chosen based on non-failure and minimal moisture penetration. The test concluded that the least penetration was achieved by applying the wax seal to the surface of the hot specimens, which helped the wax adhere to the specimen. As a result, the second batch of testing required more than eight weeks for the water penetration to reach the top of the sample and no failures on the edges, compared to 24 hours of penetration using first method of application.

Figure 4.8 Partial immersion test on sealant

A set of six specimens was tested independently for each type of CLT. During the test, each specimen was weighed at an offset of one minute to provide time for adjusting the container height at the start of the test and for measuring the weight of the specimens. Measurements were taken at 0, 10, 20, 30, 50 minutes, and 1, 1.5, 2, 4, 12, and 24 hours due to non-linear decreasing rate of moisture absorption. The specimens were released from the stand, excess water was removed from the bottom of the specimens using paper towel, and the samples were weighed on a scale with an accuracy of $1x10^{-6}$ kg. The mass gained was divided by the surface area of the

specimen (Equation 4.1). The water absorption coefficient was calculated from the mass gained per square root time (Equation 4.2).

$$Mass\ gain = \Delta m_t = \frac{(m_t - m_i)}{A} \qquad \text{Equation 4.1}$$

Water Absorption Coefficient:

$$A_W = \frac{\Delta m_{t2} - \Delta m_{t1}}{\sqrt{t_{2-1}}} \qquad \text{Equation 4.2}$$

Where Δm_t is the mass gain (kg/m^2), m is the mass of the specimen (kg), A is the face area (m^2), A_w is the absorption coefficient (kg/(m$^2 \cdot$s$^{0.5}$)), t_{2-1} is time from mass gain 1 to mass gain 2 (s).

4.4 Water Vapour Transmission

Water vapour transmission in CLT was tested using the cup method, discussed in section 3.5.1. In this method, the material is sealed to the open mouth of a cup to allow moisture movement from the atmosphere to the cup through the specimen. The cup and the cup's surrounding environment are set to different humidity levels, which causes the water vapour to move from the higher RH environment to the lower RH environment. The rate of moisture transfer is assigned to the average RH surrounding the material.

Both desiccant method and water method were used to determine the moisture transfer rate, as specified in ASTM E96 (2010). The desiccant method requires the cup to be filled with desiccant representing 0% RH. This method can be used to determine the moisture transport at average RH of up to 50%. On the other hand, the water method requires the cup to be filled with water representing 100% RH. This method is used to determine the moisture transport for average RH above 50%. The moisture transfer rate for each material varies based on the average RH surrounding the material. Depending on the type of test, the cup is at either 0% RH or 100% RH,

where the RH of the surrounding environment on the other side of the material can be adjusted using saturation salts or mechanical RH regulators.

The test specimen from the thermal conductivity test was cut into eight specimens per set. Four specimens from each set were tested using the desiccant method and the other four specimens were tested using the water method. The specimens were cut into cylinders, with a diameter of 150 mm and a thickness of 18 mm, based on the shape and size of the cups available. Because thicker material requires more time to for the moisture movement to stabilize, the thickness of all the specimens was reduced and a layer of lamination was kept to determine the effect of the lamination. The first layer of wood was 12 mm thick while the second layer was 6 mm thick. The variation in the thickness of each layer helped to determine the effect of a glue layer on the moisture movement through the specimen. Each layer in the CLT contains abutting boards that form a joint, which could become a gap during wood shrinkage at low RH. To consider the effect of the abutting boards, a joint of two abutting boards was located at the center of the top side of the specimen, as shown in Figure 4.9. The joint between the boards was used to estimate the effect of moisture and air movement between abutting boards.

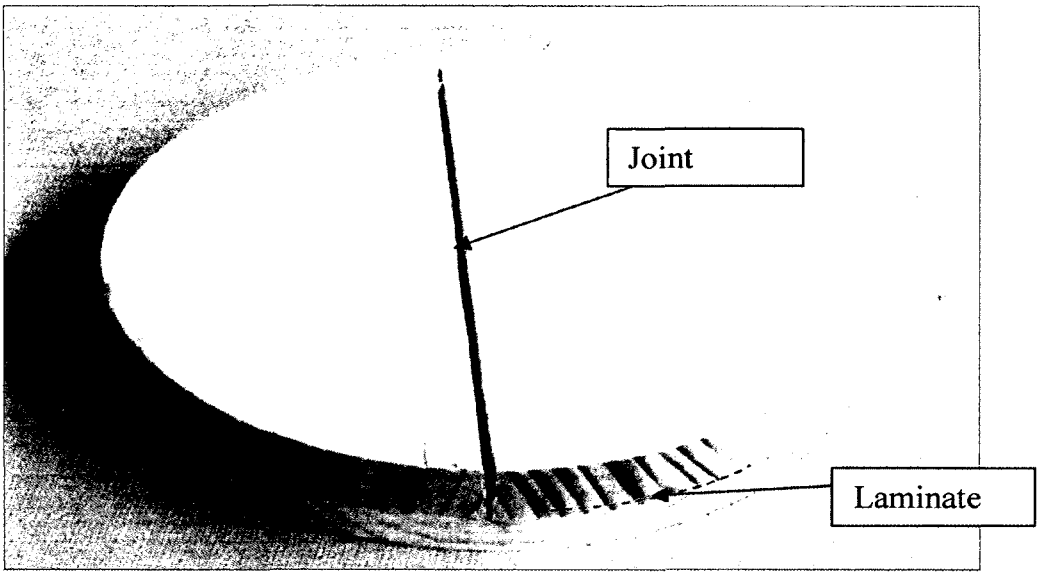

Figure 4.9 Water vapour transmission specimen before testing

To avoid any leakage around the specimen, wax was used to seal the gaps between the cup and the specimen. The wax was composed of 50% beeswax and 50% rosin and was applied at 135°C. The wax was applied on the edge of the round specimens before fitting in the lid, and then again between the specimen and the lid of the cup. After filling the cup with either water or desiccant, another layer of wax was also applied between the lid and the cup, as shown in Figure 4.10.

The tests were conducted under different surrounding conditions using chambers that are environmentally controllable. Each chamber was set to a different RH: 50%, 70% or 90%. Based on the combination of the chamber RH and the cup RH, the average RH within the specimen is considered the average as shown in Table 4.2. To stabilize the RH in the chambers and avoid sudden temperature changes, the chambers were located in a room with controlled humidity and temperature of 50% RH and 22 ±1°C. Pressure, temperature, and RH of the room and the chambers were continuously monitored during the experiment. The change in mass of the

specimens was measured using an analytical balance with a sensitivity of $\pm 1 \times 10^{-6}$ kg, and a maximum mass of 5 kg.

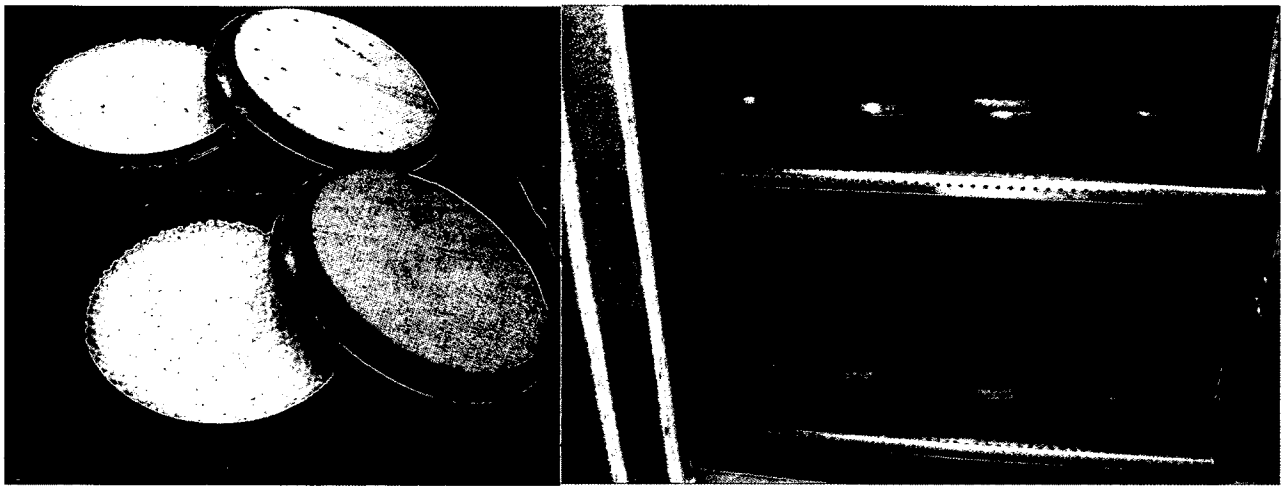

Figure 4.10 Water vapour transmission specimens (desiccant method) (left) and specimens in the chamber (right)

Table 4.2: Water vapour transport RH: based on average surface RH from inside cup and chamber

Cup content		Chamber RH		
Substance:	(RH)	50%	70%	90%
Desiccant	0%	25%	35%	45%
Water	100%	75%	85%	95%

All four sets of eight specimens were placed in the appropriate chamber (Figure 3.10), until a constant rate of transmission was reached. The cups containing the specimens were weighed daily to quantify the movement of water vapour. A buoyancy correction factor was applied to the mass of the specimens to account for the changes in atmospheric pressure which occurred throughout the testing period (ASTM E96 2010). The linear regression in Figure 4.11 is

calculated based on the last six linear data points that show a linear moisture movement rate throughout the specimen.

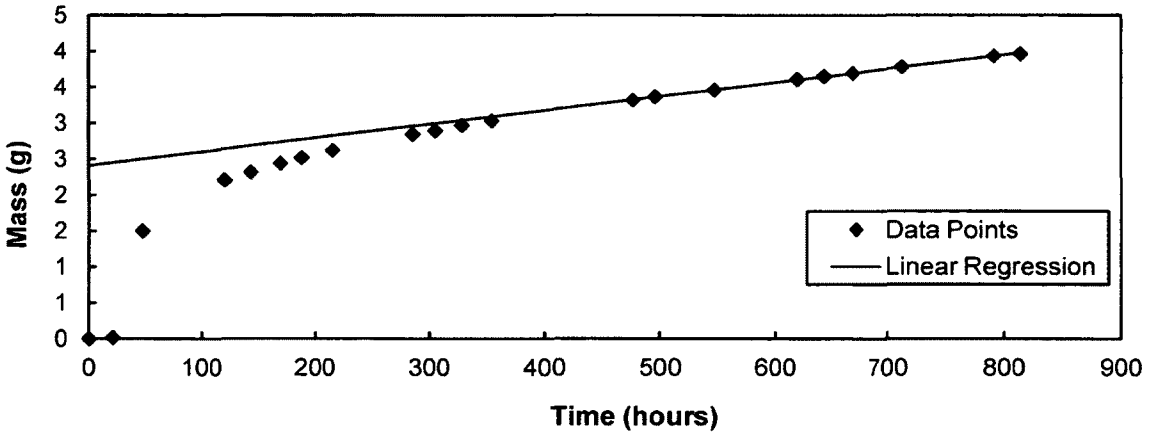

Figure 4.11 Water vapour transport to constant linear rate

Once a constant moisture transfer rate was reached, the specimens were transferred from the lower RH chamber to the higher RH chamber. During the transfer, the wax was visually inspected for any moisture around the specimen. Also, the mass of the desiccant was checked to ensure that the mass of absorbed moisture did not exceed 10% of the original desiccant mass. The desiccant was replaced after completing the rate measurement in the 70% RH chamber. The data was calculated after applying the buoyancy correction factor and the correction for still air and specimen surface. The measurements were collected using the calculated water vapour transport rate based on the average RH present throughout the specimen.

The water vapour transport measurements were completed over three months period since the specimens required at least two weeks for the transport rate to stabilize. While the samples were weighed on a daily basis, the stability of the vapour transport rate was checked using the Excel spreadsheet developed by IRC, which adjusts measurements using a buoyancy correction factor.

After a stable water vapour transfer rate was achieved, the permeability rate was adjusted for still air, as suggested in ASTM E96 (2010).

4.5 Equilibrium Moisture Content (EMC) of Wood

CLT is composed of two materials, wood and glue, therefore measuring the EMC of CLT is a challenging and time consuming task. This is because it is difficult to prepare scaled down specimens representing both wood and glue. However, since glue's durability is usually dependent on the EMC of wood and the glue comprises less than 1% of the CLT weight, the EMC of the CLT was considered equivalent to the EMC of wood. As a result, the EMC of the glue had negligible effect on the overall EMC of the CLT specimen.

The tests included specimens from both longitudinal and tangential directions, as shown in Figure 4.12, where weight of each specimen was about 15 g. The longitudinal specimens were of size 3 cm x 5 cm x 0.4 - 0.7cm and tangential direction specimens were of size 4 cm x 4 cm x 0.4 - 0.7 cm.

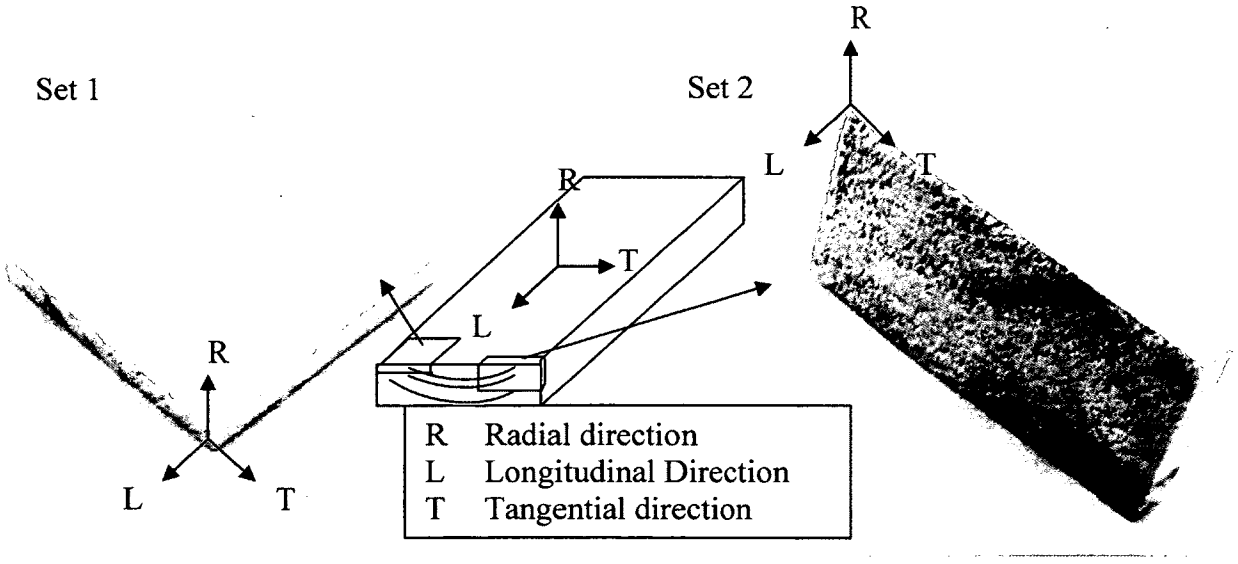

Figure 4.12 Cut orientation differences between set 1 and set 2

The tests were conducted following ASTM C1498 (2004). The specimens were tested for adsorption in four different chambers. Before the initial tests, the specimens were dried in an oven at 107°C until they had a constant mass. The specimens were then tested for adsorption in chambers with RH at 50, 70, 90, and 95% consecutively. The specimens were weighed daily until they had constant mass for three consecutive days. The EMC was calculated using Equation 4.3 based on the steady moist mass of the specimen and dry mass of the specimens, in which the mass was steady within 10% for three days.

$$MC = \frac{(m-m_0)}{m_0} \qquad \text{Equation 4.3}$$

Where MC is the moisture content, m is the moist weight of the specimen and m_0 is the dry weight of the specimen.

4.6 Air Flow Permeability

Air flow resistance is inversely related to the air permeability of the material. To determine the air permeability of CLT, the movement of air through the CLT was measured by recording the air pressure differential at both ends and the air flow at one end. These tests were conducted on the specimens that were used for the water vapour transmission experiments.

A cylindrical chamber with specimen mounted in the lid of the chamber was used to measure the air flow resistance (Figure 4.13), the method was based on Bomberg and Kumaran (1986). The chamber was well sealed, and the specimen was waxed to the chamber to insure no leaks. Air was passed through an air flow regulator and into the chamber, while the pressure monitor measured the pressure difference across the specimen. As the air flowed through the specimen at

different rates, the instrument gathered the stabilized pressure differential within the chamber to extract the results.

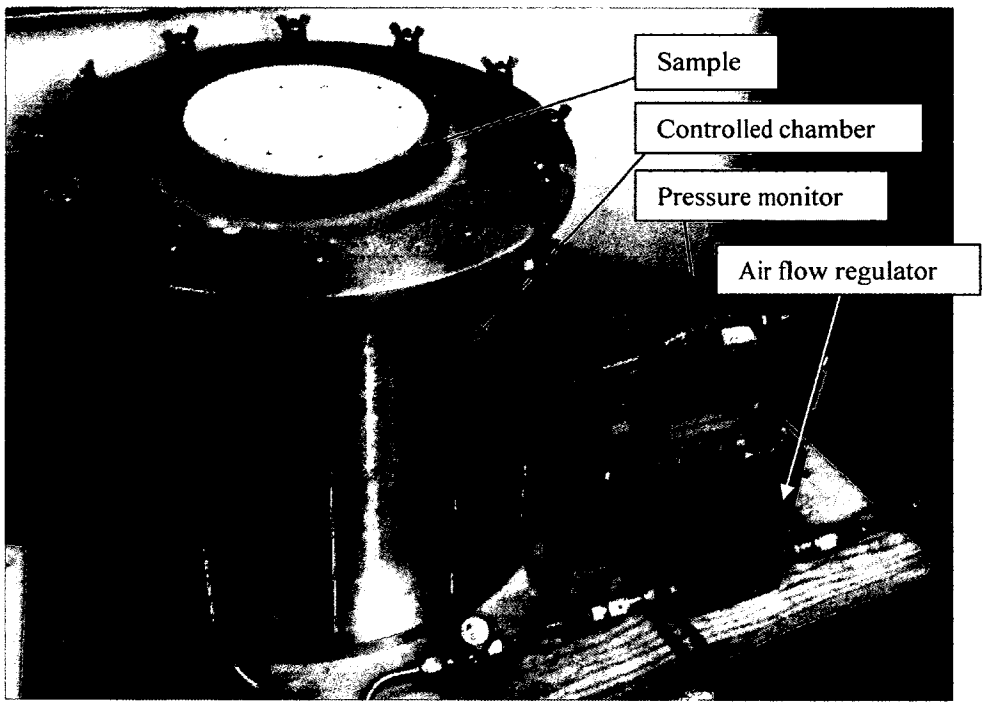

Figure 4.13 Air permeability testing apparatus

The method used to determine the air permeability follows ASTM C522 (2009). A software developed by the National Research Council (NRC) of Canada was used to record the pressure differences under various airflow rates, and compute the air permeability. As the air flows through the specimen, the pressure within the chamber would stabilize at certain pressure and the air permeability, k_a (kg/m·Pa·s) was calculated using Equation 4.4 (Bomberg and Kumaran 1986):

$$k_a = J_a(dx/(A \cdot \Delta p)) \qquad \text{Equation 4.4}$$

Where, J_a is the air flow rate (kg/s) across an area A (m^2), dx is the thickness of the specimen (m), and Δp is the difference in air pressure across the specimen surfaces (pa).

Similarly, the air permeance, K_a (kg/m^2·Pa·s), of a product at a given thickness is calculated from the above measurements using Equation 4.5:

$$K_a = J_a / A \cdot \Delta p \qquad \text{Equation 4.5}$$

In the event that the pressure in the chamber continuously increased, the specimen was deemed to be impermeable.

Chapter 5 **Experimental: Results and Discussion**

The experimental work for this research was conducted at the National Research Council, Ottawa. The hygrothermal properties of CLT produced from Canadian harvested wood species and European harvested wood species were determined, and compared to a European CLT and previous research on wood-based materials.

The average densities of the materials used during these experiments are presented in Table 5.1. The densities were measured using the sorption specimens composed of only wood, as the weight of the adhesive is less than 1% of the overall weight of CLT, as mentioned earlier. Five to six specimens were measured from each material, with total weight of each material being $15x10^{-3} \pm 1x10^{-3}$ kg. Theses specimens were weighed individualy using a scale with an accuracy of $\pm 1x10^{-6}$. The dimensions of the specimens were measured with an accuracy of ±0.1mm

Table 5.1: CLT density

	Dry Density (kg/m^3)
Hem-Fir:	380 ±24.2
ESPF:	370 ±23.8
WSPF:	440 ±25.0
Euro:	340 ±12.7

5.1 **Thermal Conductivity**

Thermal conductivity results as shown in Table 5.2 show similarities to the studies conducted using plain wood and published by other researchers (Kumaran 2001, Wu 2007, Galss and Zelinka 2010), and Staked Laminated Timber (Raji et al. 2009). Moreover, it can be noticed that the thermal conductivity of CLT is related to its density. The denser the wood, the higher is the

thermal conductivity. No effect on the thermal conductivity values of the specimens, shown in table 5.2, was recorded despite the glue between the layers of lumber, when compared to table 3.3. Similar conclusions were made by Raji et al. (2009) study on stacked laminated solid wood planks. Table 5.2 shows the thickness and the temperature range surrounding the tested specimens to measure the thermal conductance value. The conductivity was calculated based on the conductance and the thickness of the specimen, as the relation is shown in equation 5.1.

$$\lambda = C\,(dx) \qquad \text{Equation 5.1}$$

Where λ is the thermal conductivity$(W/m \cdot K)$, C is the thermal conductance$(W/m^2 \cdot K)$and dx is the thickness (m)

Table 5.2: Thermal conductivity results

Specimen	Thickness (cm)	Hot Surface Temp. (°C)	Cold Surface Temp. (°C)	Mean Temp. (°C)	Themal Conductance W/(m²·K)	Thermal Conductivity W/(m·K)
Hem-Fir	13.2	34.3	13.4	23.8	0.855	0.113 ±0.002
ESPF	13.1	35.0	12.9	23.9	0.813	0.106 ±0.002
WSPF	13.1	35.1	12.7	23.9	0.877	0.117 ±0.003
Euro Test 1	8.90	34.8	13.1	24.0	1.162	0.103 ±0.002
Euro Test 2	8.87	35.4	13.2	24.3	1.176	0.104 ±0.002

5.2 **Water Absorption**

The water absorption by wood specimens was measured in the tangential and radial directions, while the measurement in the longitudinal direction was excluded. In each set, six specimens were tested and the results, represented as diffusion coefficient, are based on the linear slope of the cumulative weight measurements in each set of specimens per square root time, as simplified from equation 3.6. As the diffusion coefficient calculated for Hem-Fir 1 was influenced by the break in the wax seal on the longitudinal surfaces of the specimens, an extra test method was required to identify the best method for sealing the specimens.

Out of the five specimens tested for the seal method selection, as discussed in Section 4.3, two specimens, using methods 4 and 5, immediately failed during the test as the seal broke during the test. After removing the specimens from the water, it was noticed that the specimen from method 1 had a break in the seal, whereas the specimens sealed using method 2 and method 3 did not fail. As the three methods were disqualified due to breaks in the seal, the only two methods which lasted without a break in the seal were method 2 and method 3. Method 2 is the brush application on heated specimen edge without aluminum tape. Method 3 is the brush application of wax on top of an aluminum tape on the central half of specimen edge. Figure 5.1 illustrates the results of the sealant method test.

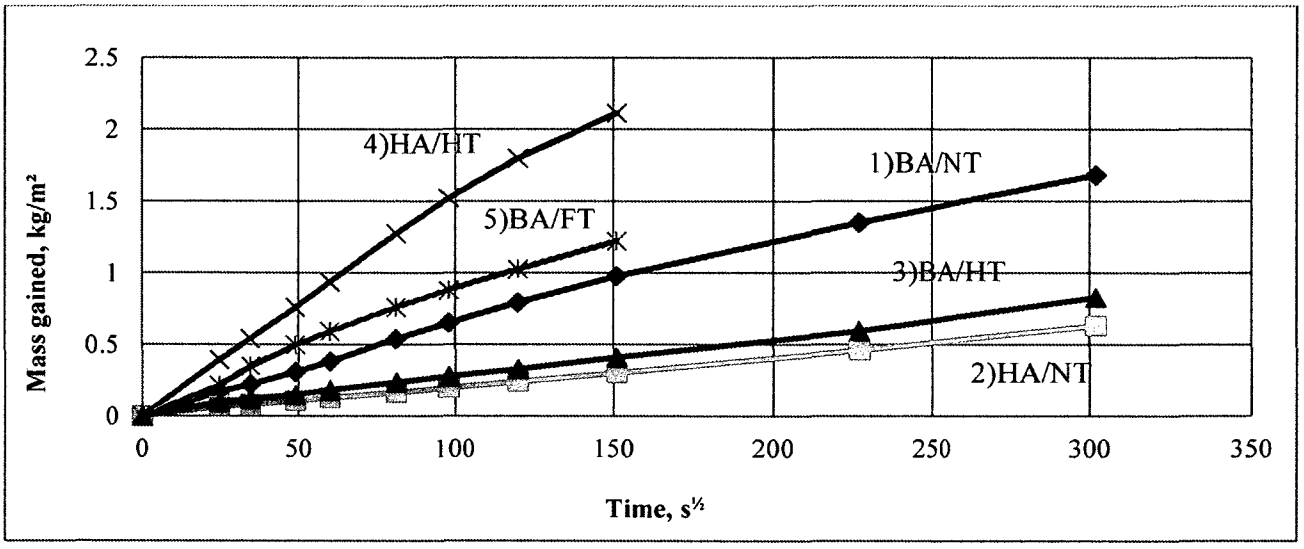

Figure 5.1 Partial immersion results for sealant test labeled by method number and sealant index (different configurations using aluminum tape and wax. Tape: NT = No tape, HT = Tape on central half of specimen edge, and FT = Tape on full specimen edge. Wax: BA = Brush application on non-heated specimen edge and HA =Brush application on heated specimen edge).

Since the brush application on heated specimen edge application is least permeable, easier to apply and does not use tape, it was chosen as the preferred method to seal the edges of the CLT

specimens. After testing Hem-Fir again and testing the other specimens using an improved wax seal, the diffusivity was found to be two times lower as shown in Figure 5.2 with a difference between Hem-Fir 1 and Hem-Fir 2. The diffusion coefficient, or diffusivity, of the CLT specimens is presented in Table 5.3. These coefficients can be noticed by the linear slope of the gain per square root time.

Table 5.3: Diffusion coefficient of CLT specimens

Material	Diffusion Coefficient ($kg/m^2 \cdot s^{1/2}$)	Standard Deviation
Hem-Fir 1	5.55×10^{-3}	$\pm 9.80 \times 10^{-4}$
Hem-Fir 2	2.49×10^{-3}	$\pm 1.93 \times 10^{-4}$
ESPF	1.97×10^{-3}	$\pm 2.10 \times 10^{-4}$
WSPF	1.89×10^{-3}	$\pm 3.64 \times 10^{-4}$
Euro	1.63×10^{-3}	$\pm 3.29 \times 10^{-4}$

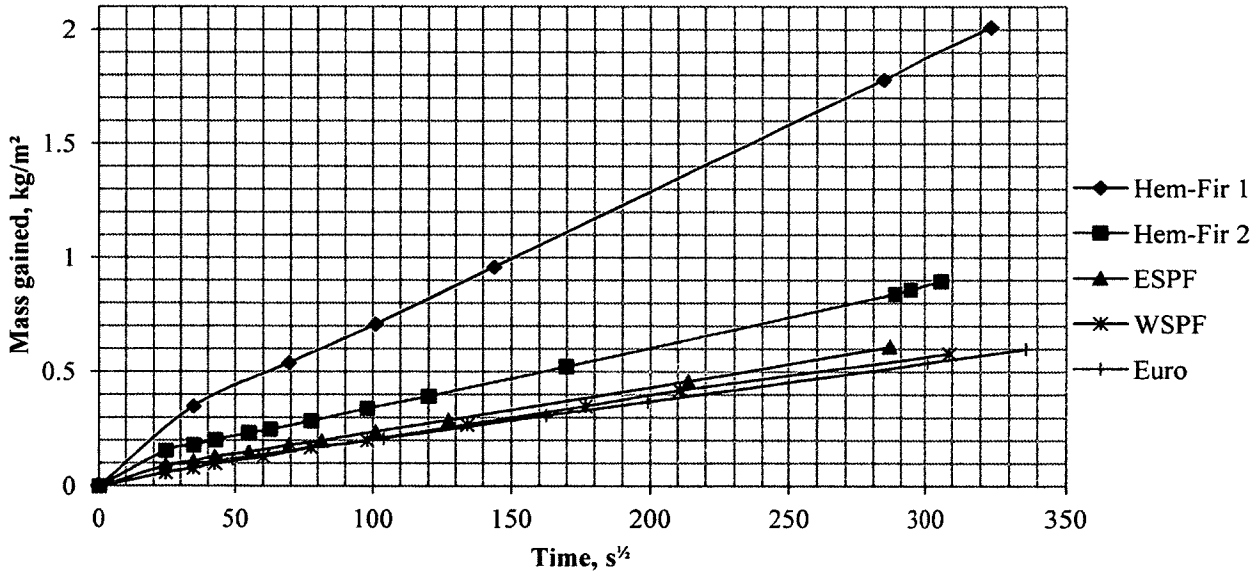

Figure 5.2 Results from the partial immersion tests

Results from previous studies by Wu (2007) reported that spruce has an absorption coefficient of 12 $x10^{-3}$ $kg/m^2 \cdot s^{1/2}$. This number shows how moisture is absorbed faster in without the laminate layer, in which it is six times more permeable than ESPF, WSPF and the European specimen, which has an absorption coefficient of 1.97 x 10^{-3} , 1.89 x 10^{-3} and 1.63 x 10^{-3} $kg/m^2 \cdot s^{1/2}$, respectively. This demonstrates that the adhesive layer limited the movement of air and moisture across the specimen used in this research.

5.3 Water Vapour Transport

After calculating the water vapour transport for four CLT specimens, it can be noticed that the water vapour permeability of CLT is almost similar. The results from the permeability tests are presented in Figure 4.3, along with the permeability rates obtained from previous research for comparison purposes. Due to limited literature on CLT, the water vapour permeability of plain wood was used for comparison. In general, permeability of CLT, Canadian and European specimens, and the permeability of plain wood are similar (Figure 5.3).

Table 5.4: Water vapour permeability measurements

		Water vapour permeability (kg/m·s·Pa)		
Chamber RH:		50%	70%	90%
Desiccant method 0% RH	Hem-Fir	(6.76 ±1.55) $x10^{-13}$	(9.04 ±1.45) $x10^{-13}$	(11.7 ±0.81) $x10^{-13}$
	ESPF	(5.71 ±2.15) $x10^{-13}$	(9.25 ±1.94) $x10^{-13}$	(13.5 ±1.30) $x10^{-13}$
	WSPF	(4.11 ±1.25) $x10^{-13}$	(8.87 ±2.16) $x10^{-13}$	(10.8 ±1.64) $x10^{-13}$
	Euro	(7.59 ±0.82) $x10^{-13}$	(12.7 ±1.46) $x10^{-13}$	(25.2 ±3.68) $x10^{-13}$
Water method 100% RH	Hem-Fir	(42.8 ±4.94) $x10^{-13}$	(60.2 ±5.41) $x10^{-13}$	(126 ±9.11) $x10^{-13}$
	ESPF	(42.8 ±7.98) $x10^{-13}$	(63.6 ±10.7) $x10^{-13}$	(135 ±19.0) $x10^{-13}$
	WSPF	(38.3 ±4.80) $x10^{-13}$	(56.4 ±6.41) $x10^{-13}$	(93.8 ±9.59) $x10^{-13}$
	Euro	(60.3 ±11.9) $x10^{-13}$	(83.4 ±18.6) $x10^{-13}$	(110 ±25.7) $x10^{-13}$

Raji et al. (2009) measured the water vapour permeability through a stacked laminated timber wall using the gravimetric method, and found a higher WVP for a solid wood pine than a laminated pine as the adhesive in the material acted as a seal for the moisture movement.

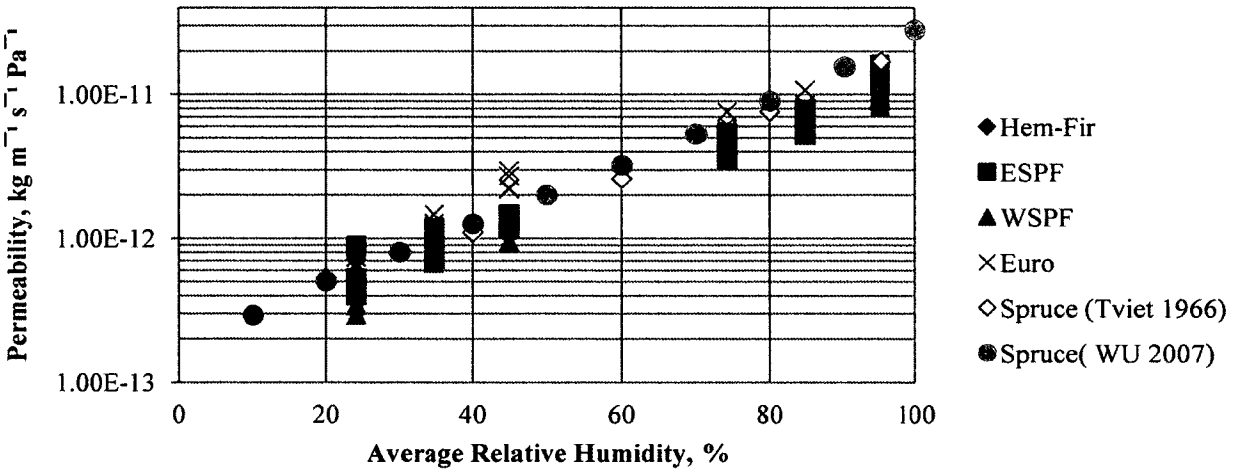

Figure 5.3 Water vapour permeability of CLT specimens (logarithmic scale)

5.4 Equilibrium Moisture Content (EMC)

The EMC experiment was performed on plain wood specimens cut from the CLT. The EMC of the glue was not measured especially that the glue's weight represents less than 1% of the overall weight of CLT; therefore, calculating the EMC of CLT could be assumed to be similar to the EMC of wood. The results of this experiment are presented in Table 5.5 as measured from the lab experiments.

The sorption results for two groups from four different sets of CLT specimens provided similar results, as well as following the same curve as plain wood that was reported by other researchers (Ahlgren 1972, Absetz 1993, Tveita 1966, Time 1998, Raji et al. 2009). Five to six specimens per set per specie was tested for adsorption. The results of this study have been fitted to a Hailwood and Horrobin model as the parameters for the different values are shown in Table 5.6

and the curve have been plotted in Figure 5.4. These model have their uncertainty analyzed using the sum of squares of residual per number (Sr/n) which was discussed previously. Figure 5.4 shows the adsorption results for every set of specimens tested in this experiment. It can be noticed that most of the specimens had similar EMC within the range of 50% RH to 95% RH. Because the EMC of various set are the same, an overall EMC was calculated, as shown in Table 5.5, to compare to the previous literature (Tviet 1966, Ahlgren 1972, Absetz 1993, Time 1998, Raji et al. 2009, Glass and Zelinka 2010).

Table 5.5: Measurements of EMC of CLT by adsorption

Specimens MC		Adsorption			
		50%	70%	90%	95%
Hem-Fir	set 1	7.80 ±0.25%	11.1 ±0.39%	20.3 ±0.90%	23.5 ±1.12%
Hem-Fir	set 2	8.05 ±0.13%	11.2 ±0.21%	20.5 ±0.62%	21.2 ±0.76%
ESPF	set 1	7.93 ±0.12%	11.2 ±0.16%	20.0 ±0.37%	21.4 ±1.62%
ESPF	set 2	7.93 ±0.22%	11.0 ±0.30%	19.2 ±0.52%	21.4 ±0.67%
WSPF	set 1	7.64 ±0.33%	10.9 ±0.43%	19.8 ±0.70%	20.6 ±0.85%
WSPF	set 2	7.82 ±0.21%	10.8 ±0.24%	18.9 ±0.50%	22.5 ±0.95%
Euro	set 1	8.00 ±0.05%	11.3 ±0.09%	20.3 ±0.21%	21.0 ±0.48%
Euro	set 2	7.92 ±0.09%	11.0 ±0.11%	19.3 ±0.24%	23.7 ±0.37%

Table 5.6: Results based on Hailwood and Horrobin model

Specimens		Method	Temp. (°C)	A	B	C	Sr/n
Hem-Fir	set 1	Adsorption	22 ±1	2.3731155	0.1495744	0.0013942	0.61
Hem-Fir	set 2	Adsorption	22 ±1	0.0854001	0.1972873	0.0016125	1.21
ESPF	set 1	Adsorption	22 ±1	0.0653117	0.2018391	0.0016576	1.21
ESPF	set 2	Adsorption	22 ±1	0.0655211	0.2083085	0.0017179	0.42
WSPF	set 1	Adsorption	22 ±1	0.0775600	0.2044250	0.0016715	1.32
WSPF	set 2	Adsorption	22 ±1	0.0775710	0.2048340	0.0016940	0.40
Euro	set 1	Adsorption	22 ±1	0.1817230	0.1926035	0.0015679	1.03
Euro	set 2	Adsorption	22 ±1	0.1817418	0.1932943	0.0016019	0.40
All Specimens Overall		Adsorption	22 ±1	1.8401560	0.1601540	0.0014200	1.02

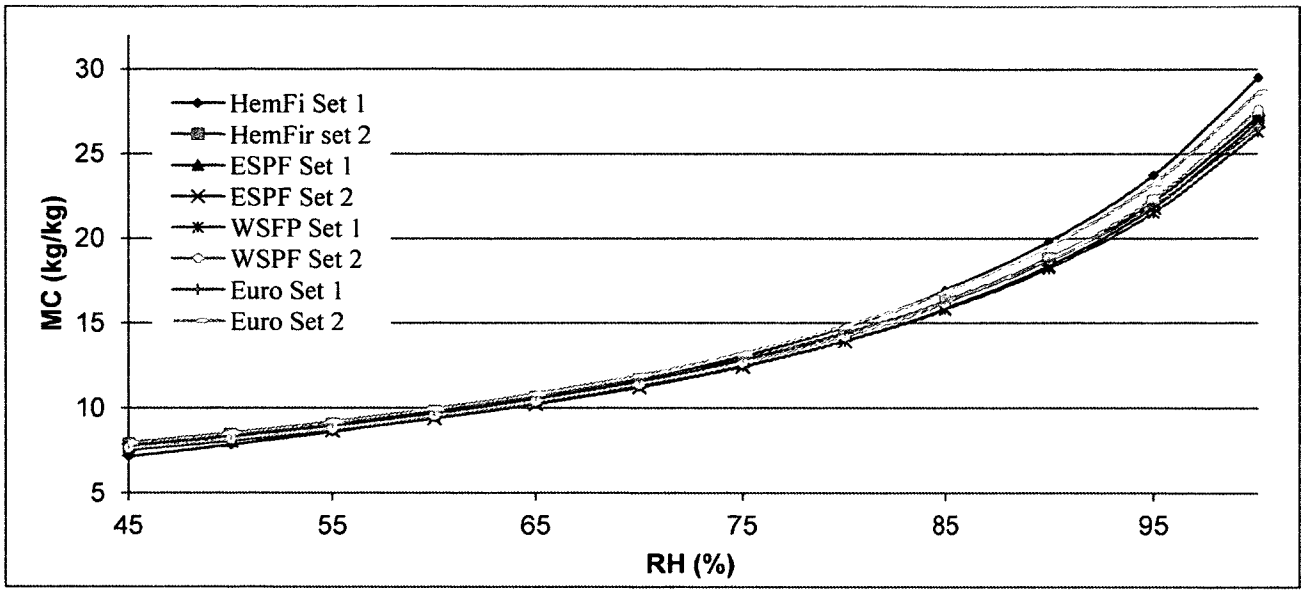

Figure 5.4 Comparison of adsorption in this study

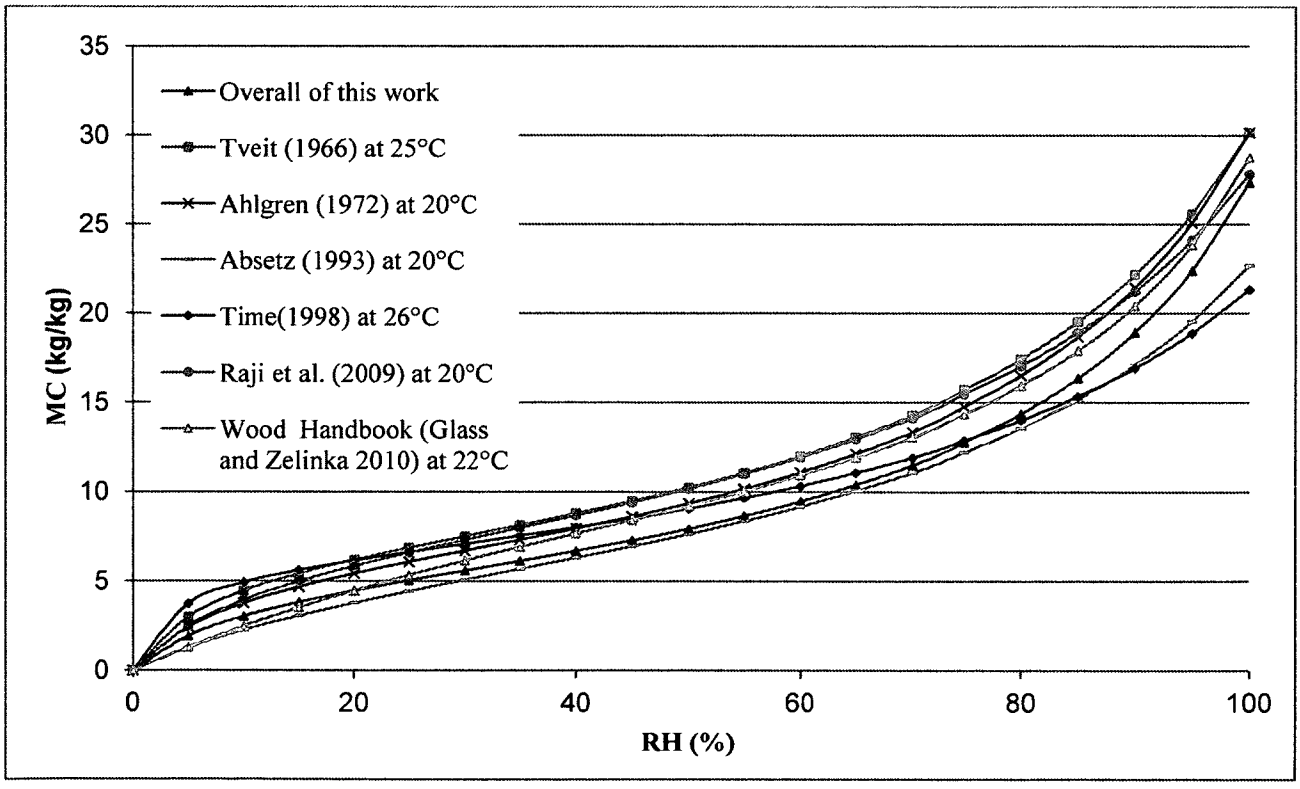

Figure 5.5 Adsorption comparison of the overall of this work to previous studies except for Tviet(1966) and Glass and Zelink(2010) which are sorption.

5.5 **Air Permeability**

At a temperature of 22°C, the air permeability tests showed that six specimens were impermeable, with no measurable air flow under the applied high pressure gradient. The least favorable air flow was found in specimen "Hem-Fir 1" that had a visible gap, as shown in Figure 5.6. The results of this experiment are presented in Table 5.7 as it shows the thickness of the materials and its permeability. Under these test conditions, impermeable does not necessarily mean that air cannot flow through the specimen, but that the air movement is very low and requires a more sensitive air flow measuring system.

Table 5.7: Air permeance and permeability of CLT specimens

Sample #	Thickness (mm)	Permeance l/((75 Pa)m²·s)	Permeability l/((75 Pa)m·s)	Permeability kg/Pa·m·s	Mean Permeability (Standard Dev.)
Hem-Fir 1	18.39	452×10^{-3}	8.31×10^{-3}	133×10^{-9}	53.6×10^{-9} (69.4×10^{-9})
Hem-Fir 2	18.45	13.6×10^{-3}	0.25×10^{-3}	4.02×10^{-9}	
Hem-Fir 3	18.48	79.9×10^{-3}	1.48×10^{-3}	23.7×10^{-9}	
ESPF 1	18.85	356×10^{-3}	6.72×10^{-3}	108×10^{-9}	58.4×10^{-9} (69.7×10^{-9})
ESPF 2	18.29	32.0×10^{-3}	0.585×10^{-3}	9.36×10^{-9}	
ESPF 3	18.48	Impermeable	Impermeable	Impermeable	
WSPF 1	18.84	Impermeable	Impermeable	Impermeable	4.06×10^{-9}
WSPF 2	18.87	Impermeable	Impermeable	Impermeable	
WSPF 3	18.97	13.4×10^{-3}	0.254×10^{-3}	4.06×10^{-9}	
Euro 1	18.39	Impermeable	Impermeable	Impermeable	Impermeable
Euro 2	18.69	Impermeable	Impermeable	Impermeable	
Euro 3	17.80	Impermeable	Impermeable	Impermeable	

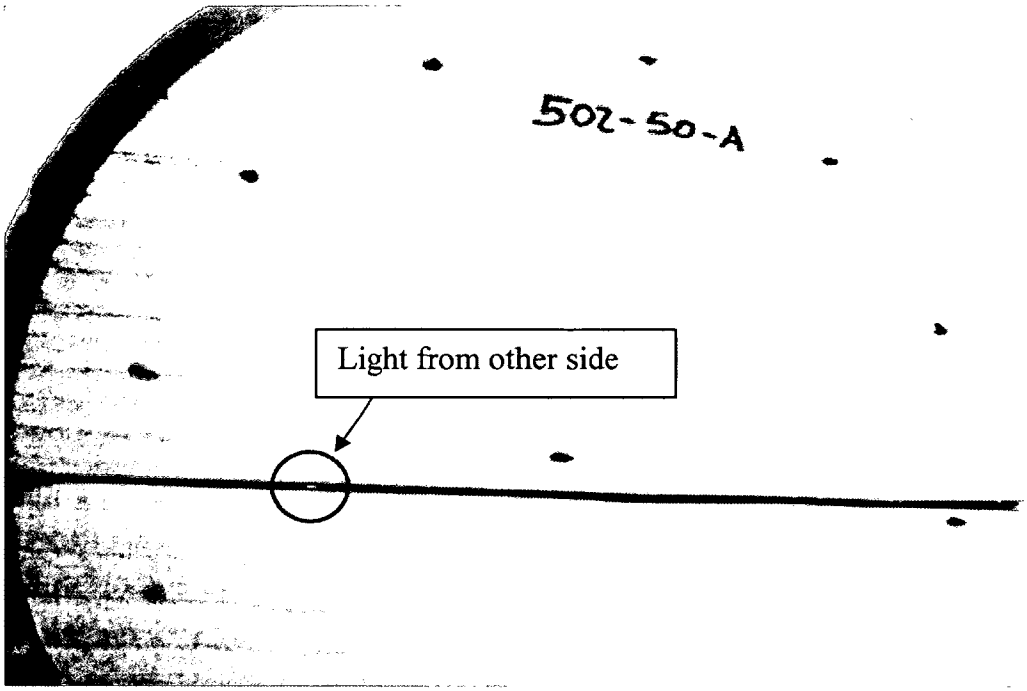

Figure 5.6 Specimen (Hem-Fir 1) with most air flow due to small gap between the connections

Results showed that Hem-Fir is the most permeable while ESPF is next permeable. WSPF is least permeable especially that two specimens were impermeable; however, European spruce was impermeable to air. Although theses data show the air permeability of CLT specimens with only one adhesive layer, the air permeability of CLT is expected to be much less due to the additional layers of adhesive. To compare these results to previous data, CLT is less permeable compared to wood used in building construction. As Wu (2007) reported that spruce had a permeability of $(7.2 \pm 1) \times 10^{-9}$ kg/m·Pa·s, which is higher compared to European spruce and WSPF. As one layer of adhesive was experiment, these experiments proved that wood could be impermeable to air especially that CLT thickness is above 100mm and is composed of more than one layer of adhesive.

5.6 Summary

The tests performed were part of an investigation for evaluating methods to quantify the hygrothermal properties of CLT. Most of these tests have successfully derived results that are comparable to investigations performed on wood and stacked laminated timber. Plain wood, European CLT and Canadian CLT showed similar results when tested for thermal conductivity, EMC, and water vapour permeability. Meanwhile, the water absorption test showed a difference between plain wood and CLT; as CLT was capable of absorbing moisture at a lower rate while plain wood absorbed moisture at a high rate. As for air permeability, most CLT specimens were robust to air flow except for some specimens, which were Hem-Fir and ESPF, in which Hem-Fir contained a visible gap within the joints. The CLT method of construction will require more than one layer of laminate so that these gaps will not be present due to the moisture retention stored in the core of the CLT panel.

Chapter 6 **Wood Moisture Content at High Relative Humidity**

6.1 **Introduction**

Determination of the Equilibrium Moisture Content (EMC) of wood at near-saturated relative humidity (RH) is a challenging task. However, EMC at near-saturated RH (greater than 95 % RH) is very important for the assessment of moisture management performance of the wood or wood-based building materials in humid locations. There is a disagreement among researchers concerning the methodology used to determine EMC of wood at high RH using the pressure plate apparatus. The pressure plate apparatus was originally developed to study the moisture content of soils, but this method has been used for wood by Mukhopadhyaya et al. (2011) and Almeida and Hernandez (2006), and is applied to various building materials by ASTM C1699 (2009). It is worth mentioning that this method is the only available method to determine the EMC of wood at high RH. However, Wang et al. (2011) questioned the use of the pressure plate apparatus to determine the EMC at near-saturated conditions. Due to the limited information on EMC of wood at high RH, an interpolation of the wood EMC using a sorption curve and full saturation was used to verify the response of the material at near saturated RH. This is done by considering the best fit of the EMC of wood from sorption, which is considered between 0% RH to 95% RH and is determined using the chamber method (ASTM C1498 2004), and full saturation, which is considered at 100% RH and is determined by immersing wood in water (ASTM C1699 2009).

As the EMC at high RH is considerably critical for very humid location, this study assessed the response of wood within a building wall using a state of the art simulation technique. Although identifying the exact EMC property of wood at high RH is a challenging task, it can be

approached by initially simulating the approximate EMC properties in wood to determine its hygrothermal response. This response will help determining the criticality of EMC at near saturated RH ranges in humid locations.

The sorption-desorption properties of red pine were determined by Mukhopadhyaya et al. (2009) in the NRC-IRC's laboratory using humidity chambers (ASTM C1498 2004) and pressure plate apparatus (ASTM C1699 2009), as discussed earlier. Four different cases of EMC at near-saturated RH levels (i.e. part of the sorption isotherm) were considered for red pine to critically assess the impact of wood EMC property at near-saturated RH. The assessment used NRC-IRC's hygrothermal simulation tool called hygIRC-2D based on a case study testing wood frame stucco walls using a wall model tested by Mukhopadhyaya et al. (2009). The only variable component was the sorption isotherm of red pine, which involved four different cases (discussed below), and the remaining hygrothermal properties of red pine were taken of eastern white pine properties, as available in the NRC-IRC's materials properties database (Kumaran et al. 2002). The interpolated cases of EMC at high RH were combined with the other properties of wood to determine the different effects on the durability of the wood.

6.2 Varying Equilibrium Moisture Content Cases

The cases of EMC were interpolated from the report of Mukhopadhyaya et al. (2011). Since most researchers agree on the results for RH up to 95 %, the interpolation was based on changes in the EMC results above 95 %. Four different cases were considered for this parametric study, as outlined below:

Case 1: The best fit curve derived from the sorption results (using humidity chambers) and pressure plate results available in Mukhopadhyaya et al. (2011).

Case 2: The best fit curve for sorption up to 100 % RH, derived from humidity chamber and capillary saturation measurement data.

Case 3: The best fit curve derived from humidity chamber measurements, up to 95 % RH, and then linear to capillary saturation measurement data to FSP at 100 % RH.

Case 4: The best fit curve derived from humidity chamber measurement, up to 95 % RH, then another best fit curve for pressure plate measurement data from 95 % to 100 % RH.

Cases 2, 3 and 4 have the same sorption results from 0 to 95 %, while Case 1 has small differences due to including the pressure plate apparatus measurements, which requires ignoring the result from sorption at 95 %, as shown in Figure 6.1. Further details on the model of each case are presented in Appendix C.

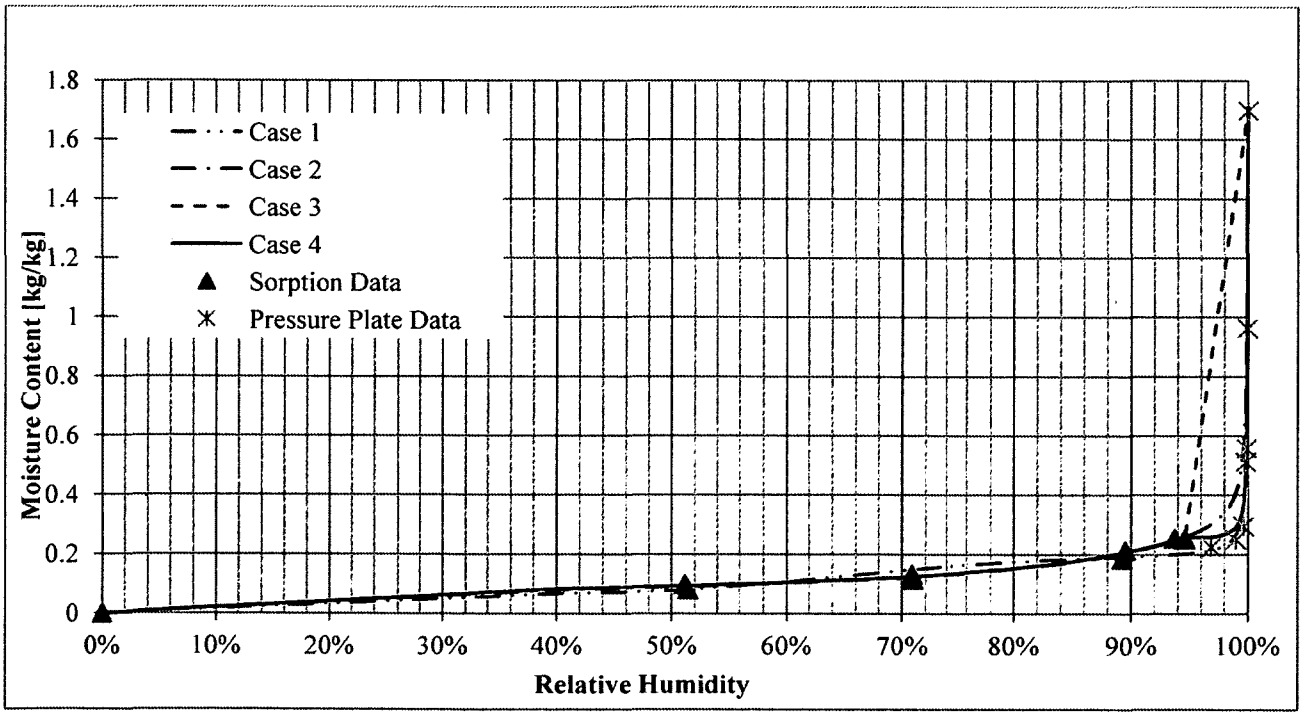

Figure 6.1 Sorption curve for the various cases

6.3 Hygrothermal Modeling Parameters

Based on some of the previous modeling tests that were conducted at NRC (Mukhopadhyaya et al. 2009), HAM transfer modeling was performed to check the hygrothermal effects on a wood frame stucco wall assembly, as shown in Figure 6.2. The materials used in the wall assembly were the same as the materials used by Mukhopadhyaya et al. (2009), and the properties of the materials were based on the NRC database (Kumaran et al. 2002). However, the EMC of wood within the assembly was based on the four cases mentioned above. Each EMC case was considered in a different simulation in which all other parameters were kept constant so that the results could be comparable to one another in terms of EMC alone. The material, labelled in a matrix in Table 6.1, used in the assembly includes, from the exterior to the interior, (1) limestone stucco, (2) sheathing membrane, (3) air gap, (4) oriented strand board (OSB), (5) red pine studs, (6) glass fibre insulation, (7) polythene sheet and (8) paint coated gypsum board. Figure 6.2 shows various components of the walls and their dimensions. To simulate the assembly, the model was composed of 891 nodes in a matrix of 33x27, and each material was represented in the matrix as arranged in Table 6.1. On the horizontal and vertical axes, the nodes were distributed in a normal distribution as specified by the software.

Table 6.1: Wood frame stucco wall assembly matrix for simulation

<table>
<tr><td rowspan="3">(1)
limestone
stucco
(5x27)</td><td rowspan="3">(2)
sheathing
membrane
(3x27)</td><td rowspan="3">(3)
Air gap
(3x27)</td><td>(4)
OSB
(4x8)</td><td>(5)
Top red Pine
(9x3)</td><td rowspan="3">(6)
Polythene
sheet
(3x27)</td><td rowspan="3">(7)
Paint
coated
gypsum
board
(5x27)</td></tr>
<tr><td>(3)
Air Gap
(4x3)</td><td>(6)
Glass fibre
(9x19)</td></tr>
<tr><td>(4)
OSB
(4x16)</td><td>(5)
Bottom red
pine (9x5)</td></tr>
</table>

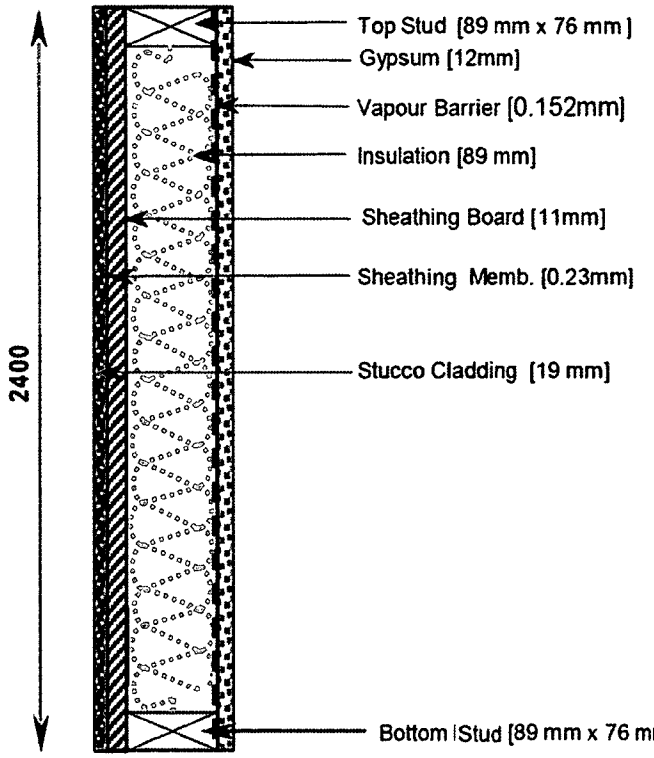

Figure 6.2 Wall assembly details (adopted from Mukhopadhyaya et al. 2009)

The interior and the exterior boundary conditions are required for the hygIRC-2D. The interior parameters required by hygIRC-2D are temperature and RH, and the exterior conditions are temperature, RH, wind velocity, wind direction, radiation (direct, diffused and reflective components), horizontal rainfall and cloud index.

The wettest boundary conditions were used to model the assembly since the purpose of the test was to determine the EMC of wood at high RH. For the interior boundary condition, the indoor temperature was set to 26 °C, and the RH was set to 65%, and for the external boundary conditions were based on the climate of Vancouver, B.C., which is considered an extreme condition since it is relatively mild and wet. The weather conditions were chosen using the Moisture Index approach as suggested by Cornick et al.(2003). The weather in the first year of the simulation was based on an average of year 1969 according to the MI approach (Cornick et al. 2003). As Cornick et al. (2003) have modeled various years to identify the wet (worst year)

and the dry (best year) years based on 5 different wall assemblies in Vancouver, BC. The wet year considered in this simulation was year 1963 as it is considered the worst year (Cornick et al. 2003).

6.4 Results

Output from the hygIRC-2D model includes RH, MC and temperature of the wall. The data was obtained from the 891 nodes in the model as performed by Mukhopadhyaya et al. (2009). Figure 6.3 shows RH contour lines related to the various RH levels within the assembly. Four different locations were probed on the wood which contained most of the moisture, as shown in Figures 6.4 and 6.5. These locations were at the interior side of the wall assembly, and at the corners of the wood studs. Based on this data, the RH and MC of the wall assembly at the location with maximum surrounding RH was measured, since the MC of the material increases relative to the RH increases.

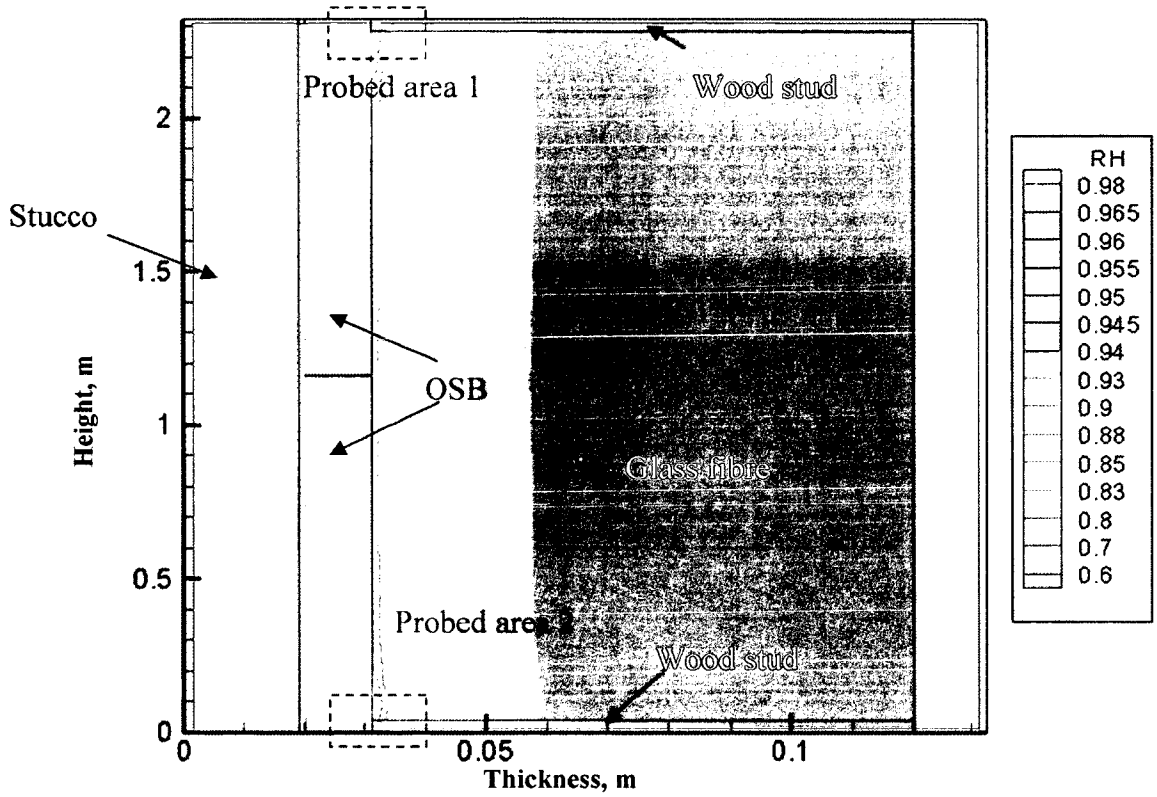

Figure 6.3 Relative humidity at day 383 of the modeling based on the cross section of the wall (expanded view, scale in meters).

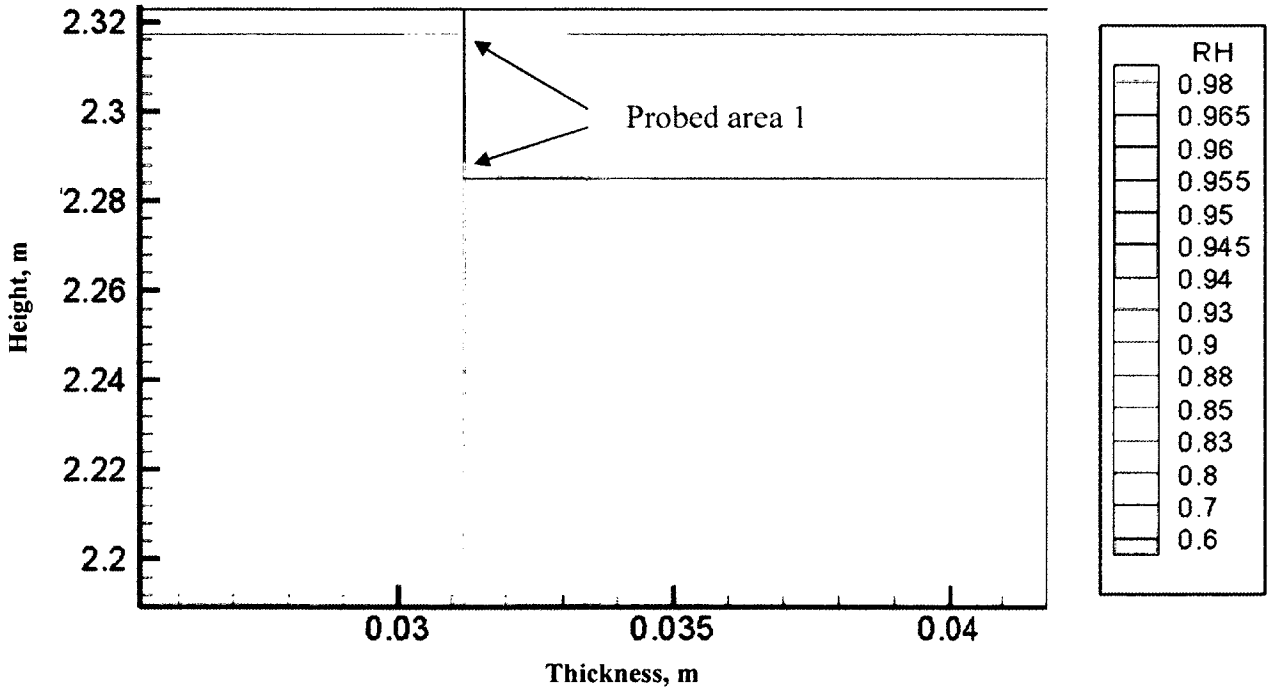

Figure 6.4 Top sill RH at day 383 (Probed area 1)

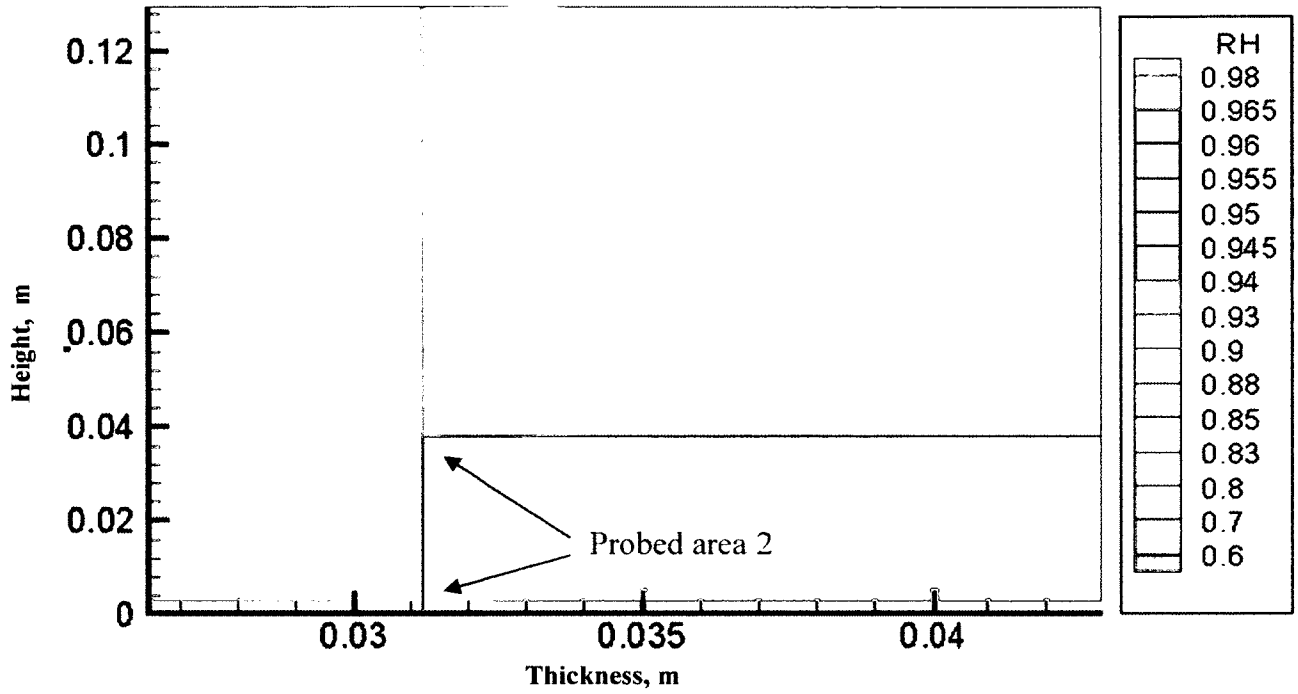

Figure 6.5 Bottom sill RH at day 383 (Probed area 2)

Based on the animation of the moisture contour movement within the wood specimen, the corners were found to be more sensitive to changes in MC. The movement of the moisture was slower at the center of the sill than at the edges. Therefore, the most sensitive areas of the wood for the short term are the edges, especially the corners, while the most affected areas for the long term are the inner portions of the specimens. The moisture movement was relatively fast at the corner of the stud which was exposed to glass fibre insulation. Because moisture movement is faster in the glass fibre, this explains the simulated characteristic of moisture movement at the corner of the sill. The bottom corner of the top sill was of main interest to this study because it contained the highest MC compared to the other corners.

Figure 6.6 and Figure 6.7 represent the RH and MC at probed location, located at the bottom corner of the top sill. Figure 6.6 shows how the RH fluctuates during a whole year. The first year (0 to 365 days) shows how the material is reaching its equilibrium state, while the second year

(365-720 days) shows the RH at the probed location during the wet year. In the simulated results, each year begins on January 1st. As shown in the Figure 6.6, the RH at that the probed location depends on the season's weather condition. Figure 6.7 is dependent on two factors: first is the RH as represented in Figure 6.6 and second is the EMC that was generated for the four cases.

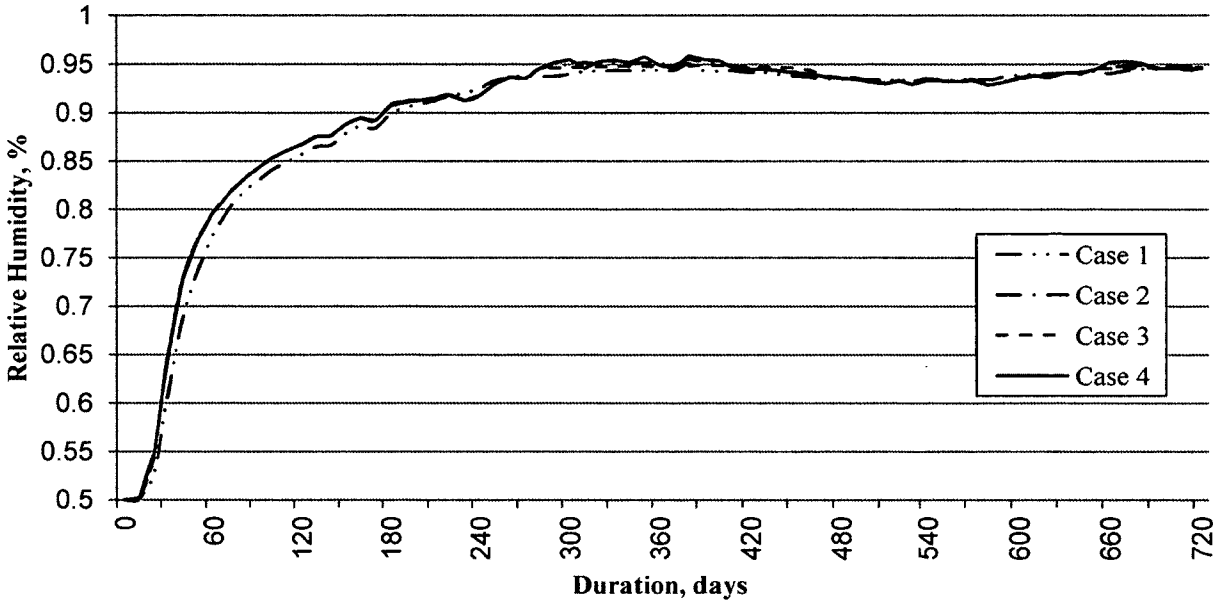

Figure 6.6 Relative humidity comparison between four different cases at bottom corner of the top sill

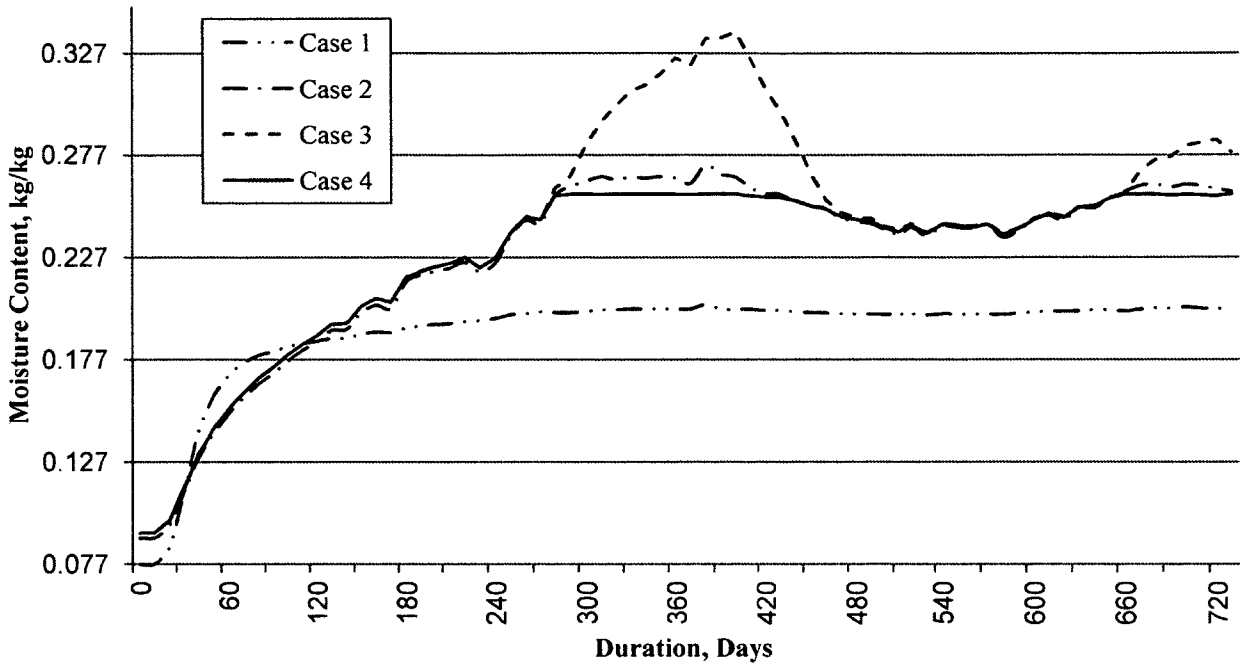

Figure 6.7 Moisture content comparison between the four different cases at bottom corner of the top sill

Based on the results presented in Figures 6.6 and 6.7, the maximum MC in Case 1 was the lowest among the four cases considered, at approximately 0.2 kg/kg, and Case 2, 3 and 4 had the MC above 0.2 kg/kg, which indicates conditions suitable to initiate decay. Moreover, the MC of these three cases varied throughout the winter months, which are from day 0 to day 60, from day 330 to day 420 and from day 700 to day 730. Although in all four cases the maximum RH remained around 94%, the maximum MC occurred during the winter months. The first observation is in the relationship between Case 1 and the other cases in which the sorption was different on most of the scale. The second observation is in the relationship between Case 2, Case 3 and Case 4, which are equivalent in the range of 0 to 95 %, but differ greatly from 95 to 100 %. The difference between these relationships is shown in Figure 6.8, as it shows the impact of EMC at certain RH ranges on the moisture content of wood during the modeled period. These

observations clearly highlight the importance of an appropriate characterization of wood sorption behaviour at near-saturated RH for the moisture management performance assessment of wood-frame constructions (e.g. wood-frame stucco wall) used in Canada.

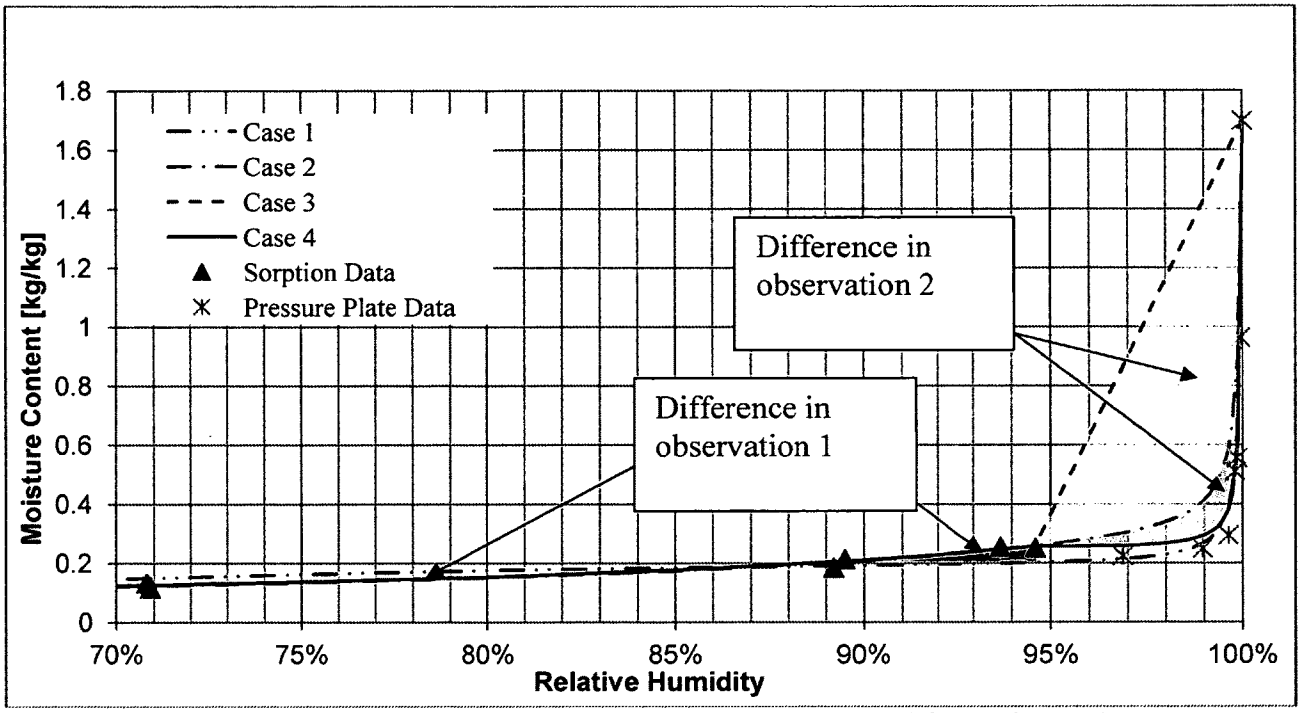

Figure 6.8 Different analysis on the model generated from Figure 6.1

6.5 Observations

6.5.1 Observation 1

Based on Figures 6.6 and 6.7, the MC in Case 1 remained the lowest at approximately 0.2 kg / kg, although the RH fluctuated around 94%. This could be due to the low sorption curve of Case 1 at 98.9% RH. Cases 2, 3 and 4 have the same sorption values up to 95%, but the moisture content and the RH of the wood deviates above 95 % RH.

Based on the EMC curve for Case 1, the MC at critical RH didn't exceed 0.21 kg / kg, although the RH at that location fluctuated around 94%. In the other cases, the MC based on a 95% RH

exposure, was considered high as reported by both the sorption analysis and pressure plate apparatus.

For observation 1, one could question the reliability of having a EMC at 95% RH and the reliability of the pressure plate apparatus results; although both of these measurement protocols are industry standards. Based on the results of standard wood frame stucco design, one can conclude that sorption of up to 95% RH could affect the overall MC of the wood.

6.5.2 Observation 2

For observation 2, the comparison was made above a RH of 95%, at which point Cases 2, 3 and 4 differ until 100 % RH. In each case, the MC fluctuated around 0.25 kg / kg, with maximum MC occurring in winter, at 0.2720, 0.3375, and 0.2579 kg / kg for Cases 2, 3 and 4 respectively. The MC of the three cases was similar during the other seasons.

From this observation, it can be seen that determining the sorption curve above 95% is critical, because it quantifies the speed at which biological elements can grow on wood during the winter. In this analysis, the difference in sorption curves above 95% would affect the curves during the winter season.

6.6 Sensitivity of Hygrothermal Analysis to the Uncertainty of the Input Data to the Model

The hygrothermal analysis for determining the effect of the changing EMC of wood on the MC of wood within the model using four different cases for EMC properties for wood was successful. However, it is needed to investigate the uncertainty in the EMC cases that were provided. This section aims to describe to what extent the model results are affected by a change

in the input, due to uncertainty. This technique was addressed by Cornick et al. (2009) who focused on making the practitioner aware "*of uncertainty by stating error bands for their prediction of performance*". Cornick et al. (2009) did so by studying the uncertainty of wind driven rain and using various rainfall intensity to identify the error bands for different rainfall intensities. In the study by Cornick et al. (2009), the error bands were analysed for the MC of wood at the same location that was analysed in this study. The error bands from the uncertainty were demonstrated in mean bias error (MBE), which uses the following equation:

$$MBE = \frac{1}{n}\sum_{i=1}^{n}[(x_{band} - x_{base})/x_{base}] \qquad \text{Equation 6.1}$$

Where *MBE* is the mean bias error, n is the number of data points assessed, X_{band} is the error band, and X_{base} is the base data. It is worth noting that the error band and base data measured in this study is the output moisture content of the wood during the modeled duration.

Additional uncertainties were considered in this analysis. These include internal temperature and internal RH. The uncertainty in the EMC of wood, internal temperature and internal RH was assumed to be ±10%. These uncertainty values were modeled separately to identify the effect of each. The output bands, represented in MC of wood at the probed location, for the uncertainty in EMC, internal temperature and internal RH are shown in Figures 6.9, 6.10, 6.11 and 6.12 respectively; and the MBE for the bands are presented in Table 6.2. A positive MBE means that the MC band is positive in relation to the main band and vice versa.

Table 6.2: Mean bias error in MC of wood

		MBE of Moisture Content of wood			
	Adjustment	Case 1	Case 2	Case 3	Case 4
EMC +10%	EMC curve +10%	9.65%	9.08%	5.25%	9.22%
EMC - 10%	EMC curve -10%	-9.71%	-9.23%	-9.39%	-9.70%
Int. Temp +10%	Int Temp = 28.6	-0.70%	-2.99%	-6.46%	-2.20%
Int. Temp -10%	Int Temp = 23.4	0.98%	3.82%	19.2%	1.10%
Int. RH +10%	Int RH = 71.5	0.68%	2.41%	9.34%	1.17%
Int. RH - 10%	Int RH = 58.5	-0.70%	-2.17%	-5.23%	-1.54%

Based on the results shown in Table 6.2, it can be seen that an increase in the EMC of wood and internal RH increases the gain of moisture, or MC in wood, while an increase in the internal temperature reduces the gain of moisture in wood. The 10% change in the intensity of the EMC causes a major change of 9% in the moisture gain in all the cases. On the other hand, Case 3 is the most sensitive to changes in EMC, internal temperature and internal RH.

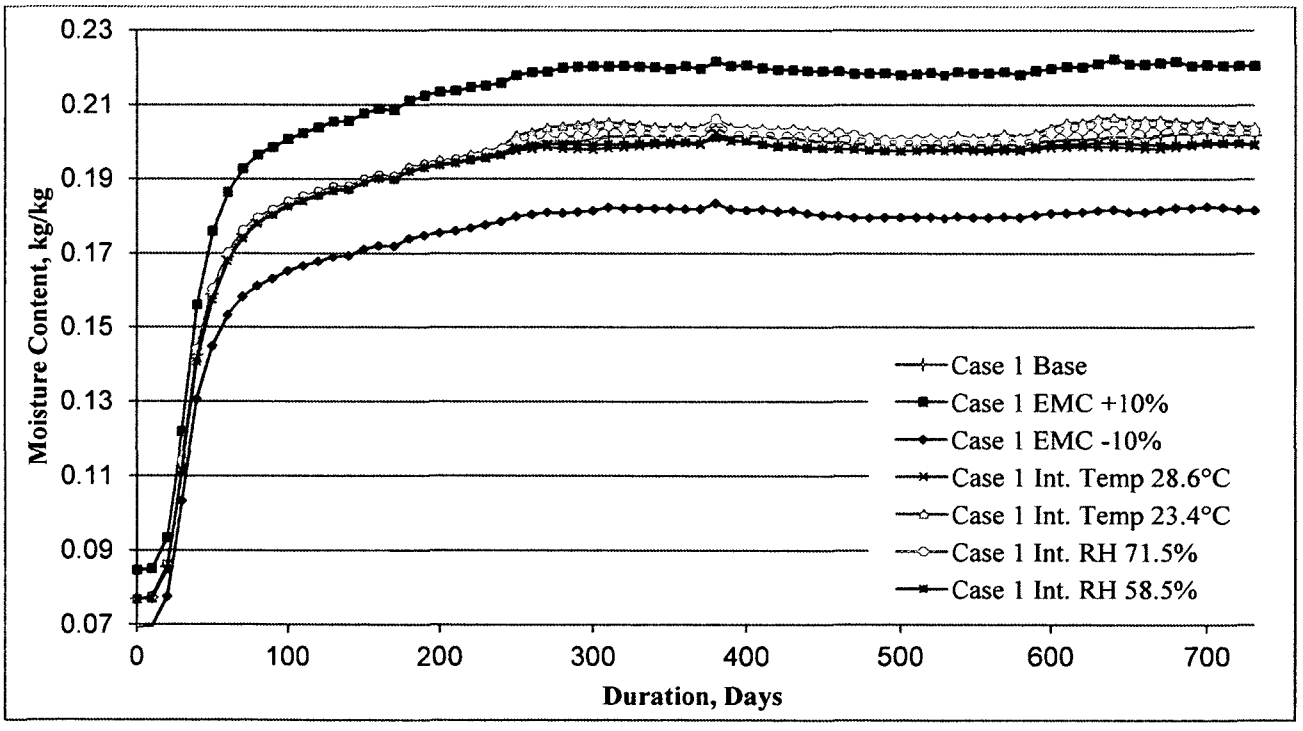

Figure 6.9 Variation in Case 1

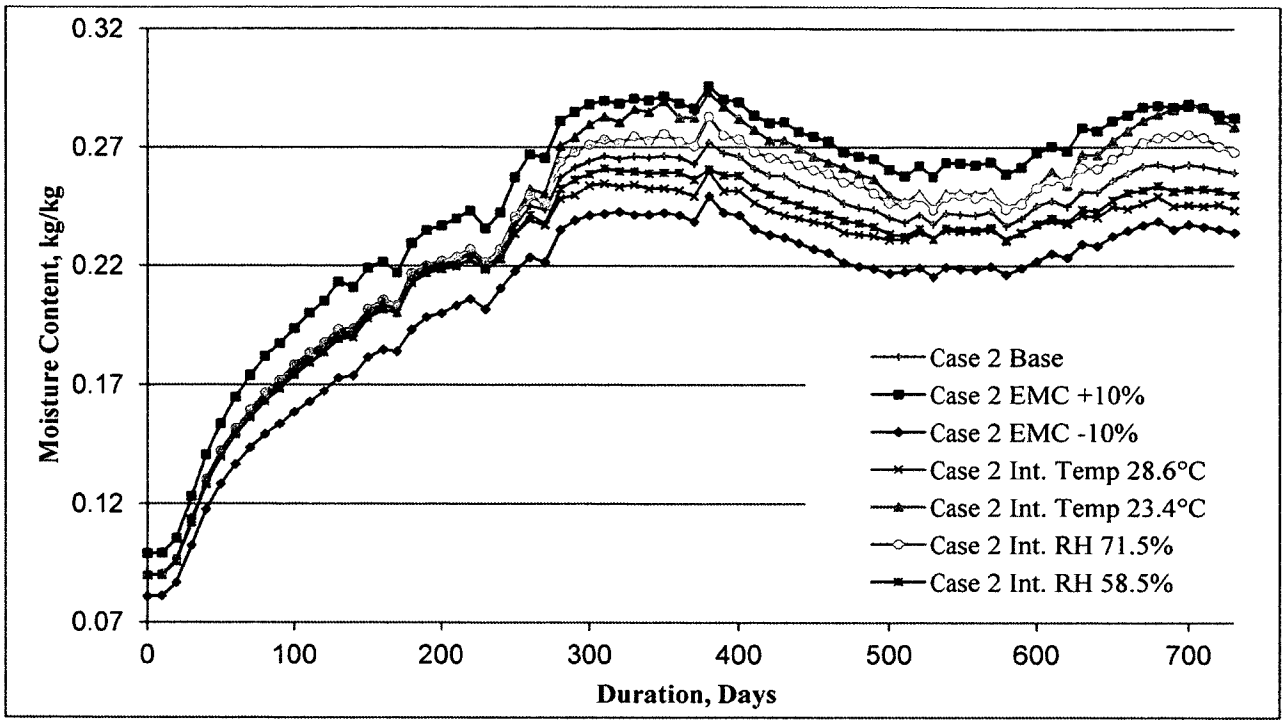

Figure 6.10 Variation in Case 2

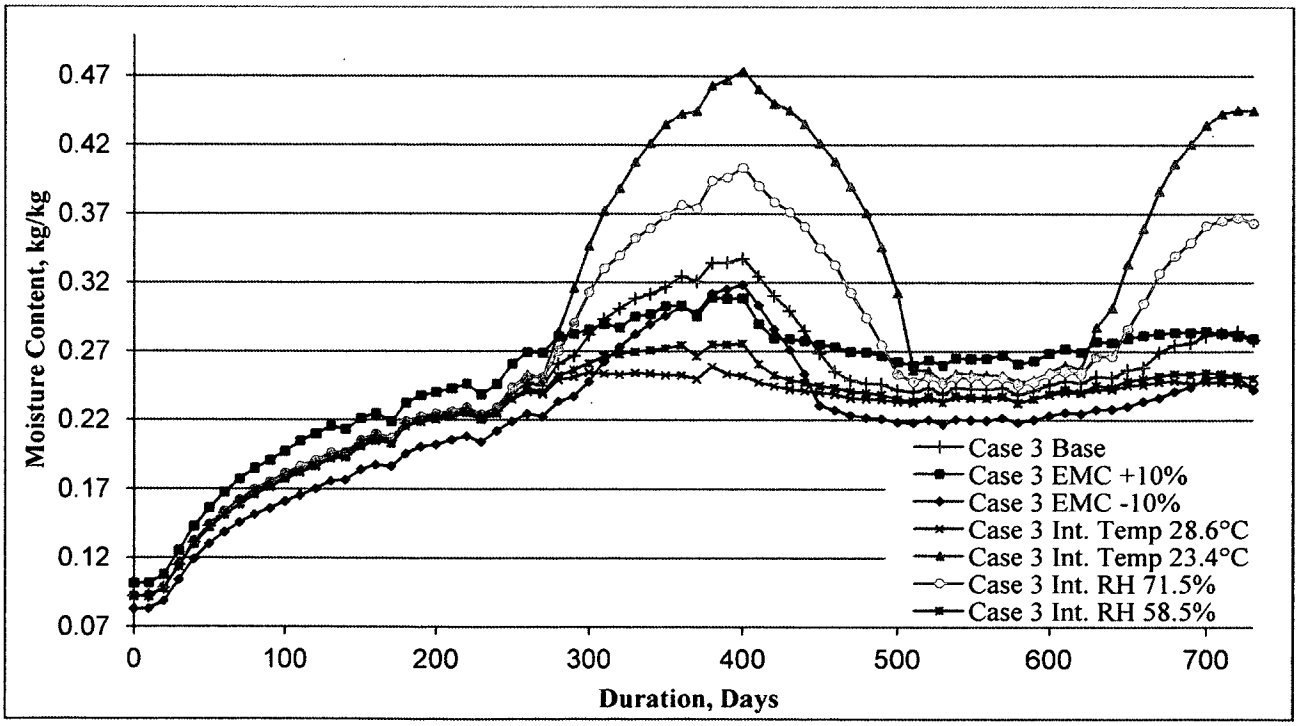

Figure 6.11 Variation in Case 3

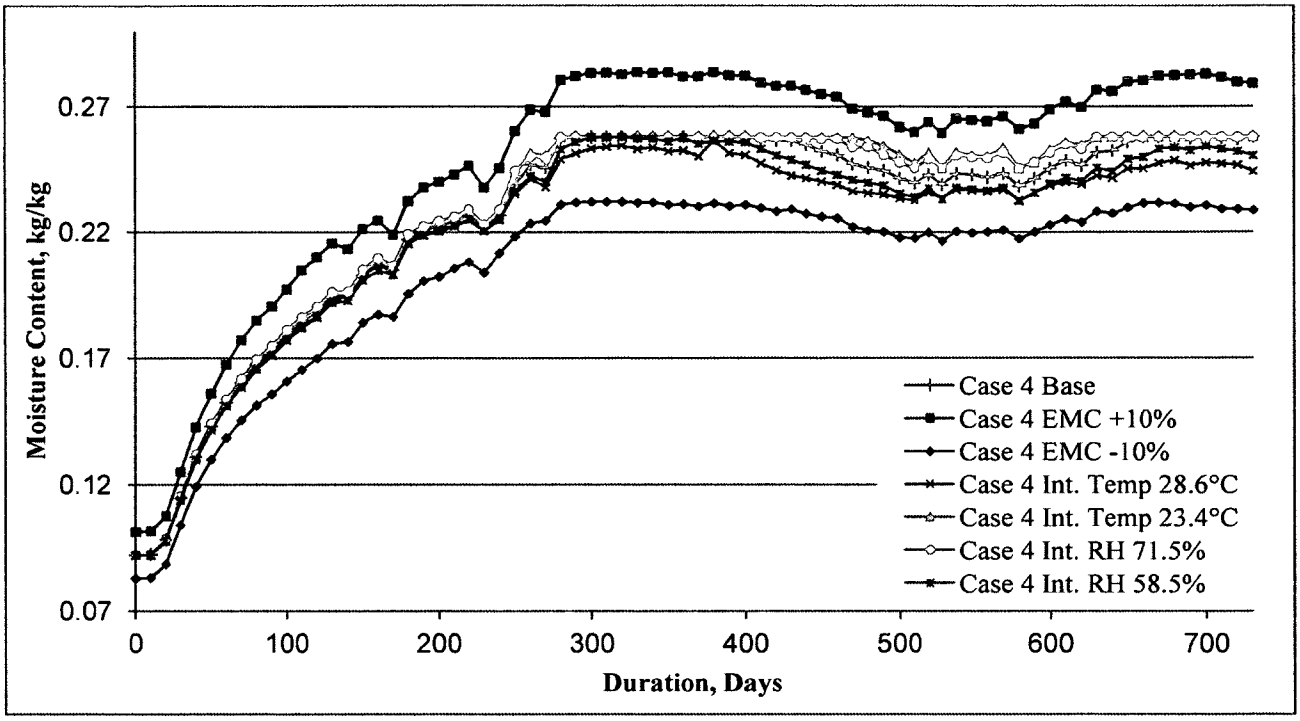

Figure 6.12 Variation in Case 4

6.7 Summary

The EMC of wood at high RH have been assessed based on the 4 possible EMC curve cases that are generated from sorption data and pressure plate apparatus test data tested from wood pine samples. The EMC of wood in Case 1, which is the best fit from the sorption data and the pressure plate apparatus test data, has a different effect on the MC of wood in a wood frame stucco wall assembly from the EMC of wood in Cases 2, 3 and 4, which is the fit using the sorption data (up to 95%). This effect was observed throughout the duration of the simulation. On the other hand, it could be observed from the differences in the EMCs of the wood in Cases 2, 3 and 4, which are different at high range of 95 to 100% RH that simulated wall was affected in winter seasons. Based on the sensitivity of the hygrothermal analysis, the uncertainty of 10%

in the EMC of wood, internal temperature and internal RH did not affect the recognized observations.

Chapter 7 **Conclusion and Recommendations**

This study investigated and presented the hygrothermal properties of Cross Laminated Timber (CLT). Experiments were conducted on four CLT specimens. Three specimens from different Canadian wood species combinations (Eastern Spruce-Pine-Fir, Western Spruce-Pine-Fir, and Hem-Fir) and one European spruce specimen. The findings from this study contribute towards evaluation of existing test methods for the determination of hygrothermal properties of wood-based materials and the determination of the hygrothermal properties of CLT.

The influence of Equilibrium Moisture Content (EMC) of wood-based material at high RH on the moisture management performance of a wood-frame wall assembly was also investigated in this study. This investigation is particularly important for appropriate determination of the adsorption / desorption isotherms for wood and wood-based materials.

7.1 **Conclusions**

The following conclusions were derived from the analysis of date in this study:

1. This study has successfully characterized the hygrothermal properties of the four CLT specimens. The hygrothermal properties determined included thermal conductivity, water vapour permeability, liquid water absorption, equilibrium moisture content (EMC), and air permeability.
2. Two properties of CLT were found to be different from wood materials commonly used in building construction:
    a. Liquid water absorption coefficients of CLT specimens were found to be lower than construction wood material properties available in the major literature.

b. The air permeability values of CLTs were dependant on the continuity of glue between the layers. While most CLT specimens were found to be impermeable, a few CLT specimens were permeable to air due to air leakage through the joint.

3. Various studies on EMC of wood were reviewed with focus on the high relative humidity (RH) range. Dissimilarities in the data for high RH were noticed in different studies. Four different possibilities of wood EMC between ≈95%-100% RH were generated from the experimental data obtained from sorption and pressure plate experiments by Mukhopadhyaya et al.(2011) .
4. The four possibilities of EMC have been critically analyzed using hygIRC-2D simulation software. The simulations were conducted for two years on a conventional wood-frame stucco wall assembly. The simulations resulted in two major findings:
    a. EMC differences at a higher RH range (i.e. 90% - 95%) result in major differences in the moisture content (MC) of the wood specimens throughout the modeling period.
    b. EMC differences at the highest RH range (i.e. 95% - 100%) result in variations in the MC of wood during winters months only.

7.2 **Recommendations for Future Research**

The introduction of CLT to the North American market has created a necessity for further investigation and research on CLT. This study has identified several ideas for future investigations that are presented below:

1. In previous testing of adhesives, various diffusion curves have been noted by Sonderegger et al. (2010) for different adhesives. Since the adhesive could affect

diffusion of moisture at high RH of over 70%, a standard protocol is required to determine the best method for applying the adhesive on the material. Moreover, the various adhesives available could have significant impacts on rupture strength, service life and permeability of the specimen. Further research is needed to determine the effect of adhesives between wood layers, and its relationship to the structural durability of the specimen under variable moisture conditions.

2. Moisture plays a major role in deforming the shape of boards, and this reaction is largely dependent on the orientation of the wood. Published literatures has identified cross lamination as an effective method for limiting board deformations. However, contraction and expansion still occur at the surface of the material. Further research is required to develop the best method to manage the effect of surface contraction and expansion in CLT.

3. The findings from the study on wood EMC at high RH, using hygIRC-2D simulation tool, indicate the need for an appropriate test method to determine the EMC of wood at near saturated RH to reflect the transition in the moisture presence in wood and to differentiate between capillary water and hygroscopic water. Further investigations are needed to develop an exclusive standard test procedure for the determination of sorption/desorption behavior of wood using both environmental chambers and pressure plate test apparatus.

References

Absetz, I. (1993). "Sorption isotherm and moisture diffusivity comparison of spruce and pine." Seminarium I Tra¨mekanik, Sweden.

Ahlgren, L. (1972). "Moisture fixation in porous building materials." (in Swedish) *Report* 36, Division of Building Technology, Lund Institute of Technology, Sweden.

Almeida, G., and Hernández, R. E. (2006). "Changes in physical properties of yellow birch below and above the fiber saturation point." *Wood Fiber Science,* 38(1):74–83.

American Society for Testing and Materials (ASTM C177) (2010). " Standard test method for steady-state heat flux measurements and thermal transmission properties by means of the guarded-hot-plate apparatus" C177, ASTM International, West Conshohocken, PA, 2010, DOI: 10.1520/C0177-10, www.astm.org

American Society for Testing and Materials (ASTM C518) (2010). "Standard Test Method for Steady-State Thermal Transmission Properties by Means of the Heat Flow Meter Apparatus" C518, ASTM International, West Conshohocken, PA, 2010, DOI: 10.1520/C0518-10, www.astm.org

American Society for Testing and Materials (ASTM C522) (2009). "Standard Test Method for Airflow Resistance of Acoustical Materials" C522, ASTM International, West Conshohocken, PA, 2009, DOI: 10.1520/C0522-09, www.astm.org

American Society for Testing and Materials (ASTM C1498) (2004) e1. "Standard Test Method for Hygroscopic Sorption Isotherms of Building Materials" C1498 - 04a ,ASTM International, West Conshohocken, PA, 2004, DOI: 10.1520/C1498-04AR10E01, www.astm.org

American Society for Testing and Materials (ASTM C1699) (2009). "Standard test methods for moisture retention curves of porous building materials using pressure plate" C1699, ASTM International, West Conshohocken, PA, 2009, DOI: 10.1520/ C1699-09, www.astm.org

American Society for Testing and Materials (ASTM E96) (2010). "Standard test methods for water vapour transmission of materials" E96/E96M, ASTM International, West Conshohocken, PA, 2010, DOI: 10.1520/ E0096_E0096M-10, www.astm.org

Baker, M. C. (1969). "Decay of wood." *Canadian Building Digests, CBD-111 < http://www.nrc-cnrc.gc.ca/eng/ibp/irc/cbd/building-digest-111.html> (Dec. 15, 2011).*

Barreira, E., Delgado, J., Ramos, N., and Freitas, V. (2010). "Hygrothermal Numerical Simulation: Application in Moisture Damage Prevention." *Numerical Simulations - Examples and Applications in Computational Fluid Dynamics,* Lutz Angermann (Ed.), ISBN: 978-953-307-153-4, InTech, <http://www.intechopen.com/articles/show/title/ hygrothermal-numerical-simulation-application-in-moisture-damage-prevention> (Dec. 15,2011).

Bergman, R. (2010). "Drying and Control of Moisture Content and Dimensional Changes." General Technical Report FPL-GTR-190. *Wood Handbook: Wood as an Engineering Material,* R. J. Ross ed., U.S. Department of Agriculture, Forest Service, Forest Products Laboratory, Madison, WI.

Bomberg, M., and Kumaran, M. K. (1986). "A Test method to determine air flow resistance of exterior membranes and sheathings." *Journal of Building Physics,* 9(3), 224-235.

Bomberg, M., and Brown, W.(1993). "Building Envelope: Heat, Air and Moisture Interactions." *Journal of Building Physics*, 16 (4), 306-311.

Bowyer J., Shmulsky R., and Haygreen J. (2007) *Forest Products and Wood Science: An Introduction,* 5th ed., Blackwell Publishing, Ames, IA.

Burch, D.M. and Chi, J. (1997). MOIST: A PC program for predicting heat and moisture transfer in building envelopes. Release 3.0. National Institute of Standards and Technology,NIST special publication 917, Washington, DC.

Burke, S., Claesson, J., and Arfvidsson, J. (2008). "A New Method of Determining Moisture Flow Coefficients for both Isothermal and Non-isothermal Conditions." Proceedings of the 8th Symposium on Building Physics in the Nordic Countries, Technical University of Denmark, Copenhagen ,Denmark, 975 – 982, < http://web.byv.kth.se/bphys/copenhagen/pdf/234-2.pdf> (Dec. 16,2011) .

Cammalleri V., and Lagus, P. (2009). "Measurement Techniques and Instrumentation". *Moisture Control in Buildings: The Key Factor in Mold Prevention*, 2nd Edition, ASTM, West Conshohocken, PA.

Canadian Standards Association (CSA-O86-09). (2009). *Engineering Design in Wood.* , CSA-O86-09, CSA, Mississauga, ON.

Canadian Wood Council (CWC). (2000). *Fire Safety in Residential Buildings*, Building performance series 2 CWC, Ottawa, ON.

Canadian Wood Council (CWC). (2010). *Wood Design Manual 2010*, CWC, Ottawa, ON.

Carll, C. G., and Highley, T. L. (1999). "Decay of wood and wood-based products above ground in buildings." *Journal of Testing and Evaluation,* 27(2), 150-158.

Carpenter, J.H.(1962). *Fundamentals of Psychrometrics*. Carrier Corp., Syracuse, NY.

Cloutier, A. and Fortin,Y. (1991) "Moisture content – water potential relationship of wood from saturated to dry conditions. " *Wood Science and Technology*, 25(4), 263-280.

Cloutier, A. and Fortin,Y. (1993) "A model of moisture movement in wood based on water potential and the determination of effective water conductivity. " *Wood Science and Technology*, 27(2), 95-114.

Cornick, S., Dalgliesh W.A,.Maref, W. (2009) "Sensitivity of hygrothermal analysis to uncertainty in rain data. " *Journal of ASTM International*, 6 (4), 1-17

Cornick, S., Djebbar, R., Dalgliesh W.A. (2003). "Selecting moisture reference years using a Moisture Index approach. " *Building and Environment*, 38, 1367-1379

Dent, R.W. (1977). "A multilayer theory for gas sorption, Part I: sorption of a single gas." *Textile Research Journal*, 47, 145-152.

Djebbar, R., Kumaran, M.K., Van Reenen, D. and Tariku, F. (2002a). Hygrothermal Modeling of Building Envelope Retrofit Measures in Multi-Unit Residential and Commercial Office Buildings, Client Final Report, 187.

Djebbar, R., Kumaran, M.K., Van Reenen, D. and Tariku, F. (2002b), "Use of hygrothermal numerical modeling to identify optimal retrofit options for high-rise buildings,"12th International Heat Transfer Conference (Grenoble, France, 2002-08-18), 165-170.

Engelund, E., Thygesen, L. and Hoffmeyer P. (2010). "Water sorption in wood and modified wood at high values of relative humidity. Part 2: Theoretical assessment of the amount of capillary water in wood microvoids". *Holzforschung,* 64(3). 325-330.

Food and Agriculture Organization of the United Nations. (FAO) (2003). "Forests and forestry sector Canada.", <http://www.fao.org/forestry/country/57478/en/can/> (Mar. 16, 2012).

Forest Products Laboratory (FPL) (1999). Wood handbook : wood as an engineering material. General technical report FPL; GTR-113. U.S. Department of Agriculture, Forest Service, Forest Products Laboratory, Madison, WI.

FPInnovations. (2010). Cross Laminated Timber: A Primer. FP Innovations, Pointe-Claire, QC, ISBN: 978-0-86488-545-6, <http://www.fpinnovations.ca/files/pdfs/en/publications/cross_laminated_timber_the_book.pdf> (Dec. 17 2011).

Frihart, C. R., and Hunt, C. G. (2010). "Adhesives with Wood Materials- Bond Formation and Performance." Wood Handbook: Wood as an Engineering Material, R. J. Ross ed., U.S. Department of Agriculture, Forest Service, Forest Products Laboratory, Madison, WI.

Glass, S. V., and Zelinka, S. L. (2010). "Moisture Relations and Physical Properties of Wood", General Technical Report FPL-GTR-190. Wood Handbook: Wood as an Engineering Material, R. J. Ross ed., U.S. Department of Agriculture, Forest Service, Forest Products Laboratory, Madison, WI.

Glued Laminated Timber Research Association inc. (GLTRA) ("Studiengemeinschaft Holzleimbau e.V." in german) (2011) "Cross Laminated Timber (CLT)." <http://www.en.brettsperrholz.org> (Oct. 20, 2011).

Hagentoft, C.E. and Blomberg, T. (2000). 1D-HAM coupled heat, air and moisture transport inmulti-layered wall structures, Manual of version 2.0, Lund-Gothenburg Group for

Computational Building Physics. <http://www.buildingphysics.com/manuals/1dham.pdf>(Jul. 20, 2012).

Hailwood, A.J. and Horrobin, S. (1946), "Absorption of water by polymers: Analysis in terms of a simple model", Transactions of the Faraday Society, 42(B), 84-102.

Hens, H. (2011) Applied Building Physics, Wilhelm Ernst & Sohn, Berlin, Germany

Hukka, A., and Viitanen, H. A. (1999). "A Mathematical Model of Mould Growth on Wooden Material." Wood Science and Technology, 33(6), 475-485.

International Organization for Standardization (ISO 12572) (2001). "Hygrothermal performance of building materials and products -- Determination of water vapour transmission properties." International Organization for Standardization, Geneva, Switzerland.

International Organization for Standardization (ISO 13788) (2002). "Hygrothermal performance of building components and building elements – Internal surface temperature to avoid critical surface humidity and interstitial condensation—Calculation methods." International Organization for Standardization, Geneva, Switzerland.

International Organization for Standardization (ISO 15148) (2002). "Hygrothermal Performance of building materials and products – Determination of water absorption coefficient by partial immersion", International Organization for Standardization, Geneva, Switzerland.

Kalagasidis, A.S. (2004). "HAM-Tools: An Integrated Simulation Tool for Heat, Air and Moisture Transfer Analyses in Building Physics." Thesis, presented to Chalmers University of Technology, Gothenburg, Sweden. in partial fulfillment of the requirements for the degree of Doctor of Philosophy.

Karagiozis, A.N. (1993). "Overview of the 2-D hygrothermal heat-moisture transport model LATENITE. " Internal IRC/BPL Report, IRC/NRC, National Research Council of Canada, Ottawa, ON.

Karagiozis, A.N. (1997). "Analysis of the hygrothermal behavior of residential high-rise building components." Client report A-3052, IRC/NRC, National Research Council of Canada, Ottawa, ON.

Karagiozis, A.; Salonvaara, M.; Kumaran, M. (1996) "Numerical Simulation of Experimental freeze Condition in Glass-Fiber insulation." Building Physics in the Nordic Countries, Espoo, Finland, 455-465.

Karagiozis, A. (2001). "Advanced Hygrothermal Modeling of Building Materials using Moisture-Expert 1.0." Proceedings of the 35th International Particleboar-Composite Materials Symposium, Washington, DC, 39-47.

KLH (2012). " KLH Kreuzlagenholz Massivholzplatten, Wohnbau, Hallenbau, Industrie- und Gewerbebau: Case unifamiliari a Klagenfurt"< http://www.klh.at/it/projekte/einfamilienhaeuser/einfamilienhausinklagenfurt.html> (Jul. 10 2012).

Kuenzel, H.M. and Kiessl, K. (1997). "Calculation of Heat and Moisture Transfer in Exposed Building Components." International Journal of Heat and Mass Transfer, 40(1), 159-167.

Kumaran, K., Lackey, J., Normandin, N., van Reenen, D., and Tariku, F. (2002). "Summary report from Task 3 of MEWS project at the Institute for Research in Construction – hygrothermal properties of several building materials." Institute for Research in Construction, National Research Council, Ottawa, ON, 1-68.

Kumaran, M. K. (2009). "Fundamentals of Transportation and Storage of Moisture in Building Material and Components." ASTM Manual on Moisture in Buildings, H. R. Trechsel, and M. T. Bomberg, eds., ASTM, West Conshohocken, 1-15.

Kumaran, M. K. (2001). "Hygrothermal Properties of Building Materials." ASTM Manual on Moisture in Buildings, H. R. Trechsel, ed., American Society for Testing And Materials, West Conshohocken, 29-65.

Kumaran, M.K.(1996) "Heat, Air and Moisture Transfer Through New and Retrofitted Insulated Envelope Parts, Final report Volume 3, Task 3: Material properties." International Energy Agency.

Kumaran, M. K., Lackey, J. C., Normandin, N., Tariku, F., and van Reenen, D. (2002). "A Thermal and Moisture Transport Property Database for Common Building and Insulating Materials." <http://rp.ashrae.biz/page/rp-1018.pdf> (Jan. 5,2012).

Kurnitski, J. & Vuolle, M. (2000). "Simultaneous calculation of heat, moisture and air transport in a modular simulation environment," Proceedings of the Estonian Academy of Sciences Engineering, 6, 25.

Latta, J. K., and Garden, G. K. (1964). "Vapour Diffusion and Condensation." Canadian Building Digests, CBD-57<http://www.nrc-cnrc.gc.ca/eng/ibp/irc/cbd/building-digest-57.html> (Nov. 21, 2011).

Lebow, S.T., and White R. H. (2007). "Durability of Wood in Construction" Marks's Standard Handbook for mechanical engineers, McGraw Hill, New York, 5.129-6.131.

Lie, T.T. (1977). "A Method for Assessing the Fire Resistance of Laminated Timber Beams and Columns", Canadian journal of Civil Engineering, 4(2), 161-169.

Lstiburek, J. (1999). "Wood Durability." Research Report - 9910, Building Science Press, < http://www.buildingscience.com/documents/reports/rr-9910-wood> (Nov. 21, 2011).

Mamlouk, M., and Zaniewski, J.(1999). Materials for Civil and Construction Engineers. Addison Wesley Longman, Menlo Park, CA.

Maref, W., Lacasse, M.A., and Booth, D.G. (2002). "Benchmarking of IRC's Advanced Hygrothermal Model – hygIRC Using Mid- and Large-Scale Experiments", Research Report, Insti-tute for Research in Construction, National Research Council Canada, 126, 38.

Mendes, N., Ridley, I., Lamberts, R., Philip, P.C. and Budag, K. (1999). "UMIDUS-A PC program for the prediction of heat and moisture transfer in porous buildings elements." Building Energy Simulation, 20(4), 2-8.

Morrell, J. J. (2002). "Wood-based building components: what have we learned?" International Biodeterioration & Biodegradation, 49(4), 253-258.

Mukhopadhyaya, P., Kumaran, K., Tariku, F., and van Reenen, D. (2006). "Application of hygrothermal modeling tool to assess moisture response of exterior walls." Journal of Architectural Engineering, 12(4) 178-187.

Mukhopadhyaya, P., Ping, F., Kumaran, M. K., and Van Reenen, D. (2009). "Role of vapour barrier in wood-frame stucco wall in various North American climates-observations from hygrothermal simulation." Journal of ASTM International, 6(8), 14.

Mukhopadhyaya, P., Normandin, N., Sherrer, G. (2011) "Critical assessment of equilibrium moisture content of wood and wood-based materials at high relative humidity levels." Report B1436.1, submitted to FP Innovation , National Research Council Canada, Ottawa, ON.

Nicolai, A.; Grunewald, J. & Zhang, J.S. (2007). Salztransport und Phasenumwandlung - Modellierung und numerische Lösung im Simulations programm Delphin 5, Bauphysik, 29(3), 231-239.

Oak Ridge National Laboratory (ORNL). (2012). "BTRIC – WUFI Designing Tool – ORNL", <http://www.ornl.gov/sci/ees/etsd/btric/wufi/tool.shtml> (Aug, 30 2012).

Physibel (2007). "GLASTA Diffusion - Condensation – Drying extended Glaser method." <http://www.physibel.be/v0n2gl.htm>(Oct. 27 2012).

Raji, S., Jannot, Y., Lagiere, P., and Puiggali, J. R. (2009). "Thermophysical characterization of a laminated solid-wood pine wall." Construction and Building Material, 23(10), 3189-3195.

Rode, C. (1990). Combined heat and moisture transfer in building constructions, Ph.D. Thesis, presented to Technical University of Denmark, Denmark, in partial fulfillment of the requirements for the degree of Doctor of Philosophy.

Rode, C. & Grau, K. (2004). Calculation tool for whole building hygrothermal analysis building simulation 2000, IEA Annex 41 meeting, Zurich, Switzerland.

Rousseau, J. (1999). "Envelope moisture performance through infiltration, exfiltration and diffusion- EMPTIED", CMHM Technical Series, 99-123.

Rowell, R., Youngs, R.(1981). "Dimensional stabilization of wood in us" Research Note FPL-0243, USDA Forest products laboratories, Beltsville, MD.

Saidani-Scott, H. (1993). "Analysis of moisture transfer in porous media; Application to building material" Thesis, presented to University of Bristol,UK, in partial fulfillment of the requirements for the degree of Doctor of Philosophy.

Schaffer, E. L. (1967). Charring rate of selected woodstransverse to grain. Paper FPL 69.U.S. Department of Agriculture, Forest Service, Forest Products Laboratory, Madison, WI.

Scheffer, T. (1973). "Microbiological degradation and the causal organisms." Wood Deterioration and its Prevention by Preservative Treatments, Syracuse University Press, Syracuse, NY, 31-106.

Siau, J. F. (1995). Wood: Influence of moisture on physical properties. Dept. of Wood Science and Forest Products, Virginia Polytechnic Institute and State University, Blacksburg, VA.

Simpson, W. T. (1973). "Predicting equilibrium moisture content of wood by mathematical models." Wood Fiber Science, 5(1), 41-49.

Skaar, C. (1972) Water in Wood. Syracuse University Press, Syracuse, NY.

Sonderegger, W., Hering, S., Mannes, D., Vontobel, P., Lehmann, E., and Niemz, P. (2010). "Quantitative determination of bound water diffusion in multilayer boards by means of neutron imaging." European Journal of Wood and Wood Products, 68(3), 341-350.

Straube, J. and Burnett, E., (2005) "Building Science for Building Enclosures", Building Science Press, Westford, MA, 293-373.

Time, B. (2002). "Studies on hygroscopic moisture transport in Norway spruce (Picea abies) Part 2: Modelling of transient moisture transport and hysteresis in wood " European Journal of Wood and Wood Products, 60(6), 405-410.

Time, B. (1998). "Hygroscopic moisture transport in wood." Thesis, Presented to Norwegian University of Science and Technology. in partial fulfillment of the requirements for the degree of Doctor of Philosophy.

Timber Research and Development Association (TRADA) Technology. (2009a). "Case Study: Stadthaus, 24 Murray Grove, London: Eight storeys of apartments featuring cross-laminated timber panels Case Study: Stadthaus, 24 Murray Grove, London: Eight storeys of apartments featuring cross-laminated timber panels." <http://www.trada.co.uk/casestudies/overview/StadthausMurray Grove/> (Jan. 10 2012).

Timber Research and Development Association (TRADA) Technology. (2009b). "Cross laminated timber: Introduction for specifiers." < http://www.trada .co.uk/bookshop/view/FC70D34E-83AA-4885-888A-61CFCFE75807/WIS_23_61 _Cross_laminated_timber_Introduction_for_specifiers> (Jan. 10 2012).

Thygesen, L. and Elder, T. (2009). "Moisture in untreated, acetylated, and furfurylated Norway spruce monitored during drying below fiber saturation using time domain NMR. " Wood and Fiber Science, 41(2), 194-200.

Thygesen, L., Engelund, E. and Hoffmeyer, P. (2010). "Water sorption in wood and modified wood at high values of relative humidity. Part 1: Results for untreated, acetylated and furfurylated Norway spruce. " Holzforschung, 64(3), 315-323.

Tiemann, H.D. (1906). "Effect of moisture upon the strength and stiffness of wood." Bulletin 70,USDA Forest Service, Washington, DC.

Tveit, A. (1966). "Measurements of moisture sorption and moisture permeability of porous materials (Norges byggforskningsinstitutt." Report No. 45, Norwegian Building Research Institute, Oslo.

Van Schijndel, A. (2005). "Integrated heat, air and moisture modeling and simulation in HAMLab" Reference: A41-T3-NL-05-2, IEA ECBCS Annex 41, working meeting, Trondheim, Norway, 1-8.

Wang, J., Mukhopadhyaya, P., and Morris, P. (2011). "Wood sorption, capillary condensation and their implications for building envelopes of wood construction.", Thirteenth Canadian Conference on Building Science and Technology, Winnipeg, MB, 1-13< http://www.nrc-cnrc.gc.ca/obj/irc/doc/pubs/nrcc54434.pdf> (Jan. 15 2012).

Wu, Y. (2007). "Experimental study of hygrothermal properties for building materials." Thesis, presented to Concordia University, QC, in partial fulfillment of the requirements for the degree of Masters of Science.

Appendix A: GAB Model to Hailwood and Horrobin Model Conversion Factors

Hailwood and Horrobin model equation is given as:

$$MC = \frac{RH}{A+B\cdot RH-C\cdot RH^2} \qquad \text{Equation A.1}$$

A, B and C are variables, while MC is the moisture content and h is the Relative Humidity.

GAB Model is given as:

$$MC = \frac{C\cdot K\cdot X_m\cdot RH}{(1-K\cdot RH)(1-K\cdot RH+C\cdot K\cdot RH)} \qquad \text{Equation A.2}$$

C, K, X_m are constants, while MC is the moisture content and RH is the Relative Humidity.

Based on a mathematical conversion through the results between the Hailwood and Horrobin Model and the GAB Model, the following relationship is derived:

$$A = \frac{1}{X_m\cdot C\cdot K\ (1000)} \qquad \text{Equation A.3}$$

$$B = \frac{(C\cdot K-2K)}{X_m\cdot C\cdot K\ (1000)} \qquad \text{Equation A.4}$$

$$C = \frac{-1\ (1-C)K^2}{X_m\cdot C\cdot K\ (1000)} \qquad \text{Equation A.5}$$

Appendix B: Measure Hygrothermal Properties of CLT

B.1 Partial Immersion

Table B.1: Partial immersion for CLT

Hem-Fir 1			Hem-Fir 2		
Square root of time ($s^{1/2}$)	Water Absorption (kg/m^2)	Diffusivity ($kg/m^2 \cdot s^{1/2}$)	Square root of time ($s^{1/2}$)	Water Absorption (kg/m^2)	Diffusivity ($kg/m^2 \cdot s^{1/2}$)
34.64	0.35	0.010104[1]	24.495	0.155980	0.006368[1]
69.28	0.54	0.005485	34.641	0.180723	0.002439
101.00	0.71	0.005359	42.426	0.202056	0.002740
143.87	0.96	0.005832	54.772	0.233600	0.002555
283.57	1.78	0.005870	62.450	0.248888	0.001991
323.57	2.01	0.005750	77.460	0.286353	0.002496
412.43	2.50	0.005514	97.980	0.340636	0.002645
655.90	3.73	0.005052	120.000	0.394340	0.002439
			169.706	0.523093	0.002590
			287.750	0.841088	0.002494
Average Diffusivity:		0.0055517	Average Diffusivity:		0.002487

Note: 24.49 ($S^{1/2}$) = 10 min ([1]) Neglected from the average diffusivity

ESPF			WSPF		
Square root of time ($s^{1/2}$)	Water Absorption (kg/m^2)	Diffusivity ($kg/m^2 \cdot s^{1/2}$)	Square root of time ($s^{1/2}$)	Water Absorption (kg/m^2)	Diffusivity ($kg/m^2 \cdot s^{1/2}$)
24.49	0.09	0.003675[1]	24.49	0.06	0.002450[1]
34.64	0.11	0.001970	34.64	0.08	0.001970
42.43	0.13	0.002567	42.43	0.10	0.002567
54.77	0.15	0.001621	60.00	0.13	0.001707
69.28	0.18	0.002068	77.46	0.17	0.002291
81.24	0.20	0.001672	97.98	0.20	0.001462
101.00	0.24	0.002024	134.16	0.27	0.001935
127.28	0.29	0.001903	176.63	0.35	0.001884
213.54	0.46	0.001971	210.71	0.42	0.002054
285.66	0.61	0.002080	308.87	0.58	0.001630
Average Diffusivity:		0.001986	Average Diffusivity:		0.001944

Note: 24.49 ($S^{1/2}$) = 10 min ([1]) Neglected from the average diffusivity

Euro		
Square root of time ($s^{1/2}$)	Water Absorption (kg/m^2)	Diffusivity ($kg/m^2 \cdot s^{1/2}$)
24.49	0.09	0.003675[1]
34.64	0.10	0.000985[1]
48.99	0.12	0.001394
60.00	0.14	0.001817
77.45	0.17	0.001719
103.92	0.21	0.001511
162.48	0.31	0.001708
199.00	0.37	0.001643
301.00	0.54	0.001667
335.86	0.60	0.001721
Average Diffusivity:		0.001647

Note: 24.49 ($S^{1/2}$) = 10 min;
(1) Neglected from the average diffusivity

B.2 **Equilibrium Moisture Content**

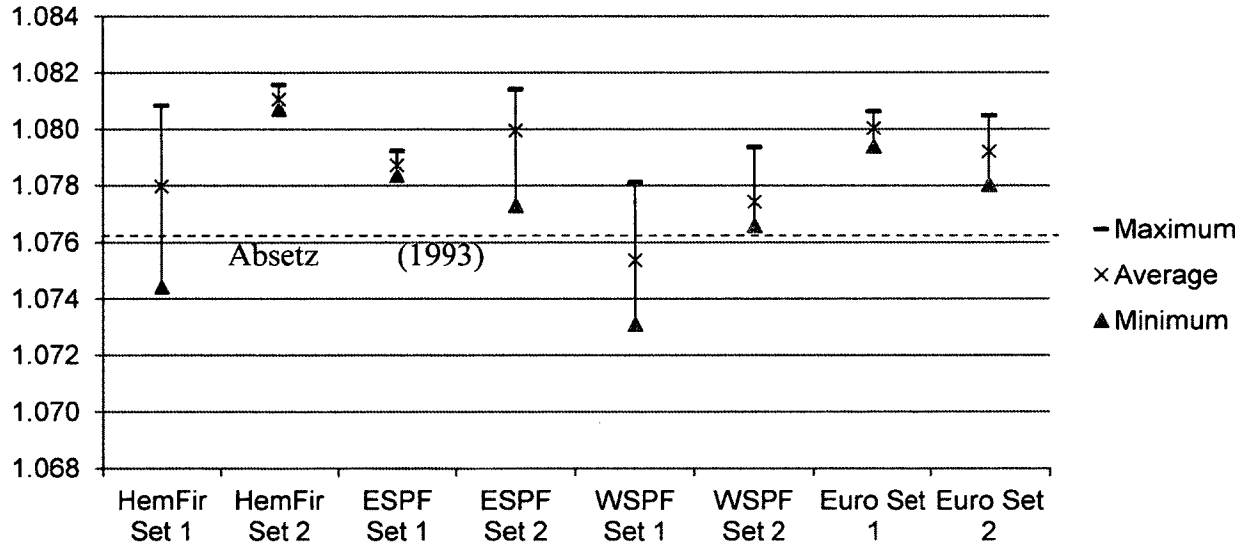

Figure B.1 Sorption at 49.8 % RH

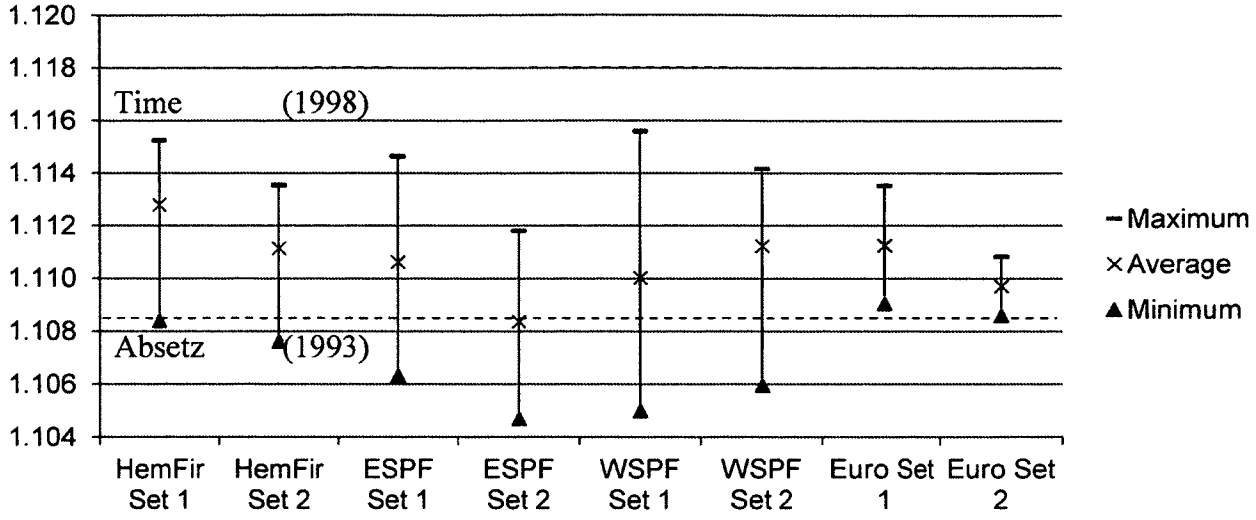

Figure B.2 Sorption at 69.4 % RH

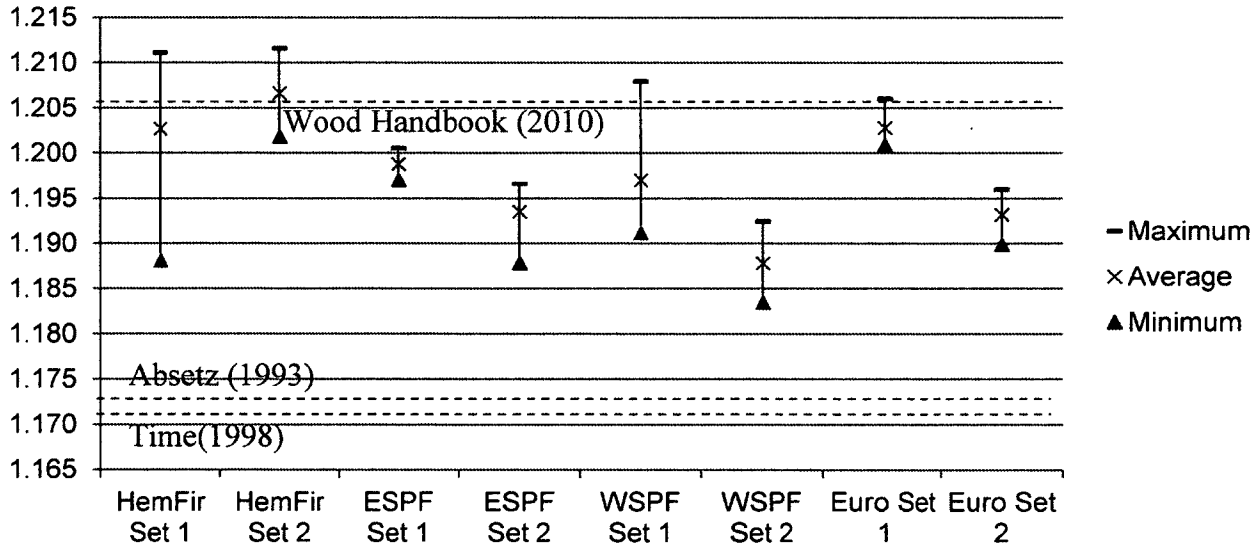

Figure B.3 Sorption at 90.3 % RH

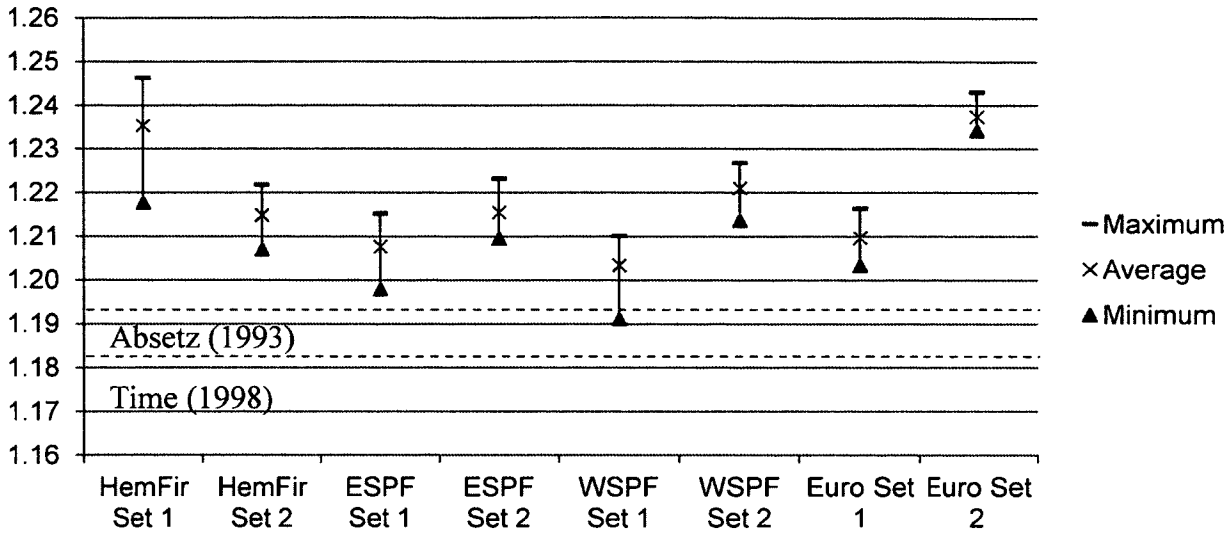

Figure B.4: Sorption at 94.4 % RH

B.3 **Water Vapour Transmission**

Table B.2: Water vapour transmission results

		RH	48.14%	69.57%	89.69%	48.14%	69.57%	89.69%
		Temp	23°C	23.1°C	23°C	23°C	23.1°C	23°C
Test Type	Material	Thick (mm)	Transmission (kg/s·m^2)			Permeability (kg/m·s·Pa)		
Dry Cup 0% RH	Hem-Fir	18.39	5.71 E-8	10.2 E-8	1.61 E-7	7.80E-13	9.55E-13	1.19E-12
		18.45	5.22 E-8	9.66 E-8	1.65 E-7	7.15E-13	9.09E-13	1.22E-12
		18.48	5.56 E-8	11.1 E-8	1.66 E-7	7.62E-13	1.05E-12	1.23E-12
		18.48	3.26 E-8	7.49 E-8	1.43 E-7	4.46E-13	7.05E-13	1.06E-12
	ESPF	18.85	3.75 E-8	8.88 E-8	1.88 E-7	5.25E-13	8.54E-13	1.42E-12
		18.29	6.51 E-8	12.6 E-8	1.84 E-7	8.84E-13	1.18E-12	1.35E-12
		18.48	2.94 E-8	7.65 E-8	1.57 E-7	4.03E-13	7.20E-13	1.17E-12
		18.05	3.53 E-8	10.3 E-8	2.04 E-7	4.72E-13	9.46E-13	1.46E-12
	WSPF	18.84	2.12 E-8	7.07 E-8	1.24 E-7	2.95E-13	6.80E-13	9.33E-13
		18.87	2.47 E-8	7.66 E-8	1.24 E-7	3.45E-13	7.39E-13	9.39E-13
		18.97	2.99 E-8	10.2 E-8	1.63 E-7	4.20E-13	9.86E-13	1.24E-12
		19.02	4.13 E-8	10.2 E-8	1.64 E-7	5.82E-13	1.14E-12	1.19E-12
	Euro	18.39	6.39 E-8	1.56 E-7	3.96 E-7	8.72E-13	1.47E-12	2.95E-12
		18.69	4.87 E-8	1.18 E-7	2.92 E-7	6.76E-13	1.13E-12	2.20E-12
		17.80	5.60 E-8	1.33 E-7	3.12 E-7	7.40E-13	1.21E-12	2.24E-12
		18.66	5.40 E-8	1.33 E-7	3.60 E-7	7.48E-13	1.27E-12	2.72E-12

		RH	48.14%	69.57%	89.69%	48.14%	69.57%	89.69%
		Temp	23°C	23.1°C	23°C	23°C	23.1°C	23°C
Test Type	Material	Thick (mm)	Transmission (kg/s·m^2)			Permeability (kg/m·s·Pa)		
Wet Cup 100% RH	Hem-Fir	18.66	3.52 E-7	2.89 E-7	1.95 E-7	4.64E-12	6.50E-12	1.35E-11
		18.39	3.56 E-7	2.85 E-7	1.89 E-7	4.62E-12	6.31E-12	1.29E-11
		17.99	2.83 E-7	2.44 E-7	1.71 E-7	3.58E-12	5.27E-12	1.14E-11
		18.22	3.34 E-7	2.73 E-7	1.83 E-7	4.28E-12	5.99E-12	1.24E-11
	ESPF	18.50	2.74 E-7	2.38 E-7	1.69 E-7	3.55E-12	5.28E-12	1.15E-11
		17.33	4.39 E-7	3.70 E-7	2.43 E-7	5.41E-12	7.83E-12	1.60E-11
		18.58	3.04 E-7	2.68 E-7	1.85 E-7	3.98E-12	5.99E-12	1.28E-11
		17.71	3.34 E-7	2.97 E-7	2.04 E-7	4.17E-12	6.34E-12	1.35E-11
	WSPF	18.42	2.77 E-7	2.39 E-7	1.24 E-7	3.58E-12	5.26E-12	8.28E-12
		18.64	2.79 E-7	2.41 E-7	1.33 E-7	3.64E-12	5.37E-12	9.02E-12
		18.18	2.77 E-7	2.45 E-7	1.45 E-7	3.54E-12	5.34E-12	9.65E-12
		18.78	3.43 E-7	2.91 E-7	1.53 E-7	4.54E-12	6.60E-12	1.05E-11
	Euro	18.99	4.28 E-7	3.40 E-7	1.43 E-7	6.20E-12	3.34E-12	1.09E-12
		17.83	3.74 E-7	2.91 E-7	1.15 E-7	5.08E-12	2.68E-12	8.21E-13
		18.76	5.64 E-7	4.64 E-7	2.08 E-7	8.20E-12	4.53E-12	1.57E-12
		19.06	4.51 E-7	3.66 E-7	1.56 E-7	6.61E-12	3.62E-12	1.19E-12

Appendix C: EMC models for four cases considered

Table C.1: EMC cases for red pine

Case 1: $M = \frac{a + ch^{½} + eh + gh^{1.5}}{1 + bh^{½} + dh + fh^{1.5}}$		Case 2: $M = \frac{a + c\ln(x) + e\left(ln(x)\right)^2}{1 + b\ln(x) + d\left(ln(x)\right)^2}$	
At RH = (0-100%)		At RH = (0-100%)	
a=	0.106908626	*a*=	1.698999224
b=	-3.37404522	*b*=	-1072.27813
c=	-0.39296665	*c*=	-344.803494
d=	3.863811168	*d*=	7911.462522
e=	0.486844315	*e*=	350.006569
f=	-1.48973299		
g=	-0.20072987		

Case 3: Two equations			
$M = \frac{1}{a + be^h}$		$M = a + \left((h/100 - b)c\right)$	
At RH = (0% - 94.6%)		At RH = (94.6%- 100%)	
a=	23.22726886	*a*=	0.257886756
b=	-7.51327635	*b*=	0.946
		c=	26.68726793

Case 4: Three Equations					
$M = \frac{1}{a + be^h}$		$M = a + \left((h/100 - b)c\right)$		$lnM = \frac{(a + ch)}{(1 + bh)}$	
At RH = (0% - 94.6%)		At RH = (94.6%-96.7%)		At RH = (96.7% - 100%)	
a=	23.22726886	*a*=	0.257886756	*a*=	-1.41660293
b=	-7.51327635	*b*=	0.946	*b*=	-0.99891419
		c=	0.02746649	*c*=	1.417243314

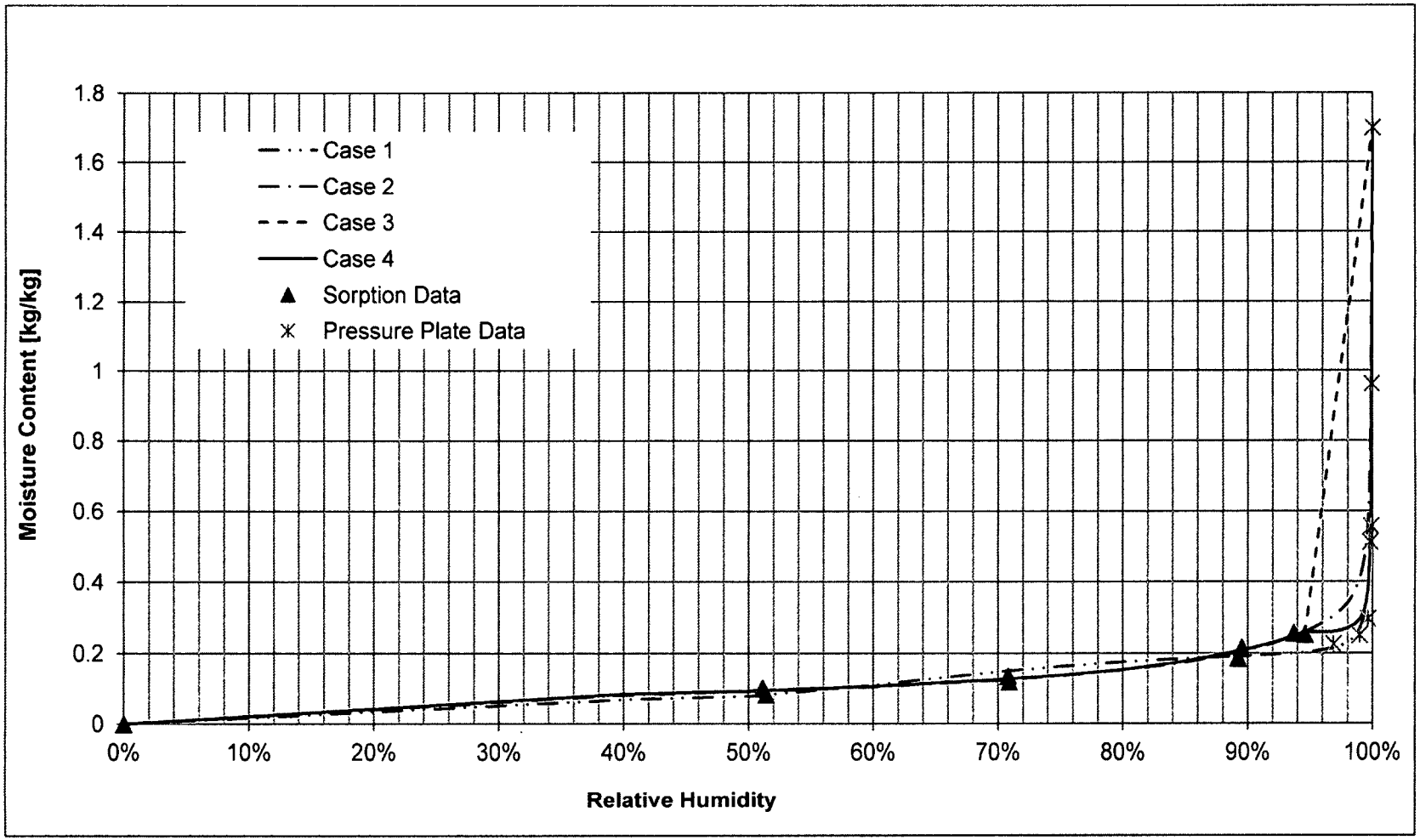

Figure C.1 Generated models for EMC cases

Appendix D: Modeling Software

Table D.1: Modeling software sources

Software	Originating	website
1D-HAM	Sweden	http://www.buildingphysics.com/1d-ham.htm
Bsim2000	Denmark	http://en.sbi.dk/publications/programs_models/bsim
DELPHIN 5	Germany	http://www.bauklimatik-dresden.de/delphin/documentation.php?aLa=en
EMPTIED	Canada	-
GLASTA	Belgium	http://www.physibel.be/v0n2gl.htm
HAMLab	Netherlands	http://archbps1.campus.tue.nl/bpswiki/index.php/Hamlab
HAM-Tools	Swed./Den.	-
hygIRC-1D	Canada	http://www.nrc-cnrc.gc.ca/eng/projects/irc/hygirc.html
IDA-ICE	Sweden	http://www.equa.se/eng.ice.html
MATCH	Denmark	http://www.ornl.gov/sci/roofs+walls/codes/code04.html
MOIST	USA	http://www.ornl.gov/sci/roofs+walls/codes/code03.html
MOIST-EXP	USA	-
UMIDUS	Brazil	http://www.pucpr.br/pesquisa/1st/
WUFI	Germ./USA	http://www.ornl.gov/sci/ees/etsd/btric/wufi.shtml